

NASA  
CR  
1607  
[v.]3  
c.1



NASA CR-1607

LOAN COPY RETURN

AFWL (WLOL)

KIRTLAND AFB, NM

TECH LIBRARY KAFB, NM  
0060875

# NASA CONTRACTOR REPORT

NASA CR-1609

## DETERMINATION OF WELDABILITY AND ELEVATED TEMPERATURE STABILITY OF REFRACTORY METAL ALLOYS III - Effect of Contamination Level on Weldability of Refractory Metal Alloys

*by D. R. Stoner*

*Prepared by*  
WESTINGHOUSE ASTRONUCLEAR LABORATORY  
Pittsburgh, Pa. 15236  
*for Lewis Research Center*

NATIONAL AERONAUTICS AND SPACE ADMINISTRATION • WASHINGTON, D. C. • SEPTEMBER 1970



0060875

1. Report No. NASA CR-1609		2. Government Accession No.		3. Recipient's Catalog No.	
4. Title and Subtitle DETERMINATION OF WELDABILITY AND ELEVATED TEMPERATURE STABILITY OF REFRACTORY METAL ALLOYS III - EFFECT OF CONTAMINATION LEVEL ON WELDABILITY OF REFRACTORY METAL ALLOYS		5. Report Date September 1970			
		6. Performing Organization Code			
7. Author(s) D. R. Stoner		8. Performing Organization Report No. WANL-PR-(P)-015			
9. Performing Organization Name and Address Westinghouse Astronuclear Laboratory Pittsburgh, Pennsylvania 15236		10. Work Unit No.			
		11. Contract or Grant No. NAS 3-2540			
12. Sponsoring Agency Name and Address National Aeronautics and Space Administration Washington, D.C. 20546		13. Type of Report and Period Covered Contractor Report			
		14. Sponsoring Agency Code			
15. Supplementary Notes					
16. Abstract <p>This program was undertaken to determine the tolerance of three promising, highly weldable tantalum and columbium alloys to in-service oxygen contamination and subsequent repair welding. The alloys evaluated were FS-85, T-111, and T-222. These alloys were surface oxidized at low oxygen partial pressure and subsequently vacuum annealed to diffuse the oxygen contamination throughout the material. The detrimental effects of oxygen contamination were measured by bend tensile and restrained weld tests. Five oxygen contamination levels, ranging from residual oxygen content to 1000 ppm, were selected for this investigation. In addition, the most promising alloy, T-111, was aged for 1000 hours under ultra-high vacuum conditions to evaluate the effect of oxygen contamination on the thermal stability of base and weld metal. All three alloys exhibited a reasonable tolerance for contamination up to 100 to 200 ppm oxygen, above which ductility impairment became excessive. T-111 proved to be the most tolerant to oxygen contamination. The thermal history had a greater effect on the mechanical properties of T-111 than total oxygen content per se, apparently by altering the form and distribution of the oxide precipitates. Weld metal mechanical properties were nearly equal to base metal properties over the range of oxygen contamination investigated.</p>					
17. Key Words (Suggested by Author(s)) Refractory metals Welding Thermal stability			18. Distribution Statement Unclassified - unlimited		
19. Security Classif. (of this report) Unclassified	20. Security Classif. (of this page) Unclassified	21. No. of Pages 111	22. Price * \$3.00		



## FOREWORD

This evaluation was conducted by the Westinghouse Astronuclear Laboratory under NASA contract NAS 3-2540. Mr. P. E. Moorhead, of the Lewis Research Center Space Power Systems Division, was the NASA Project Manager for the program. Mr. G. G. Lessmann was responsible for performance of the program at the Westinghouse Astronuclear Laboratory.

The objectives delineated and results reported herein represent the requirements of Task IV of contract NAS 3-2540. Additional comprehensive investigations which were conducted as a part of this program are the subjects of additional reports. The final reports for this contract are the following:

- I - Weldability of Refractory Metal Alloys (CR-1607)
- II - Long-Time Elevated Temperature Stability of Refractory Metal Alloys (CR-1608)
- III - Effect of Contamination Level on Weldability of Refractory Metal Alloys (CR-1609)
- IV - Post Weld Annealing Studies of T-111 (CR-1610)
- V - Weldability of Tungsten Base Alloys (CR-1611)

Additional salient features of this program have been summarized in the following reports:

G. G. Lessmann, "The Comparative Weldability of Refractory Metal Alloys," The Welding Journal Research Supplement, Vol. 45 (12), December, 1966.

G. G. Lessmann and R. E. Gold, "The Weldability of Tungsten Base Alloys," The Welding Journal Research Supplement.

D. R. Stoner and G. G. Lessmann, "Measurement and Control of Weld Chamber Atmospheres," The Welding Journal Research Supplement, Vol. 30 (8), August, 1965.

G. G. Lessmann and D. R. Stoner, "Welding Refractory Metal Alloys for Space Power System Applications," Presented at the 9th National SAMPE Symposium on Joining of Materials for Aerospace Systems, November, 1965.

D. R. Stoner and G. G. Lessmann, "Operation of  $10^{-10}$  Torr Vacuum Heat Treating Furnaces in Routine Processing," Transactions of the 1965 Vacuum Metallurgy Conference of the American Vacuum Society, L. M. Bianchi, Editor.

G. G. Lessmann and R. E. Gold, "Thermal Stability of Refractory Metal Alloys", NASA Symposium on Recent Advances in Refractory Metals for Space Power Systems, June, 1969.

D. R. Stoner, "Welding Behavior of Oxygen Contaminated Refractory Metal Alloys," Presented at Annual AWS Meeting, April, 1967.

## TABLE OF CONTENTS

	<u>Page No.</u>
I. INTRODUCTION	1
II. EXPERIMENTAL PROCEDURES	12
III. RESULTS	33
PHASE I	33
PHASE II	64
IV. CONCLUSIONS	100
V. REFERENCES	102

## LIST OF FIGURES

	<u>Page No.</u>
1. Program Outline	2
2. Program Outline for Contaminated Alloy Weldability Evaluation	3
3. Effect of Oxygen and Nitrogen Content on the As-Cast Hardness of Unalloyed Columbium	5
4. Effect of Interstitial Content on Bend Ductility of Unalloyed Columbium	6
5. Effect of Welding Atmosphere on Weld Bend Ductility of B-66	8
6. Comparative Reactivity of Cb-1Zr to Interstitial Contamination	9
7. Effect of Oxygen on the Hardness of Cb-Hf and Cb-Zr Alloys	10
8. Calculated Effect of Annealing on Redistribution of Surface Oxides	13
9. Oxygen Concentration Gradient for T-222 Following 50 Hour Vacuum Annealing	14
10. FS-85 Contaminated to 750 ppm Oxygen	16
11. Schematic of Oxygen Contamination Apparatus	17
12. Controlled Oxygen Contamination Equipment	18
13. Correlation Between Weight Gain and Chemical Analysis	21
14. Vacuum Annealing Equipment	26
15. Vacuum Purged Welding Chamber	27
16. High Oxygen Content Weld Transverse Sections	28
17. Bend Test Description	31
18. Weld Restraint Patch Tests	32
19. Phase I Program Outline	34
20. Typical Bend Test Results. Intermediate Oxygen Contamination Levels	36
21. Bend Ductility Versus Oxygen Content for 3 Alloys	37
22. Transverse Weld Tensile Properties of T-111	40
23. Transverse Weld Tensile Properties of T-222	41
24. Transverse Weld Tensile Properties of FS-85	42
25. Tensile Properties of Ta-W-Hf-C, N, O Alloys in the Recrystallized Condition as a Function of Temperature	46

## LIST OF FIGURES (CONTINUED)

	<u>Page No.</u>
26. T-111, Photographs of 2200°F Tensile Specimens	47
27. T-222, Photographs of 2200°F Tensile Specimens	48
28. FS-85, Photographs of 2200°F Tensile Specimens	49
29. T-111, As-Welded Following 1800°F-50 Hrs. Diffusion Anneal	53
30. T-222, As-Welded Following 1800°F-50 Hrs. Diffusion Anneal	54
31. FS-85, As-Welded Following 1800°F-50 Hrs. Diffusion Anneal	55
32. Effect of Oxygen Content on Weld Interface Shape	56
33. Weld Hardness Traverse of T-111	57
34. Weld Hardness Traverse of T-222	58
35. Weld Hardness Traverse of FS-85	59
36. Transverse Hardness Traverses for FS-85	61
37. Hardness Versus Oxygen Content for 3 Alloys	63
38. Phase II Program Outline	65
39. Bend Transition Temperature Summary for Aged T-111	67
40. Bend Ductility of Vacuum Oxidized FS-85	69
41. Measured Oxygen Concentration Gradients for Vacuum Oxidized FS-85	70
42. Bend Ductility Comparison of Aged and Unaged T-111	71
43. Elevated Temperature Transverse Weld Tensile Properties of T-111, Aged 1000 Hours	76
44. Room Temperature Transverse Weld Tensile Properties of T-111, Aged 1000 Hours	77
45. 1800°F Comparison of Weld and Base Metal Tensile Properties	78
46. Room Temperature Comparison of T-111 Weld and Base Metal Tensile Properties	79
47. Comparison of Aged and As-Welded Yield Strength	81
48. Comparison of Aged and As-Welded Tensile Strength	82
49. Comparison of Aged and As-Welded Tensile Elongation	83
50. Elevated Temperature Fracture Profiles of T-111 Weld Tensile Specimens	85



## LIST OF FIGURES (CONTINUED)

	<u>Page No.</u>
51. Room Temperature Fracture Profiles of T-111 Weld Specimens	86
52. Fracture Profiles of T-111 Base Metal Specimens	87
53. T-111, Aged 1000 Hours at 1500°F	88
54. T-111, Aged 1000 Hours at 1800°F	89
55. T-111, Aged 1000 Hours at 2200°F	90
56. Weld Hardness Traverse of T-111 Uncontaminated	91
57. Weld Hardness Traverse of T-111	92
58. Weld Hardness Profiles Expected in Age Hardenable Material	93
59. Hardness Versus Oxygen Content for Aged T-111	94
60. Effect of Aging at 1800°F on Weld and Base Metal Hardness	96
61. Microstructure of Oxygen Contaminated T-111	97
62. Electron Micrograph of HfO <sub>2</sub> Precipitates	98

## LIST OF TABLES

	<u>Page No.</u>
1. Oxygen Contamination Parameters	20
2. Chemical Analysis of Phase I Bend Test Specimens	22
3. Chemical Analysis for Phase II	23
4. Comparison of Weld and Base Metal Chemical Analyses	24
5. Welding Parameters for 0.036" Sheet	29
6. As-Received Product Chemistry	29
7. Tensile Test Properties of T-111 at Five Oxygen Levels	39
8. Tensile Test Properties of T-222 at Five Oxygen Levels	44
9. Tensile Test Properties of FS-85 at Five Oxygen Levels	45
10. Weld Restraint Patch Test Inspection Results	51
11. Oxidation Program Phase II Diffusion Annealing Schedule	66
12. Tensile Test Properties Aged T-111, Weld Specimens, 1500, 1800 and 2200°F	72
13. Tensile Test Properties of Aged T-111, Weld Specimens, Room Temperature	73
14. Tensile Test Properties of Aged T-111, Base Metal, R.T. and 1800°F	74

## 1. INTRODUCTION

Tantalum and columbium base alloys are prime candidates for liquid metal Rankine or high temperature Brayton Cycle turbo-electric power systems. Their high strength at temperatures exceeding  $1800^{\circ}\text{F}$ , excellent corrosion and erosion resistance to boiling alkali metals, and proven fabricability and weldability have made them attractive choices for space power generation systems. Unfortunately, tantalum and columbium base alloys are easily contaminated by carbon, nitrogen and oxygen and their important physical properties, weldability, ductility, and corrosion resistance to liquid metals, are markedly degraded by modest contamination in the part per million range.

Although the application environment will be in contamination-free vacuum of space, considerable long time ground testing will be required for prototype systems presenting a chance of inadvertent contamination. In addition, full scale systems may be contaminated during fabrication welding and heat treatment operations. Hence, a knowledge of the comparative tolerance to interstitial contamination could be very important in the selection of alloys for hardware applications. This program was undertaken to satisfy this need. The general program outline is shown in Figure 1 and the detailed program in Figure 2.

Although carbon, nitrogen and oxygen have an equally damaging effect on alloy properties, contamination studies have indicated that columbium and tantalum base alloys are much more reactive to oxygen at typical contamination conditions. For this reason the study was limited to oxygen contamination effects.

Three refractory metal alloys were contaminated with oxygen and evaluated for changes in weldability and long time thermal stability. The columbium and tantalum base alloys, T-111 (Ta-8W-2Hf), T-222 (Ta-9.6W-2.4Hf-0.01C) and FS-85 (Cb-27Ta-10W-1Zr), are fabricable, weldable alloys designed for tubing applications. Weldability was chosen as the basic measure of performance for two reasons. First, repair and modification operations requiring welding will certainly be needed for systems with operating lives measured in years.

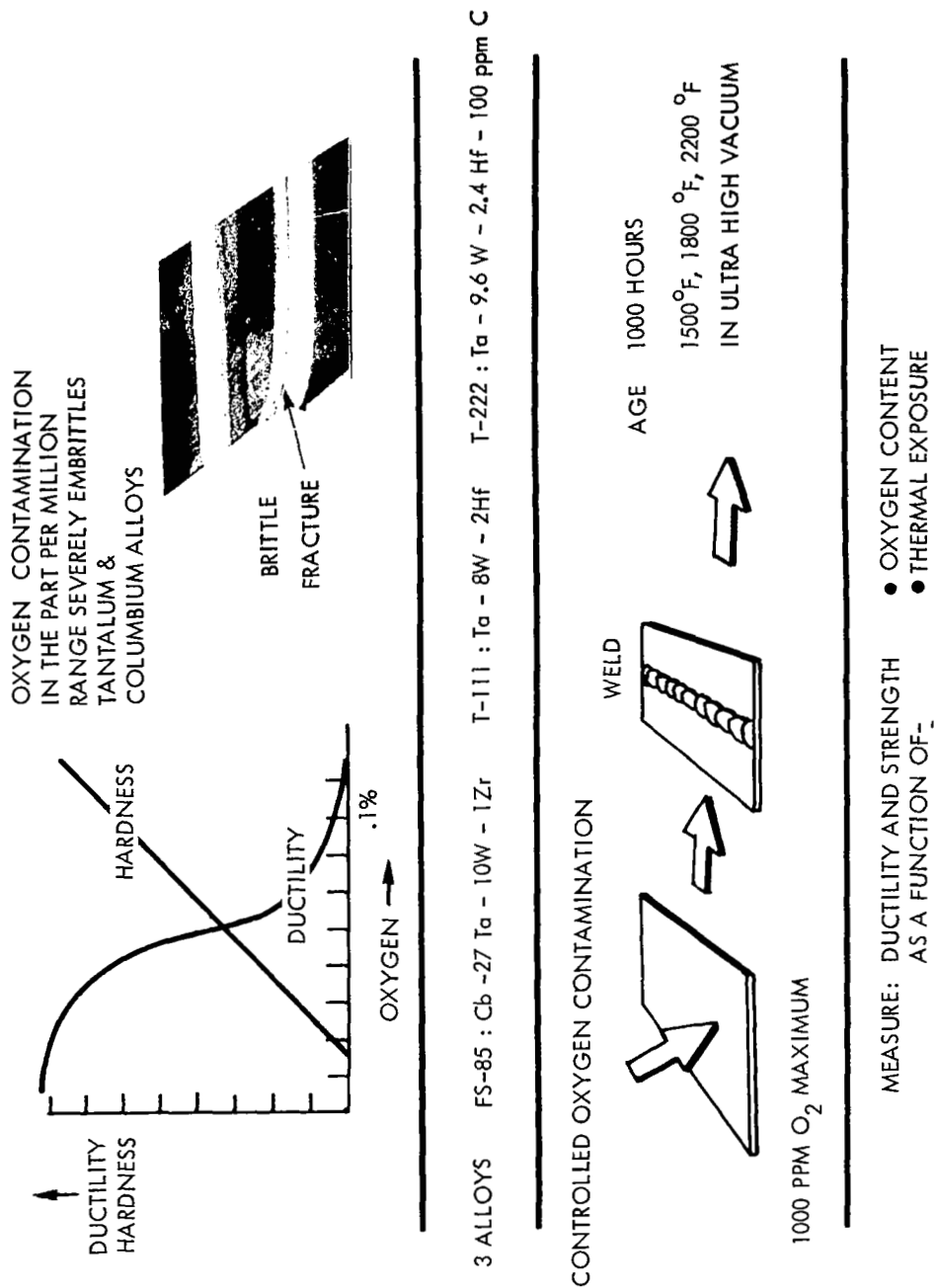
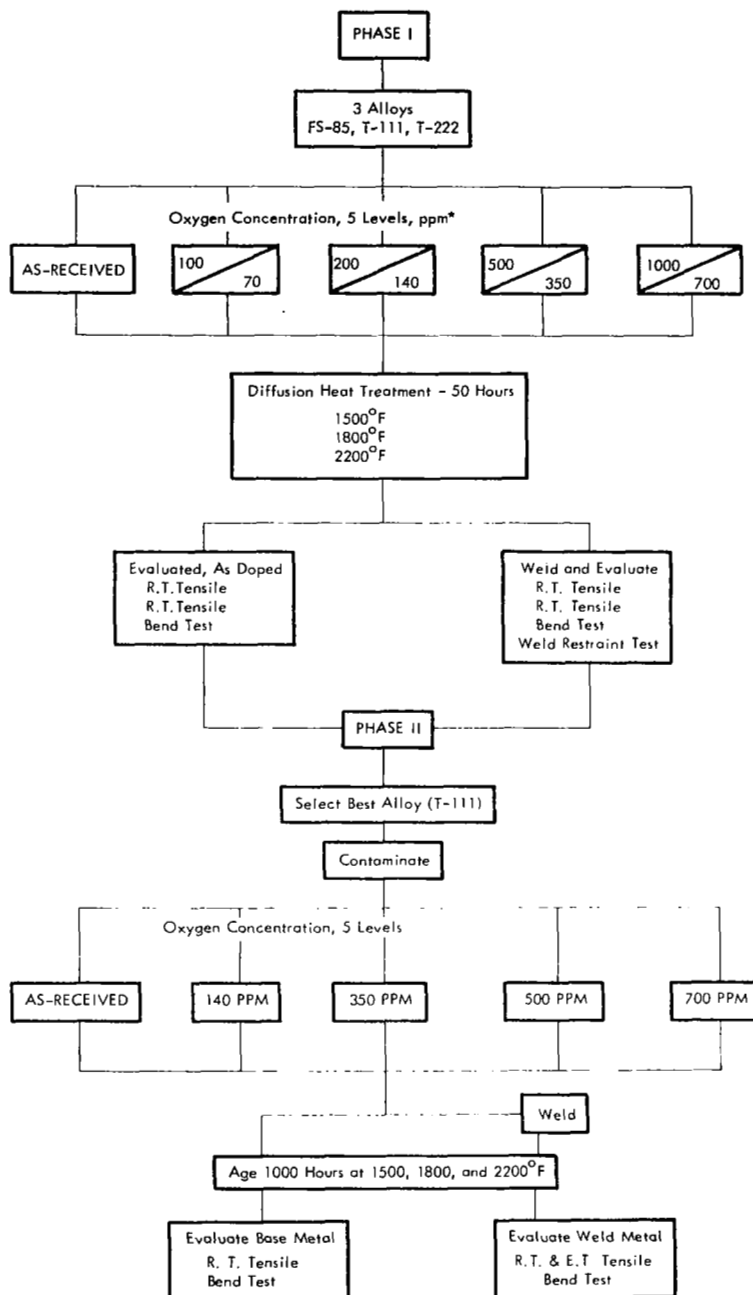


FIGURE 1 - Program Outline



\*T-111 and T-222 Contaminated  
to 70% of FS-85 for Equivalent  
Atomic % Oxygen

FIGURE 2 - Program Outline for Contaminated Alloy Weldability Evaluation

The second reason is that welds consist of a wide gamut of thermal histories, i.e., as-cast, solution treated, overaged, aged structure, etc., and are therefore very sensitive to a broad range and often to very subtle metallurgical interactions.

### Refractory Metal Oxidation

A considerable background of information exists on interstitial reactions and their effect on refractory metal properties. Unlike tungsten and molybdenum alloys, which react with oxygen at moderate temperatures forming high vapor pressure surface oxides with little internal contamination, columbium and tantalum base alloys have a high solubility for oxygen and surface oxides are quickly diffused through the material at temperatures over 1000°F.

In the late 1950's a concerted effort was made to develop tantalum and columbium alloys having a combination of high temperature strength, fabricability, and oxidation resistance. The efforts to combine oxidation resistance with other properties were generally unsuccessful and the present trend is the development of more specialized alloys. Hence, the alloys evaluated in this program are representative of alloys developed for corrosion resistance to high temperature alkali metals with a good balance between strength and fabricability. These alloys typically have negligible oxidation resistance above 800°F.

### Effects of Interstitial Contamination

The effect of interstitial content, particularly oxygen, has been observed from the early attempts to produce and evaluate pure refractory metal alloys. Figure 3 shows the effect of oxygen and nitrogen content on the hardness of as-cast columbium.<sup>(1)</sup> A pronounced hardening effect is observed and also a relationship that may be used in reverse. That is, an abnormally high hardness may be indicative of interstitial contamination. A corresponding decrease in ductility is produced with interstitial contamination as shown in Figure 4.<sup>(2)</sup>

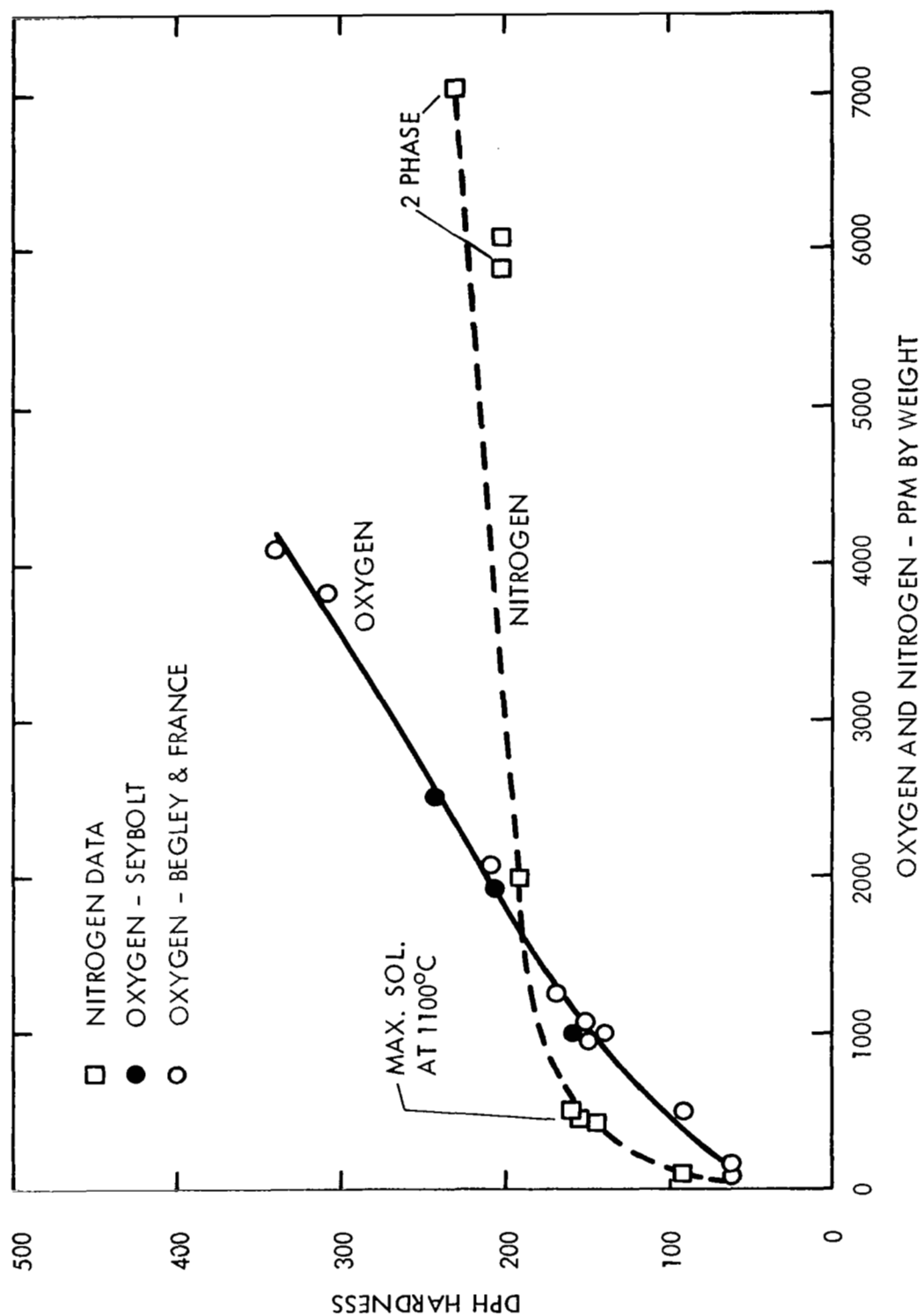


FIGURE 3 - Effect of Oxygen and Nitrogen Content on the <sup>1</sup>As-Cast Hardness of Unalloyed Columbium

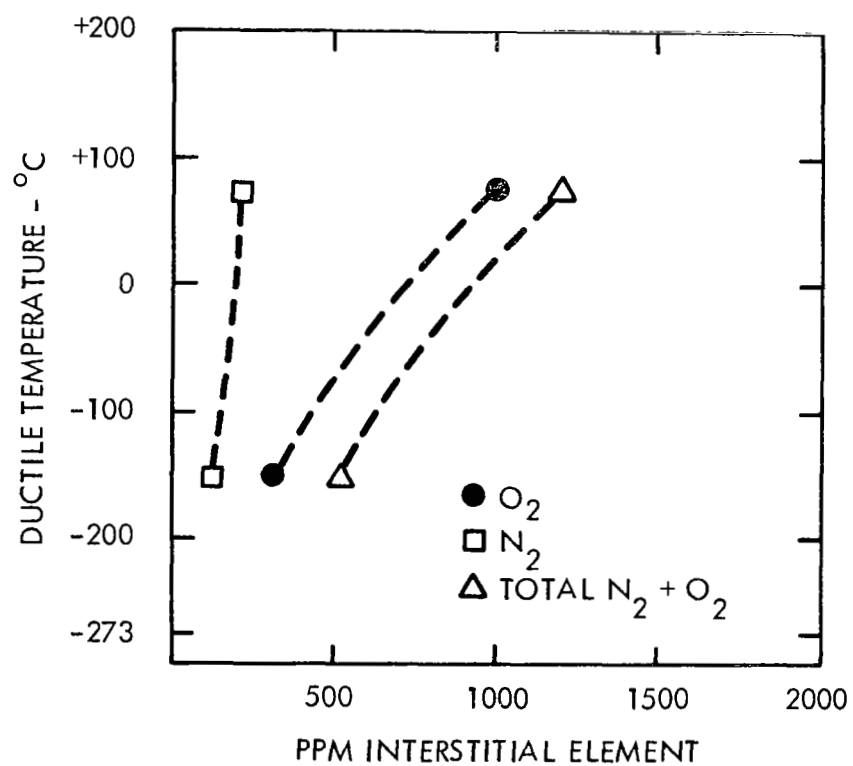


FIGURE 4 - Effect of Interstitial Content on Bend Ductility of Unalloyed Columbium



Studies of the weldability of refractory metal alloys have indicated that very high quality inert gas shielding is required to avoid weld embrittlement problems. Figure 5 shows the effect of minor air impurities in helium shielding gas on the bend ductility of a columbium base alloy B-66 (Cb-5Mo-5V-1Zr).<sup>(3)</sup> Welding atmosphere requirements for columbium and tantalum are more severe than required for titanium and even to that required for reactor grade zirconium alloys.

### Oxygen Contamination

As previously indicated, the reason for evaluating the effect on oxygen contamination rather than nitrogen and carbon, especially in view of the pronounced effects of all three interstitials, is that oxygen is much more readily assimilated than nitrogen or carbon. When nitrogen or oxygen are both present, even in the 4:1 atmospheric ratio, oxygen contamination is much more pronounced. Figure 6 shows increases in interstitial content following low pressure exposure indicating typically a much more pronounced increase in oxygen content.<sup>(4)</sup>

The alloys investigated in this program are commonly known as "gettered" refractory metal alloys. That is, they all contain a reactive alloy such as zirconium or hafnium. The reactive alloy combines with interstitial contamination, either a residual from the manufacturing process or service contamination, enhancing liquid metal corrosion resistance and, depending on the system, altering both strength and ductility. Although strengthening generally occurs with contamination anomalous behavior has also been observed; a decrease in hardness with oxygen additions is shown in Figure 7. The alloys were all prepared by melting, adding the oxygen as CbO to the melt. Using this process massive hafnium and zirconium oxides were produced which provided little strengthening and which additionally removed hafnium and zirconium from solid solution, thus decreasing the solution hardening effect of the alloy addition. A continual hardness decrease would be expected until all the hafnium or zirconium is combined with oxygen, at which point

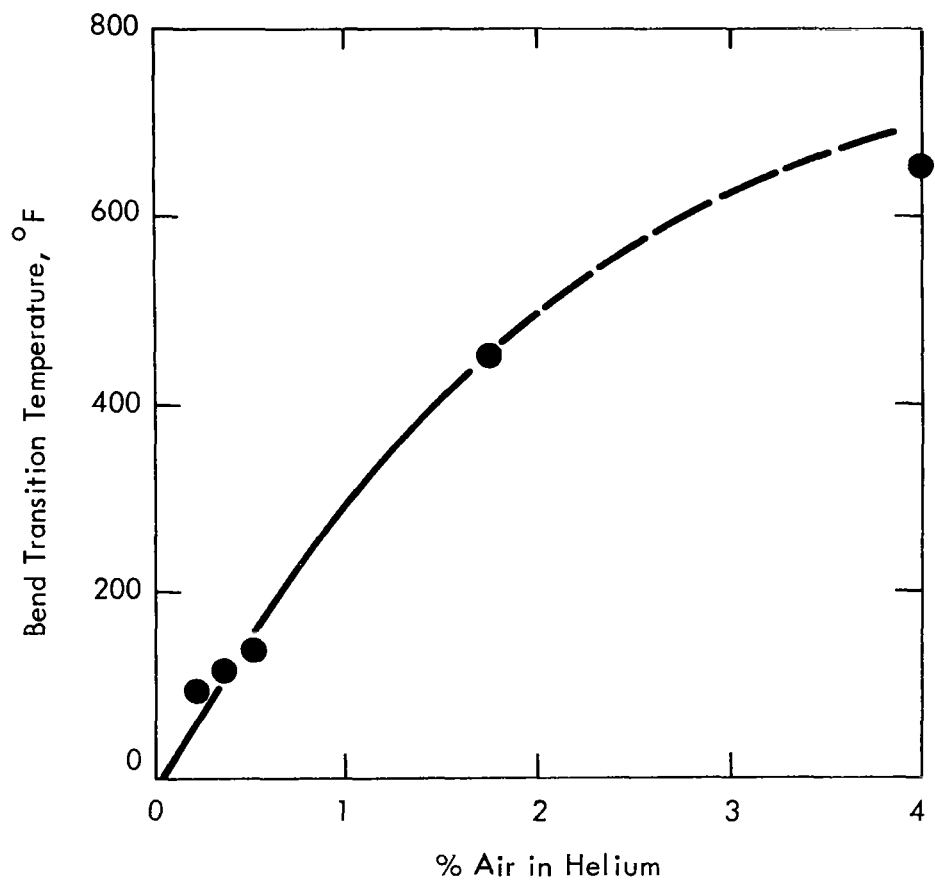


FIGURE 5 - Effect of Welding Atmosphere on Weld Bend Ductility of B-66 (Cb-5V-5Mo-1Zr)

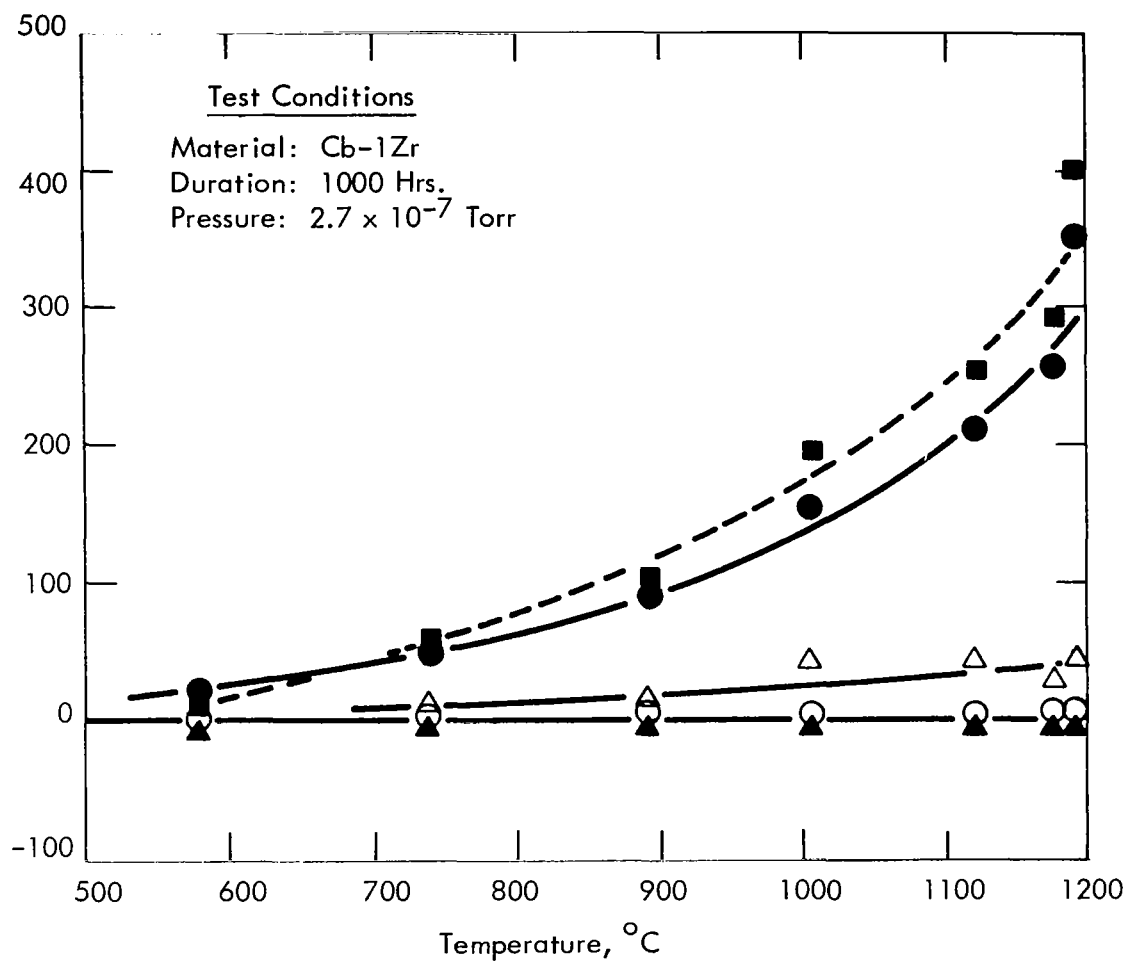


FIGURE 6 - Comparative Reactivity of Cb-1Zr to Interstitial Contamination

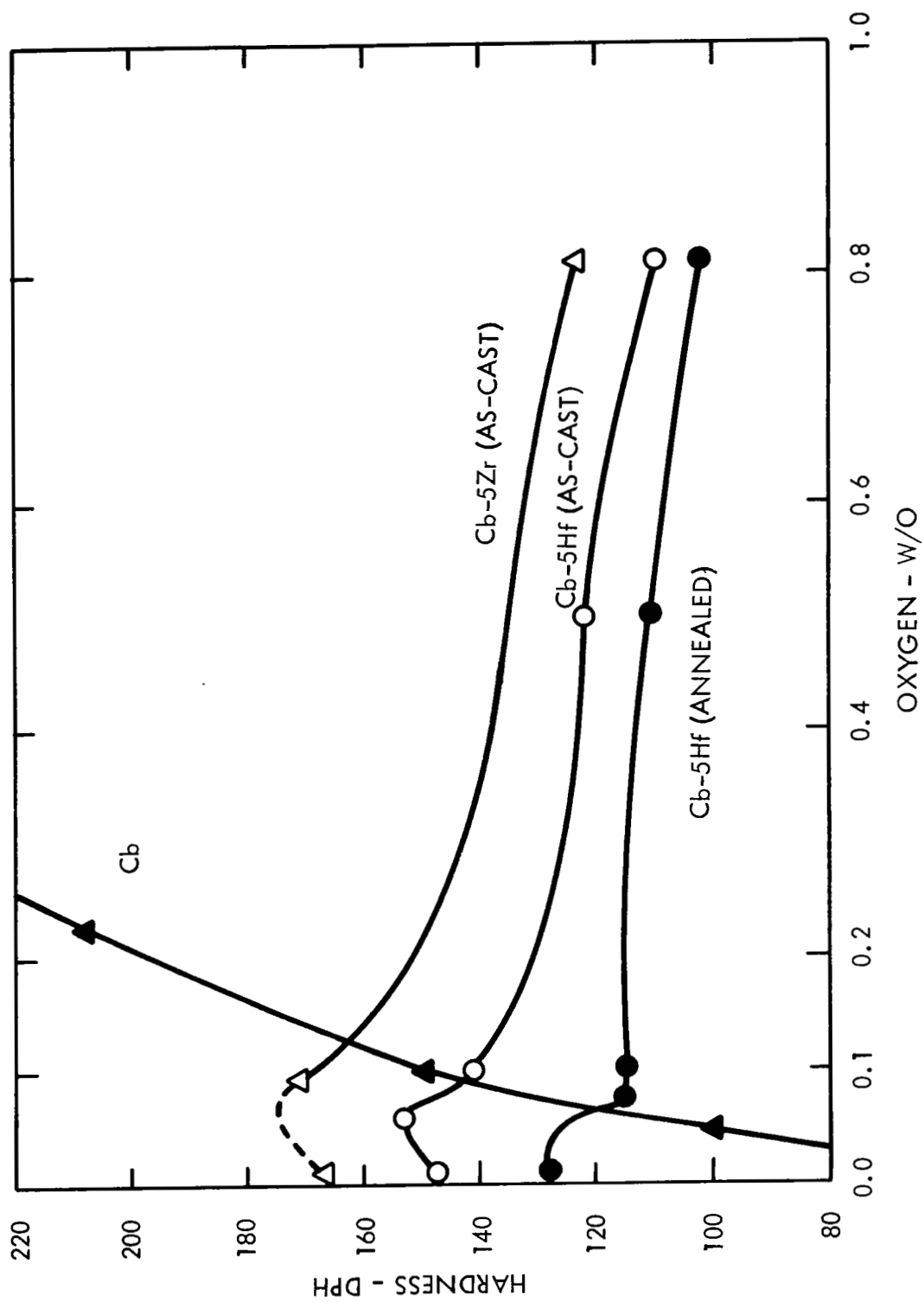


FIGURE 7 - Effect of Oxygen on the Hardness of Cb-Hf and Cb-Zr Alloys

additional oxygen would be expected to again have a potent hardening effect on the matrix. Weld metal would be expected to act similarly to the melted and cast specimens.

Under other circumstances, however, interstitial strengthening effects are observed in gettered alloys. Strengthening and strain aging effects have been observed in Cb-1W, Cb-1Zr and Cb-1W-1Zr alloys which were inadvertently contaminated with oxygen. The strength increase was explained morphologically as the formation of very small, (less than 100 Å) coherent zones of zirconium oxides. The maximum strengthening effect was produced at temperatures from 1475°F to 1650°F. At temperatures above 2200°F, the strengthening effects were much reduced and were related structurally to the formation of larger, non-coherent precipitates of zirconium oxides. The precipitation hardening observations were supported by transmission electron microscopy.

### Aging Effects

Oxygen contamination has been related to aging of refractory metal alloys. In a paper presented at the 1961 AIME conference on high temperature materials, Hobson observed oxygen related reactions in aging in Cb-1Zr.<sup>(5)</sup> At the temperature of 1700°F, classical time dependent aging was observed which resulted in an increase in strength and a loss in ductility. A prior treatment for aging was essentially a solution annealing treatment and quench with a minimum solution temperature of 2900°F. In addition, a study of the welding characteristics of Cb-1Zr made by Franco-Ferreira and Slaughter also indicated a weld aging embrittlement problem which was suspected to be related to, and aggravated by high oxygen content.<sup>(6)</sup> A decrease in ductility was observed in welds aged at 1500°F to 1800°F and was most pronounced in high oxygen content material. An overaging heat treatment at 2000°F was effective in preventing aging reactions at lower temperatures, and was suggested as a post weld heat treatment. In both of these studies the precipitation of complex zirconium oxides was suspected as the strengthening mechanism.

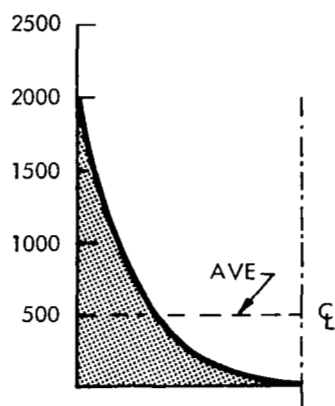
## Oxygen Concentration Gradient

Results in this program, in which oxygen was added by oxidizing the surface followed by diffusion annealing, indicated that oxygen penetration is much slower in "gettered" alloys than would be expected for unalloyed columbium and tantalum. Figure 8 shows oxygen concentration gradients calculated for unalloyed tantalum.<sup>(7,8)</sup> It was estimated that the gradient produced during an 1100°F oxidation process would be eliminated in unalloyed sheet by a 50 hour diffusion anneal at 1500°F. Figure 9 shows experimental measurements made on the tantalum base alloy T-222 following a 50 hour, 1500°F diffusion anneal. The concentration gradient was completely reduced following 50 hours at 2200°F but not at 1800°F. Apparently the reactive alloy additions form stable oxides and reduce the oxygen solubility and diffusion rate in the matrix, effectively retarding oxygen diffusion into the specimen. The oxygen concentrations were determined by mechanically removing thin layers of material and measuring the oxygen content of the remainder by vacuum fusion analysis as shown in Figure 9. Hardness traverse measurements were not reliable in following oxygen penetration, as expected, because of the complex strengthening reactions which occur in gettered alloys. Obviously, contamination and internal oxidation can easily occur in columbium and tantalum base alloys but the total effect of contamination is strongly dependent on alloy composition and thermal history and requires careful assessment.

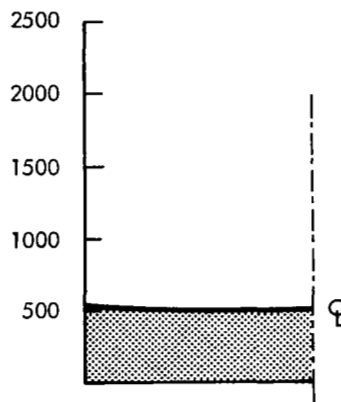
## II. EXPERIMENTAL PROCEDURES

### Oxidation Equipment

This program required the controlled oxidation of 190 specimens 4" long x 1-1/2" wide in such a way so as to simulate in-service contamination. Considerable emphasis was placed on selecting an oxidation technique which would provide controlled oxidation of a considerable quantity of material.<sup>(4,9,10,11,12,13)</sup> Since several specimens were to be oxidized at one time, an oxidation process sensitive to line of sight shielding or collision limited such as low pressure - (vacuum) oxidation, would not provide good uniformity. Of the various methods considered, including vacuum oxidation, anodizing, and modified Sievert's



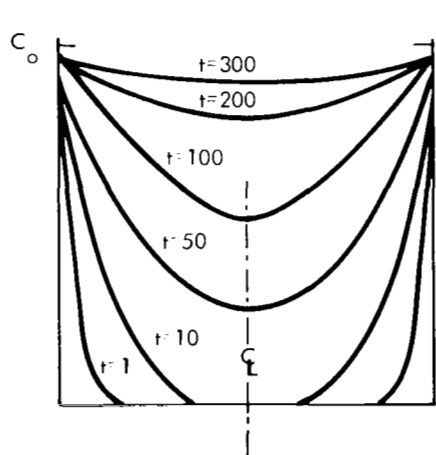
(A) 1100°F - 5 HRS.



(B) 1500°F - 50 HRS.

Calculated oxygen concentration gradients<sup>7,8</sup> in unalloyed tantalum. The 1100°F temperature represents the oxygen contaminating temperature and the 1500°F example represents the lowest diffusion annealing temperature employed in this program.

Diffusion calculations are based on diffusion into a slab from both surface as shown below:



(C) CALCULATED GRADIENTS FOR VARIOUS TIMES, CONSTANT  $C_o$

$$C_{(ave)} = C_o \left[ 1 - \frac{8}{\pi^2} \left\{ e^{-\pi^2 Dt/h^2} + \frac{1}{9} e^{-9\pi^2 Dt/h^2} + \frac{1}{25} e^{-25\pi^2 Dt/h^2} + \frac{1}{49} e^{-49\pi^2 Dt/h^2} + \dots \right\} \right]$$

$$C_{h/2} = C_o \left[ 1 - \frac{4}{\pi} \left\{ \sin \frac{\pi}{2} e^{-\pi^2 Dt/h^2} + \frac{1}{3} \sin \frac{3\pi}{2} e^{-9\pi^2 Dt/h^2} + \frac{1}{5} \sin \frac{5\pi}{2} e^{-25\pi^2 Dt/h^2} + \dots \right\} \right]$$

$D$  = diffusion cons.  $\text{cm}^2/\text{sec}$

$t$  = time, sec.

$h$  = thickness, cm.

FIGURE 8 - Calculated Effect of Annealing on Redistribution of Surface Oxides in Unalloyed Tantalum

# LAYER CHEMICAL ANALYSIS

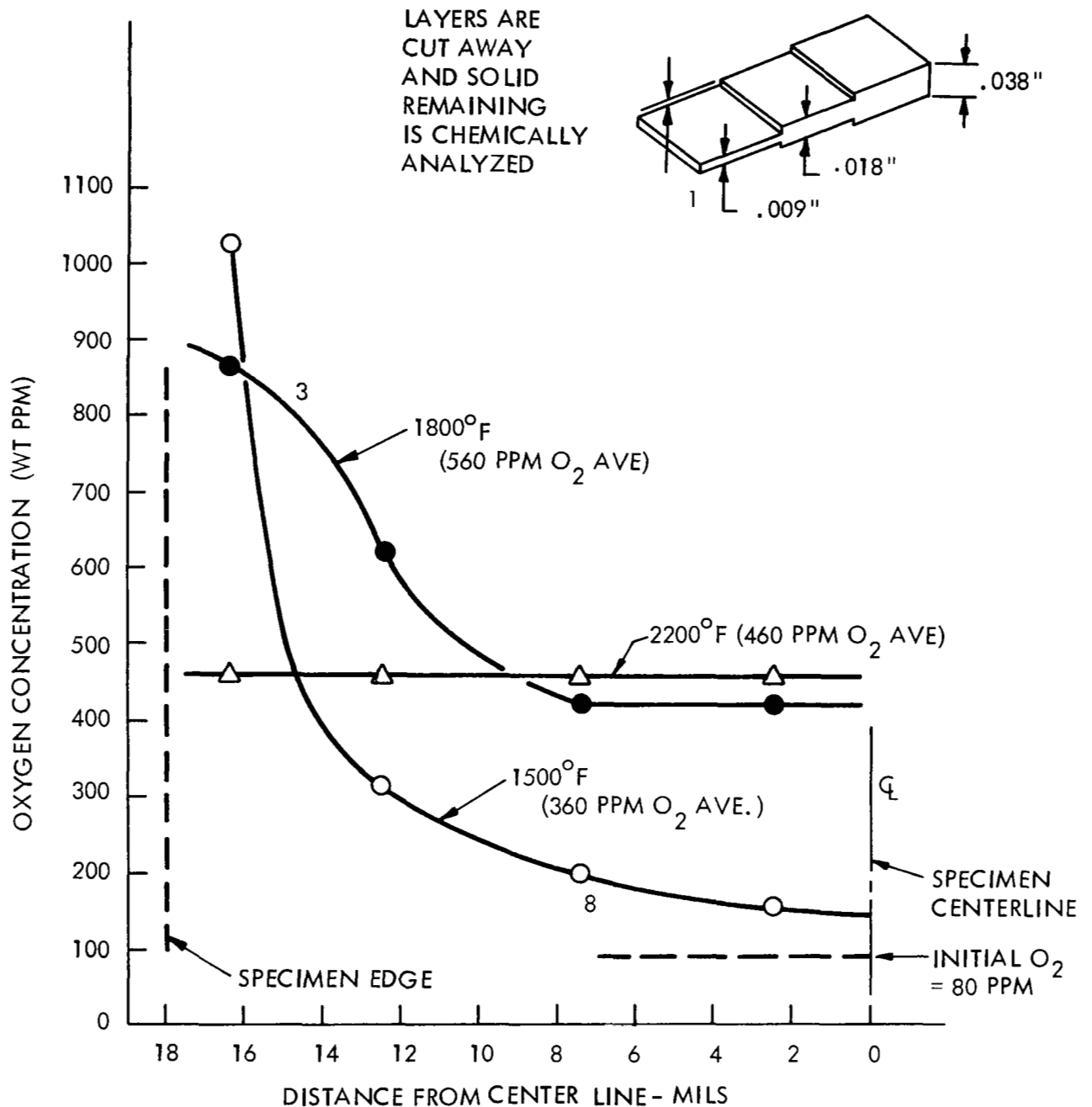


FIGURE 9 - Oxygen Concentration Gradient for T-222 Following 50 Hour Vacuum Annealing



solubility techniques, low temperature oxidation with a low partial pressure of oxygen in helium carrier gas was chosen. This method provided adequate flexibility and control to achieve a uniform surface reaction. The selected contamination parameters, 800°F to 1100°F and an oxygen partial pressure of  $7.6 \times 10^{-2}$  to  $7.6 \times 10^{-1}$  torr, produced an adherent oxide film which was subsequently diffused into the specimen at various temperatures designed to simulate oxygen concentration gradients encountered in service. Figure 10 shows typical specimens in the as-oxidized condition.

In general, about twice as much oxygen as required for the reaction was passed through the chamber. The contamination process was accomplished at slightly above atmospheric pressure using high purity helium gas doped with oxygen from 100 ppm to 1000 ppm. The contamination retort interior fixtures were constructed of stainless steel which formed a passive oxide surface layer during an initial break in period.

Figure 11 is a schematic of the oxygen contamination apparatus. The contaminating gas entered through small diameter tubing arranged in preheater coils and was distributed through a plenum chamber at the bottom of the retort. Baffles were included to limit convection currents and a water cooled baffle was located at the "O" ring sealed junction between the zirconia retort tube and the glass superstructure. Prior to introducing the contamination gas, the chamber was evacuated to  $10^{-6}$  torr and heated to 400°F to outgas the reaction chamber and reduce trace impurities.

### Process Control

Figure 12 is an overall view of the oxygen contamination apparatus. Included in the view are oxygen gages which were used to measure the oxygen content of the exhaust helium carrier gas providing an approximate measure of the reaction rate. Experience from preliminary runs had developed reaction rates at various temperatures and oxidation runs were made based on the calculated time required to achieve a given oxygen level. The time was

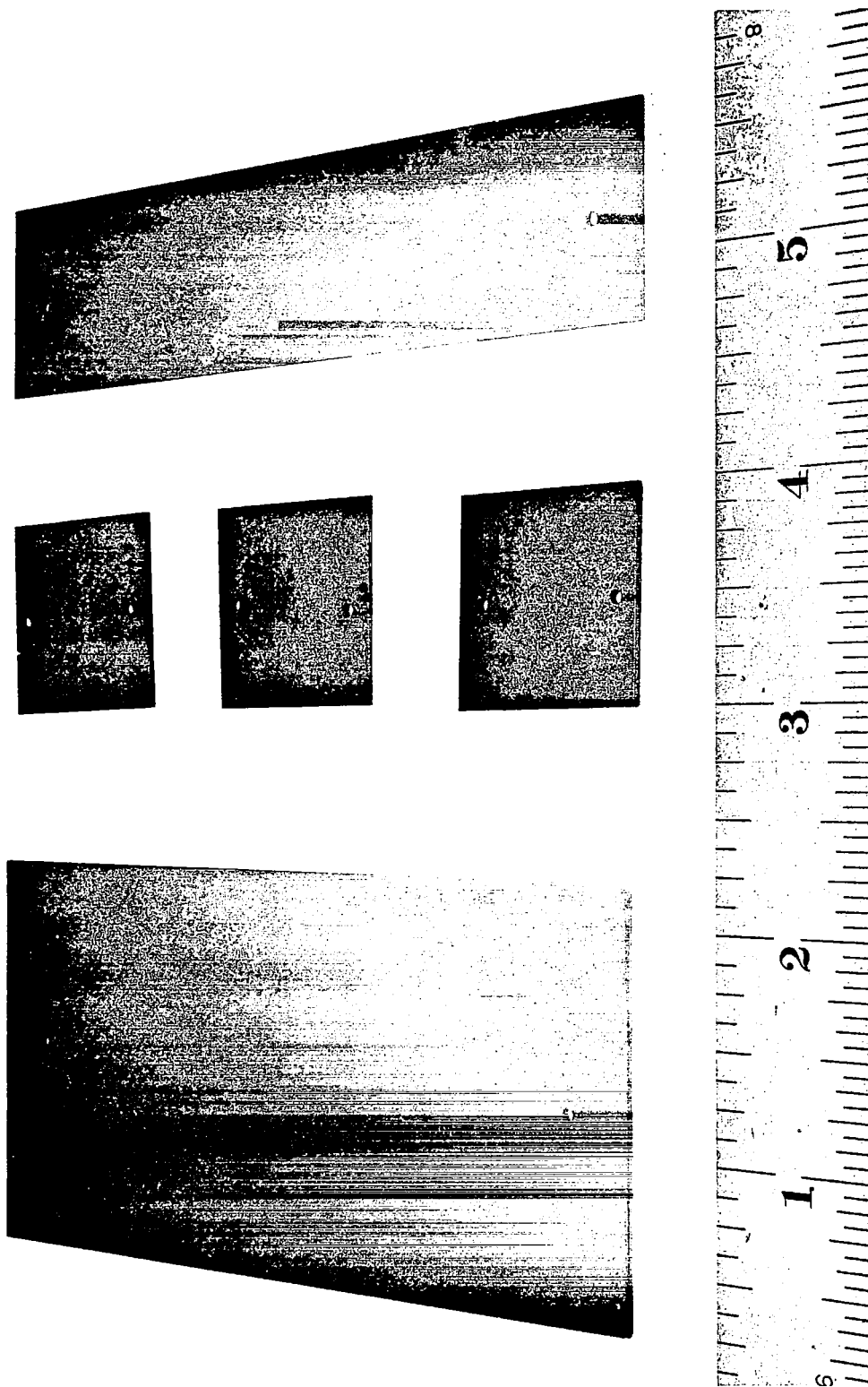


FIGURE 10 - FS-85 Contaminated to 750 ppm Oxygen

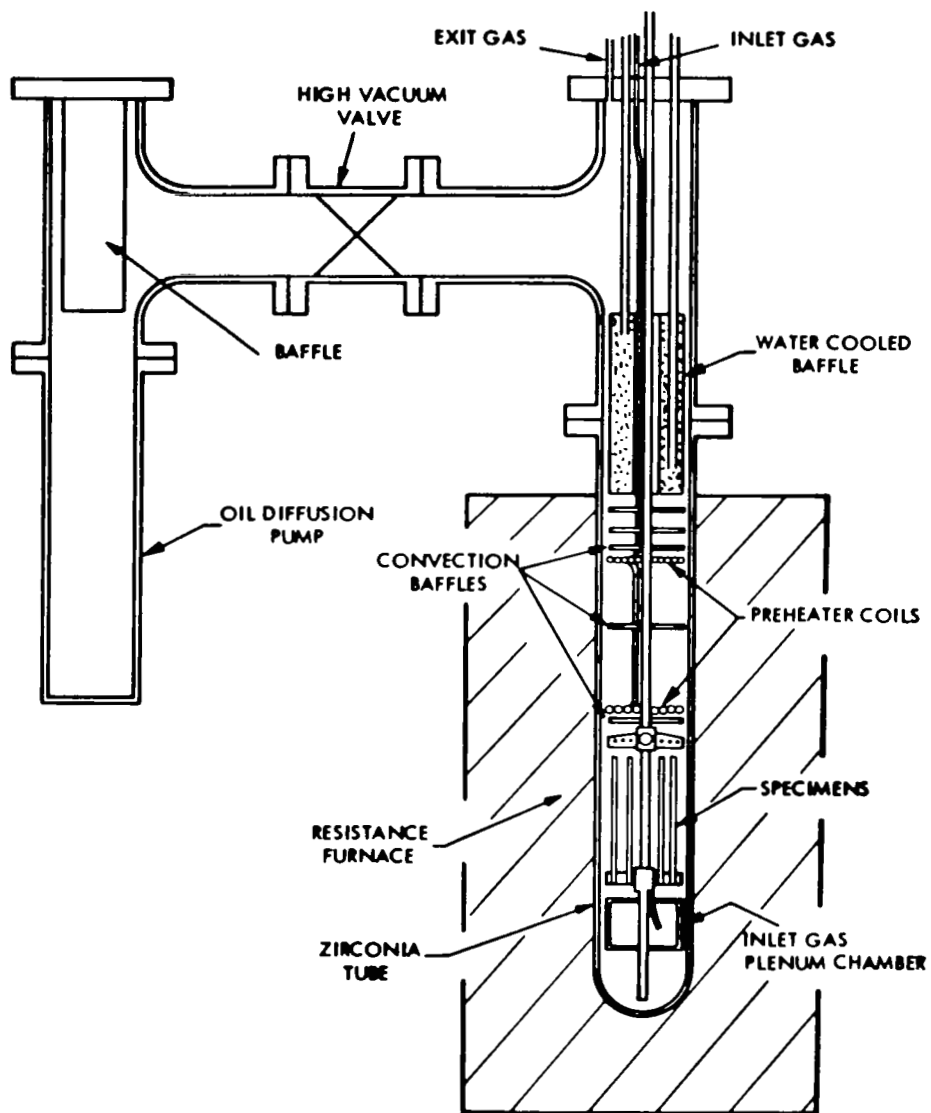


FIGURE 11 - Schematic of Oxygen Contamination Apparatus

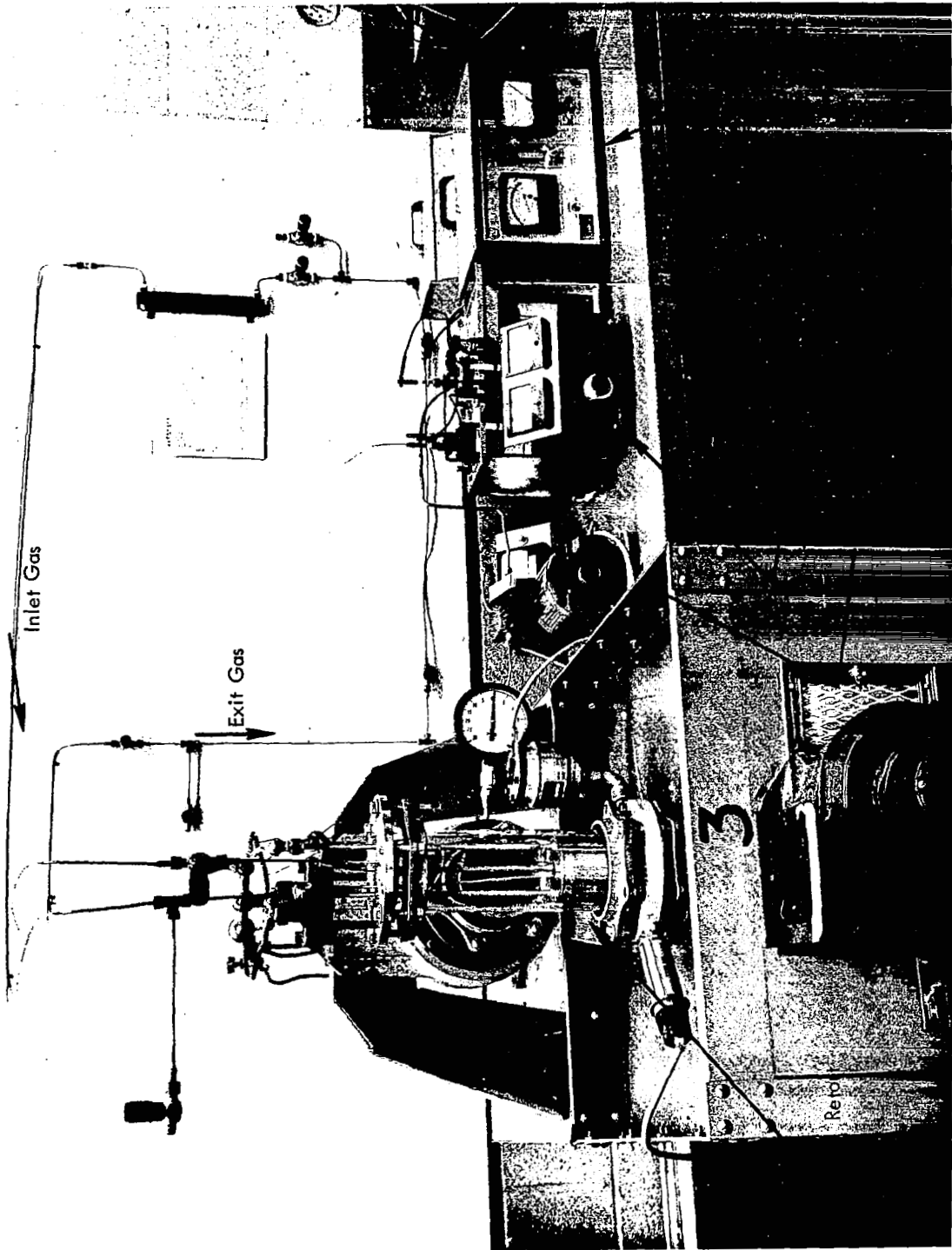


FIGURE 12 - Controlled Oxygen Contamination Equipment

usually estimated on the low side to avoid exceeding the target oxygen contamination level. Specimens which did not meet the required oxygen level were rerun. The parameters used for the contamination of the three alloys are listed in Table 1.

### Verification of Contamination Levels

The achievement of controlled oxygen contamination level from 100 ppm to 1000 ppm was necessary for a successful program. Weight gain was used as the in-process control for oxygen contamination. Although the weighing accuracy was within  $\pm 5$  ppm, weight changes could also be produced by extraneous contamination, such as carbon and nitrogen and chemical analyses were required to verify the weight gain control.

Vacuum fusion oxygen analyses were made on 1/8" square specimen sections without abrading or otherwise removing the surface layer. The exterior surfaces were included in the chemical analysis since an appreciable oxygen concentration gradient was produced and removing the oxygen rich exterior layers would lead to a misleading interpretation. Figure 13 shows the excellent correlation obtained between weight gain and chemical analysis. The two circles for each data point show how the basic weight gain data is added to a value representing the average oxygen content of the as-received material. The complete chemical analyses are presented in Tables 2 and 3. Carbon and nitrogen analyses were made as a check on extraneous contamination and are also shown in Tables 2 and 3. The data indicate a slight increase in carbon content with oxygen contamination level in FS-85. Nitrogen and carbon levels were not significantly affected in the tantalum base alloys, T-111, and T-222. The residual hydrogen content was very low as would be expected following vacuum annealing.

Comparison interstitial chemical analyses were made between the weld and base metal to determine if the welding operation was significantly altering the oxygen contamination level. As shown in Table 4, no significant difference was observed between base and weld metal composition.

TABLE 1 - Oxygen Contamination Parameters

	O <sub>2</sub> Level And Run No.	Ave. Cont.* Rate ppm/hr	Temp °F	Cont.* Time Hrs.	O <sub>2</sub> in He ppm	He Supply Rate cc/min	Cal. From Total Specimen Surface Ave ppm/hr Supplied	Total Specimen Surface Area cm <sup>2</sup>
T-111 Phase II	700-1	8	1000	12	535	100	18	310
	700-4	10	1000	12	535	100	22	257
	700-3	15	1000	45	535	200	25	464
	700-1	12	1000	30	535	200	25	464
	700-2	8	1000	6	535	100	12	464
	500-1	21	1000	22	535	200	25	464
	500-2	18	1000	1	535	200	25	464
	500-1	23	1000	23	535	200	25	464
	350-1	31	1000	2.5	535	450	55	464
	350-2	37	1000	6	535	500	60	464
	350-1	60	1000	6.5	535	500	60	464
	140-1	25	900	2.0	535	450	55	464
	140-2	10	1000	2.5	535	450	55	464
	140-3	25	1000	3.0	535	500	60	464
	140-1	34	900	3.0	535	500	60	464
	140-2	20	900	1.0	530	500	60	464
T-111 Phase I	700-1	27	900-1100	29	1000	300	55	640
	350-1	8	800	24	100	1000	16	640
	350-2	2	840	28	100	1000	16	640
	350-3	5	860	24	100	1000	16	640
	140-1	31	1000	6	535	500	45	640
	70-1	30	900	2.5	535	500	45	640
T-222 Phase I	700-1	32	900-1100	30	1000	300	55	640
	350-1	4	850	26	100	1000	16	640
	350-2	3.5	850	24	100	1000	16	640
	350-3	2.5	840	24	100	1000	16	640
	350-4	11	980	7.5	100	1000	16	640
	140-1	28	950	6	535	500	45	640
	70-1	27	915	3	535	500	45	640
FS-85 Phase I	1000-1	5	780	72	100	1000	27	640
	1000-2	5	780	174	100	1000	27	640
	500-1	7	790	24	100	1000	27	640
	500-2	3.5	790	30	100	1000	27	640
	500-3	1.5	780	64	100	1000	27	640
	500-4	3.5	790	43	100	1000	27	640
	200-1	4.0	700	50	100	500/1000	13/27	640
	100-1	4.4	700	24	500	200	27	640

\*Contamination

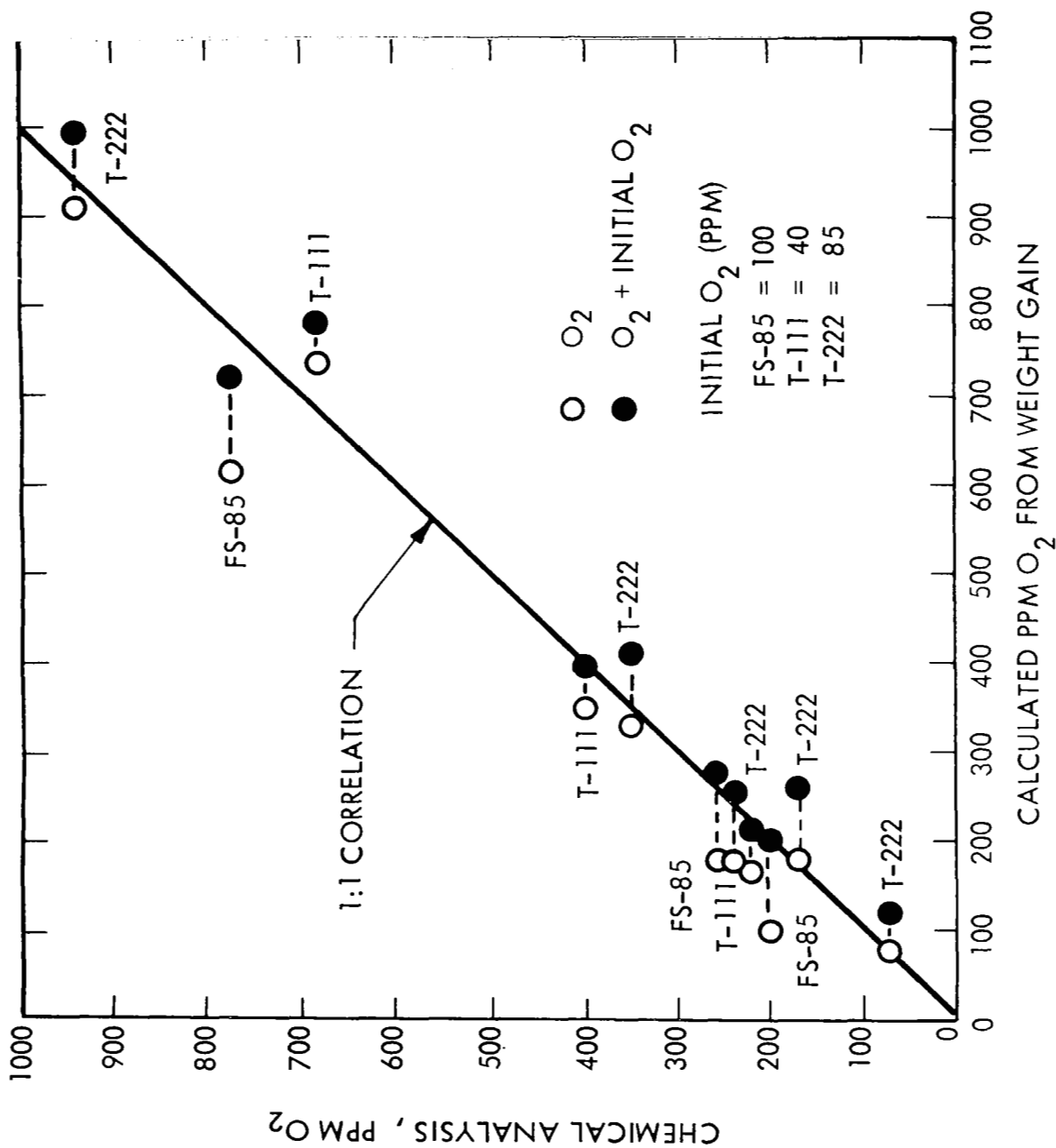


FIGURE 13 - Correlation Between Weight Gain and Chemical Analysis

TABLE 2 – Chemical Analysis of Phase I Bend Test Specimens

Alloy	O <sub>2</sub> Target Level (ppm)	$\Delta$ O <sub>2</sub> WT Gain	Oxygen (PPM)		Nitrogen (PPM)		Carbon (PPM)		Hydrogen (PPM)	
			Specimen	Analy.	Specimen	Analy.	Specimen	Analy.	Specimen	Analy.
FS-85	As Recd. 100 200 500 1000	100 175 620 830	C3CU-5-L4	110	C3CU-5-L4	36	C3CU-5-L1	24	C3CD-402	.22
			C3C5-6-L2	200	C3C5-6-L2	41	C3C5-6-L3	19		
			C3C2-5-L2	260	C3C2-5-L2	44	C3C2-5-L3	29		
			C3C1-5-L4	780	C3C1-5-L4	35	C3C1-5-L2	45		
			C3C4-5-L1	1170	C3C4-5-L1	36	C3C4-5-L2	99		
	Preliminary Specimens	330 330 330 575 745	C3CD-102	260	C3CD-102	41	C3CD-102	32		
			C3CD-402	310	C3-BL C3GL-1	49 40	C3CD-402	34		
			C3CD-402	310			C3CD-402	33		
			C3-BL	870			C3-BL	60		
			C3GL-1	920	C3GL-1	40	C3GL-1	21		
T-111	As Recd. 70 140 350 700	75 170 350 740	T1CU-6-L2	45	T1CU-6-L2	23	T1CU-6-L3	34	T1CD-303	.14
			T1C4-5-L2	75	T1C4-5-L2	38	T1C4-5-L3	43		
			T1C3-6-L2	220	T1C3-6-L2	31	T1C3-6-L3	39		
			T1C1-6-L1	400	T1C1-6-L1	19	T1C1-6-L2	42		
			T1C2-5-L1	680	T1C2-5-L1	24	T1C2-5-L2	46		
	Preliminary Specimens	110 160	T1CD-101	82	T1-CL	22	T1CD-101	35		
			T1-CL	150			T1-CL	46		
			T1CD-303	210			T1CD-303	36		
	As Recd. 70 140 350 700	175 175 330 910	T3CU-5-L2	77	T3CU-5-L2	5	T3CU-5-L3	115	T1CD-302	.24
			T3C4-5-L1	170	T3C4-5-L1	10	T3C4-5-L2	132		
			T3C3-6-L3	240	T3C3-6-L3	12	T3C3-6-L4	118		
			T3C1-6-L1	352	T3C1-6-L1	2	T3C1-6-L2	124		
			T3C2-5-L1	940	T3C2-5-L1	8	T3C2-5-L2	140		
T-222	Preliminary Specimens	180 175 275	T3-CL	180	T3-CL	10	T3-CL	120		
			T3CD-103	180	T3CD-103	130	T3CD-103	130		
			T3CD-302	275	T3CD-302	120	T3CD-302	120		



TABLE 3 - Chemical Analysis for Phase II

Target O <sub>2</sub> Level	Position	1500°F AGE						1800°F AGE						2200°F AGE					
		O <sub>2</sub>		N <sub>2</sub>		C		O <sub>2</sub>		N <sub>2</sub>		C		O <sub>2</sub>		N <sub>2</sub>		C	
		No.	ppm	No.	ppm	No.	ppm	No.	ppm	No.	ppm	No.	ppm	No.	ppm	No.	ppm	No.	ppm
As Recd. 2TICU	Base Weld	-1 L-2	40	-1 L-2	15	-1 L-2	31	-4 L-1 "-W	39 33	-4 L-1 "-W	15 15	-4 L-1 "-W	36 32	-5 L-3	25	-5 L-3	11	-5 L-3	23
40 PPMO <sub>2</sub> 2TIC2-	Base Weld	-1 L-2	120 125					-4 L-1 "-W	100 130 125					-5 L-3	140 120				
350 PPMO <sub>2</sub> 2TIC1-	Base Weld	-1 L-1	350 395					-4 L-2 "-W	350 290 390					-5 L-1	380 390				
500 PPMO <sub>2</sub> 2TIC3-	Base Weld	-4 L-1	340 452	-4 L-1	12	-4 L-1	37	-2 L-2 "-W	460 440 510	-2 L-2 "-W	21 22	-2 L-1 "-W	28 13	-5 L-1	540 485	-5 L-1	14	-5 L-1	37
700 PPMO <sub>2</sub> 2TIC4-	Base Weld	-3 L-1	700 725					-2 L-1 "-W	810 700 800					-4 L-2	720 790				



## Diffusion Annealing

A considerable amount of vacuum heat treating was required both as part of the controlled oxygen contamination process (diffusion anneals) and also to evaluate the effect of aging. To prevent extraneous contamination, particularly during the 1000 hour aging evaluation, all heat treating was accomplished in sputter ion pumped, high vacuum furnaces. These were fully qualified as described in a previous report.<sup>(14)</sup> The furnaces were operated from  $10^{-8}$  torr to  $10^{-10}$  torr during the heat treatment cycles. The intentionally added oxides were observed to be stable with respect to the high temperature and vacuum exposures as indicated by an absence of gas bursts during aging and annealing. Hence, no loss of oxygen was anticipated or observed. Figure 14 shows the high vacuum heat treatment laboratory.

## Welding

Gas tungsten arc welding was used to evaluate the effect of oxygen contamination on weldability. Automatic bead-on-plate welds were used on all specimens. The welding was accomplished in a vacuum purged inert gas welding chamber using high purity helium. The chamber was evacuated to  $10^{-6}$  torr prior to backfilling and the oxygen and moisture content of the chamber atmosphere was continually monitored during welding. Impurity levels of 1 ppm were obtained upon backfilling and all welding was accomplished below 5 ppm oxygen or water vapor. The equipment capabilities are described in detail in a previous report.<sup>(15)</sup> Figure 15 shows a view of the open welding chamber.

Typical cross sections of GTA welds of the three alloys are shown in Figure 16. These welds were through penetration bead-on-plate welds. The sheet thickness was from 0.035" to 0.037". The material was clamped in a molybdenum faced welding fixture and welded at from 15 to 30 ipm using DCSP in a helium atmosphere. The complete welding parameters are listed in Table 5. These were previously selected for good weld ductility during Task I of this program.



FIGURE 14 - Vacuum Annealing Equipment



FIGURE 15 - Vacuum Purged Welding Chamber

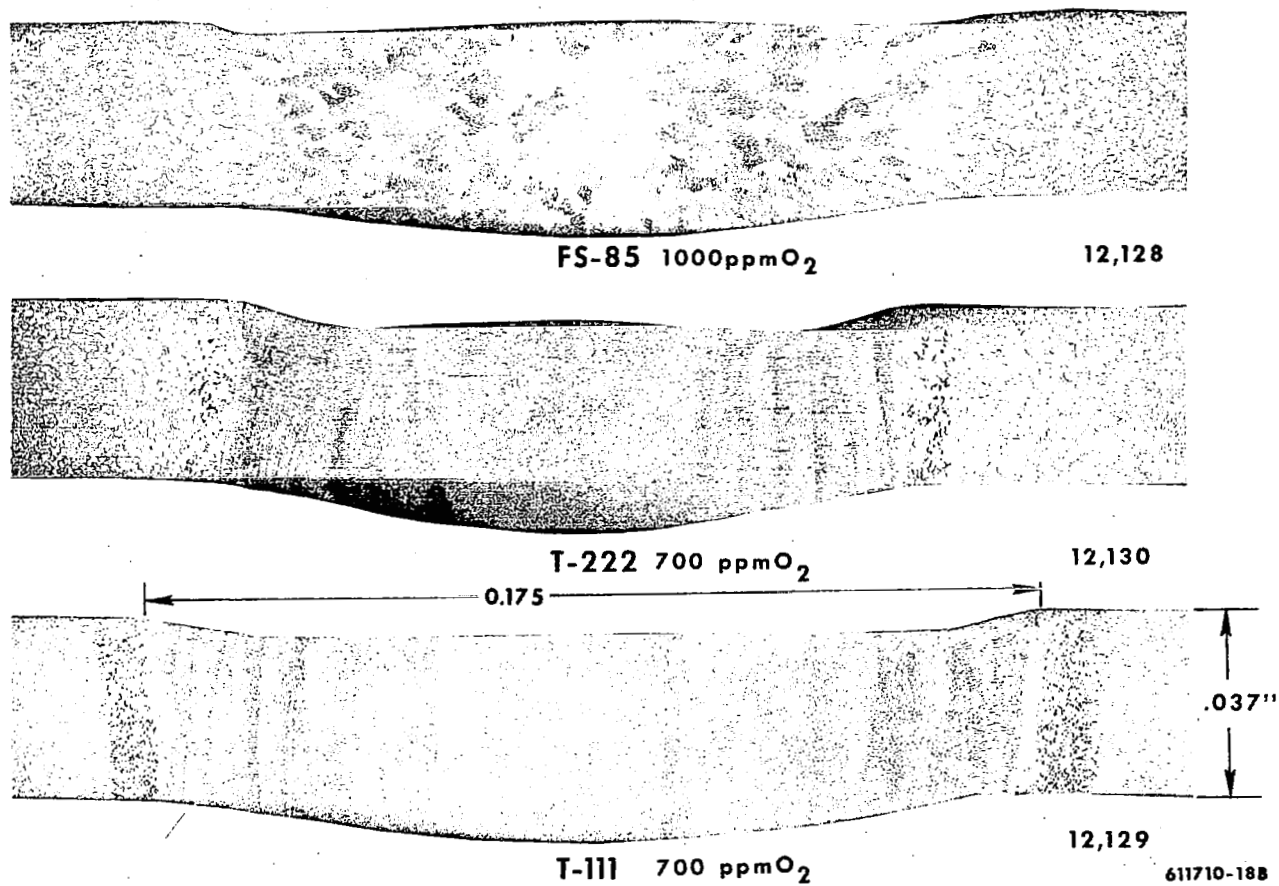


FIGURE 16 - High Oxygen Content Weld Transverse Sections

TABLE 5. WELDING PARAMETERS FOR 0.036" SHEET

Alloy	Speed ipm	Clamp Spacing (in.)	Current Amps	Arc Gap (in.)
T-111	15	3/8	115	0.060
T-222	30	1/4	190	0.060
FS-85	15	3/8	90	0.060

TABLE 6. AS-RECEIVED PRODUCT CHEMISTRY

Composition										Check Chem.		
Alloy	Supplier	Ta	Cb	W	Zr	Hf	C	O	N	C	O	N
T-111 <sup>1</sup>	Wah Chang	Bal.		8.8		2.0	80	50	35	48	15	18
T-222 <sup>2</sup>	Wah Chang	Bal.		9.2		2.55	115	50	20	100	29	10
FS-85 <sup>3</sup>	Fansteel	27.61	Bal.	10.43	0.95		40	40	52	12	98	50

1. Heat No. 6-65042-Ta
2. Heat No. 5.510-65041
3. Heat No. 85D739

## Mechanical Property Tests

Bend Ductility. The basic screening tool for this program was ductility as measured by bend testing. Ductile-to-brittle transition temperatures were defined for particular test conditions as shown in Figure 17. This test provides a sensitive indicator of changes in material structure. The small bend specimen size required enables economical testing of both base and weld metal samples from relatively thin sheet material.

The temperature range of the bend testing apparatus is from  $-320^{\circ}\text{F}$ , liquid nitrogen temperature, up to  $1000^{\circ}\text{F}$ . An infinite range of test temperatures is provided by thermocouples controlled liquid nitrogen cooling from  $-320^{\circ}\text{F}$  to room temperature and electric furnace heating to  $1000^{\circ}\text{F}$ .

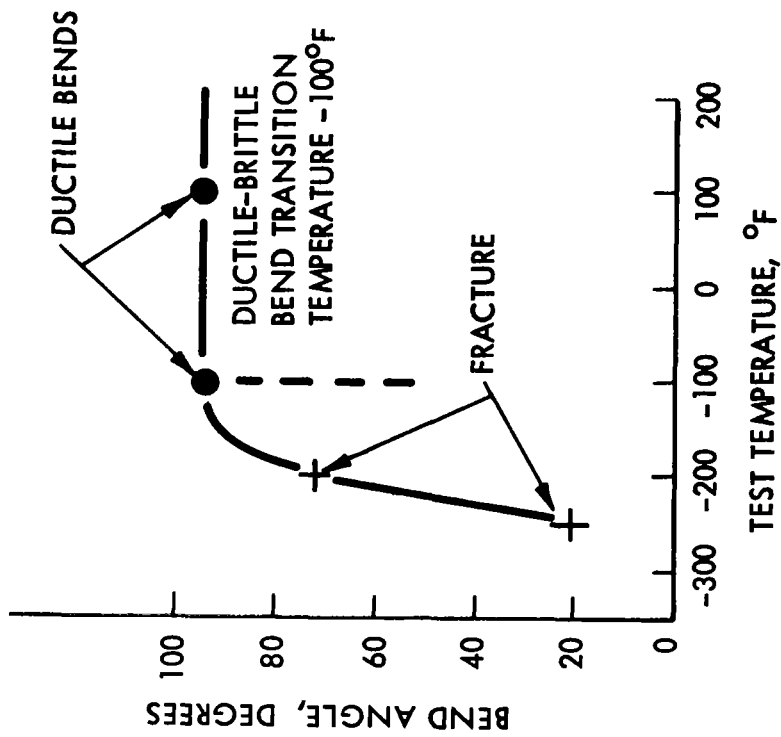
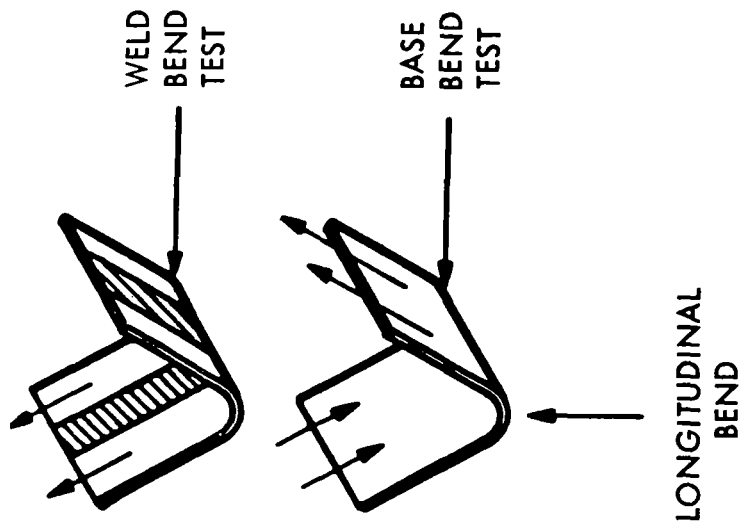
## Tensile Tests

Two types of tensile specimens were used, base metal specimens and transverse weld specimens as shown in Figure 26. To conserve material a gage length 1" long x 1/4" wide was used. Weld specimens were ground flush reducing the thickness from 0.036" to 0.030". Room temperature specimens were tested in air and the elevated temperature specimens were tested in vacuum at  $10^{-6}$  torr. A crosshead speed of 0.05 in/in/min was used.

## Weld Restraint Tests

A circular, bead-on-plate patch test was used to measure the sensitivity to weld restraint. Typical weld problems such as hot tearing, centerline cracking, and poor base metal ductility are exaggerated by the weld strains developed in this test. A 4" square section of sheet material was provided for each test as shown in Figure 18. One specimen was run for each alloy at five oxygen contamination levels. Because of size limitations in the oxygen contamination furnace, the specimens were fabricated by automatic butt welding two 2" x 4" sections. The circular weld and final cross weld were manual gas tungsten arc welds. All welds were made in the monitored, high purity helium welding chamber.

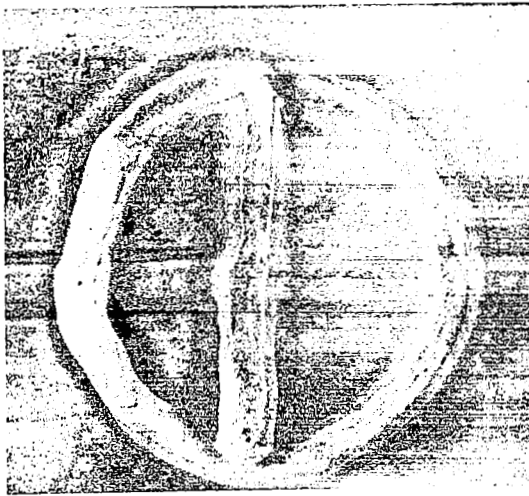




NOTE: ARROWS SHOW ROLLING DIRECTION

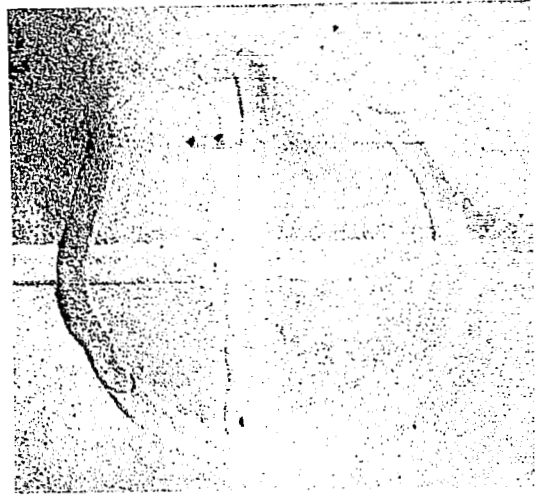
THICKNESS,  $t = 0.035$  INCH  
 WIDTH =  $12t$   
 LENGTH =  $24t$   
 TEST SPAN =  $15t$   
 PUNCH SPEED = 1 IPM  
 TEMPERATURE - VARIABLE  
 PUNCH RADIUS =  $1t$

FIGURE 17 - Bend Test Description



TICU-7-8

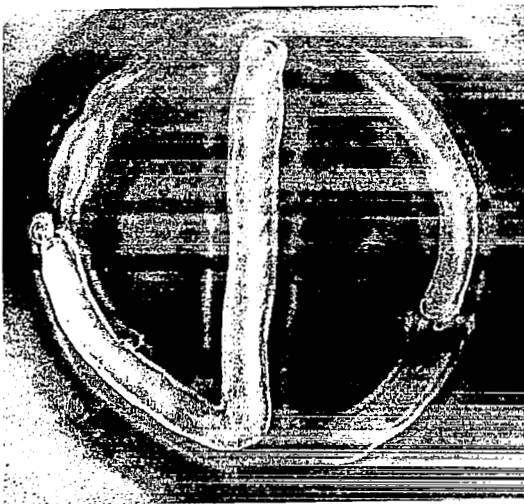
667-5



TICU-7-8

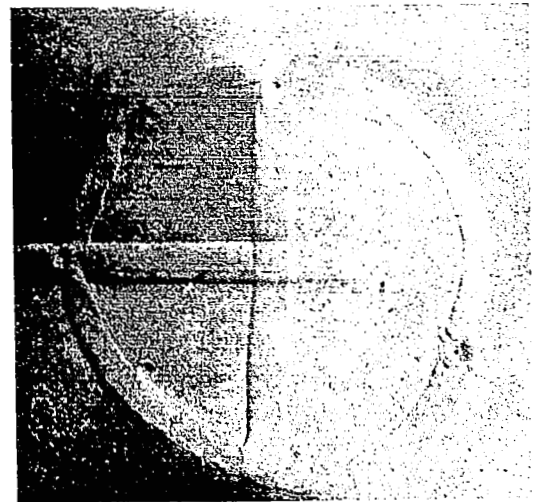
714-9

T-111 As Received



TICI-7-8

668-4



TICI-7-8

714-10

T-111 Contaminated to 335 ppm  $O_2$

As-Welded

Dye Penetrant Inspected

FIGURE 18 - Weld Restraint Patch Tests

### Specimen Preparation

The material was purchased as 0.035" thick recrystallized sheet with an ASTM grain size of 6-8. Table 6 lists the supplier and chemical analysis of the three alloys.

The initial step in specimen preparation was to degrease the sheared to size specimen and pickle in 30%  $\text{HNO}_3$ -30% HF-acid. The specimens were rinsed in distilled water and stored in individual polyethelene bags. The initial weight of the samples was measured in the pickled condition.

Following the initial oxidation step, no surface cleaning, abrasion or pickling operations were used since this would perturb the surface oxidation layer. Further, the specimens were handled with extreme care before the oxidation operation since extraneous surface contamination would affect the oxygen content values calculated from weight gain and perhaps also perturb the local oxidation rate. After diffusion annealing, handling was less critical and degreasing operations were used.

Near the later part of this study an experiment was run using surface abraided specimens. The oxygen contamination rate was much more controllable than that observed on the acid etched specimens. Apparently, the etching operation produces non-uniform passivation of the surface possibly by selectively dissolving hafnium or zirconium. The abrasion technique used consisted of polishing the specimens on 600 grit emery paper immersed in kerosine followed by alcohol degreasing.

## III. RESULTS

### Phase I

The initial phase of the program was designed to measure the effect of oxygen contamination on the as-welded ductility and strength of three refractory metal alloys as outlined in Figure 19 and detailed in Figure 2. The effect of oxygen contamination on the mechanical

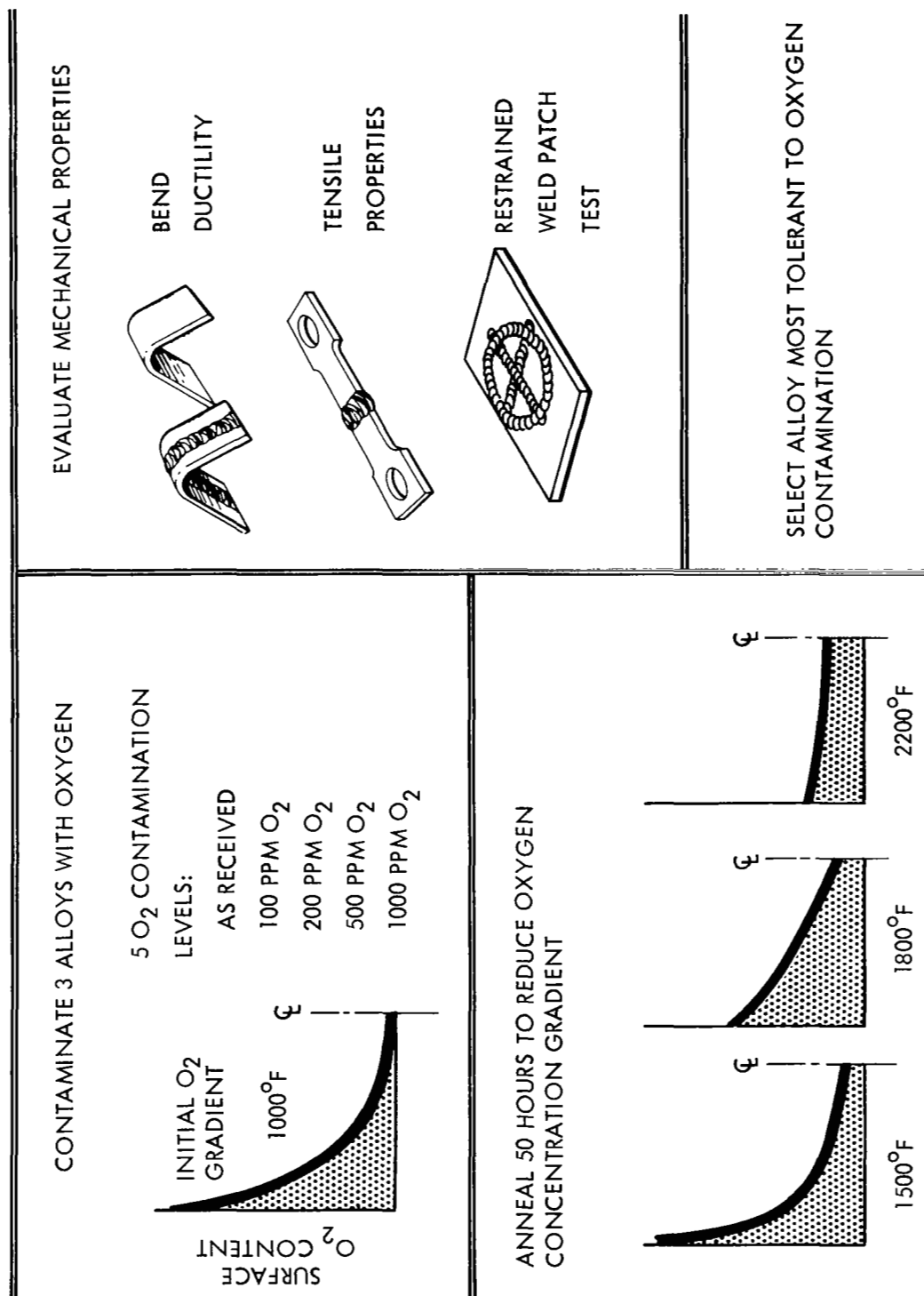


FIGURE 19 - Phase I Program Outline

properties was measured by bend ductility tests, tensile tests, and restrained weld tests. The alloy demonstrating the greatest tolerance to oxygen contamination was selected for extensive evaluation in the second phase of the program.

### Bend Ductility

The bend ductility of both welded and unwelded material proved to be the most discriminating test of the initial screening phase of the program. Figure 17 shows the test specimen design, testing parameters, and interpretation technique.

Following oxygen contamination to the required level, the bend test specimens were diffusion annealed at 1800°F for 50 hours at less than  $10^{-8}$  torr in a sputter ion pumped high vacuum furnace. Specimens selected for the as-received, baseline oxygen level were also vacuum heat treated at 1800°F along with the contaminated specimens to standardize the thermal history of the bend test specimens. A series of welded and base metal bend test specimens was run for each of the five oxygen contamination levels. A comparison of the three alloys at a moderate oxygen contamination level is shown in Figure 20. At this level, T-111 has the lowest ductile-to-brittle bend transition temperature in both the welded and unwelded condition. The target oxygen contamination level for FS-85 is higher, 200 ppm as compared to 140 ppm for T-111 and T-222, to maintain equivalent atomic ppm oxygen levels. Unless otherwise noted, all interstitial levels are reported in weight ppm.

The bend test results for the three alloys are summarized in Figure 21. The data indicate that T-111 maintains a low ductile-to-brittle bend transition temperature at higher oxygen contamination levels than either T-222 or FS-85. FS-85, the columbium base alloy, has a higher transition temperature than either T-111 or T-222 at the as-received oxygen level and although the weld specimens rapidly lose ductility with oxygen content, the base metal remains ductile to high oxygen contamination levels. T-222 rapidly loses ductility in both the welded and unwelded condition.

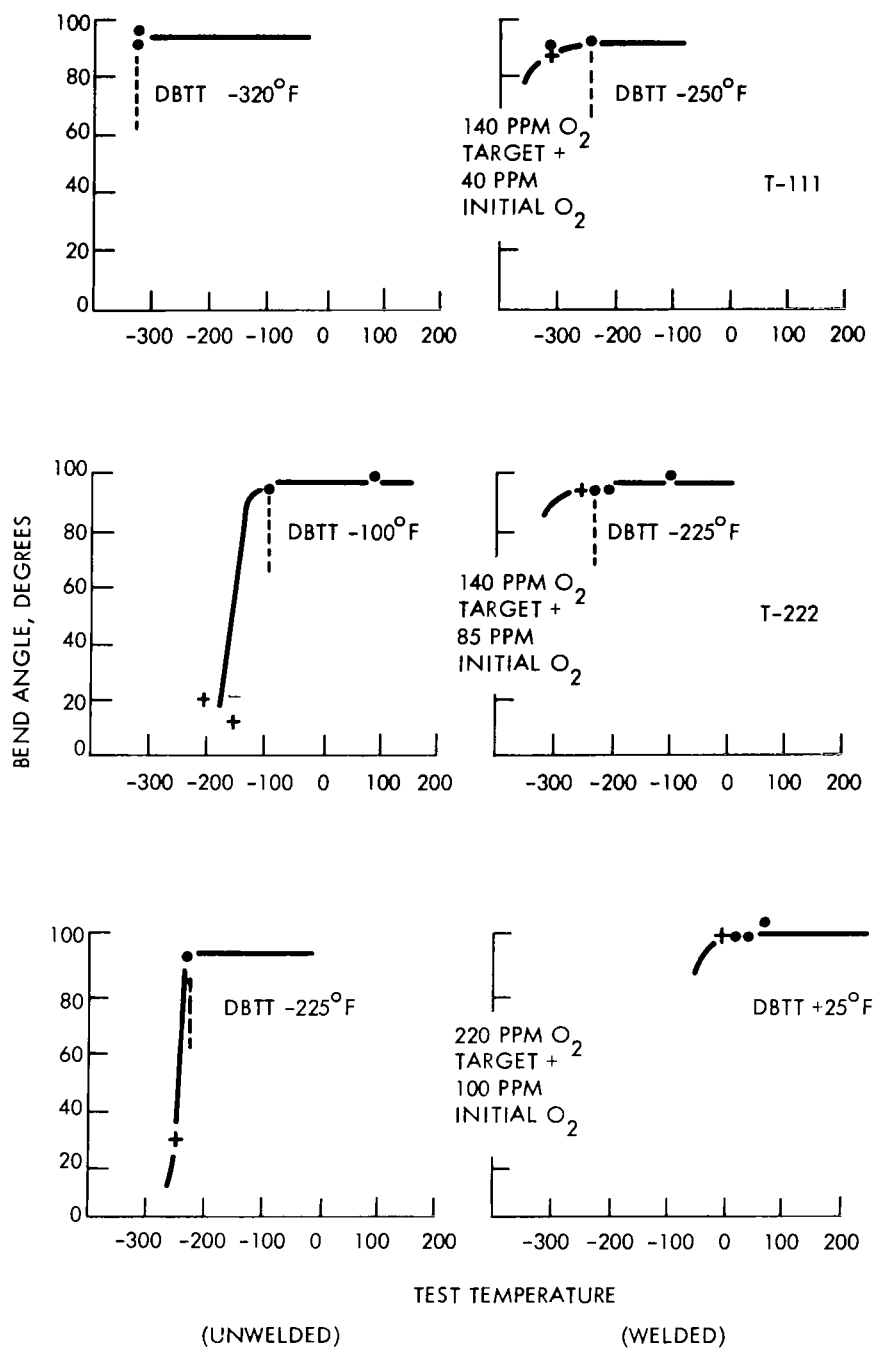


FIGURE 20 - Typical Bend Test Results. Intermediate Oxygen Contamination Levels.

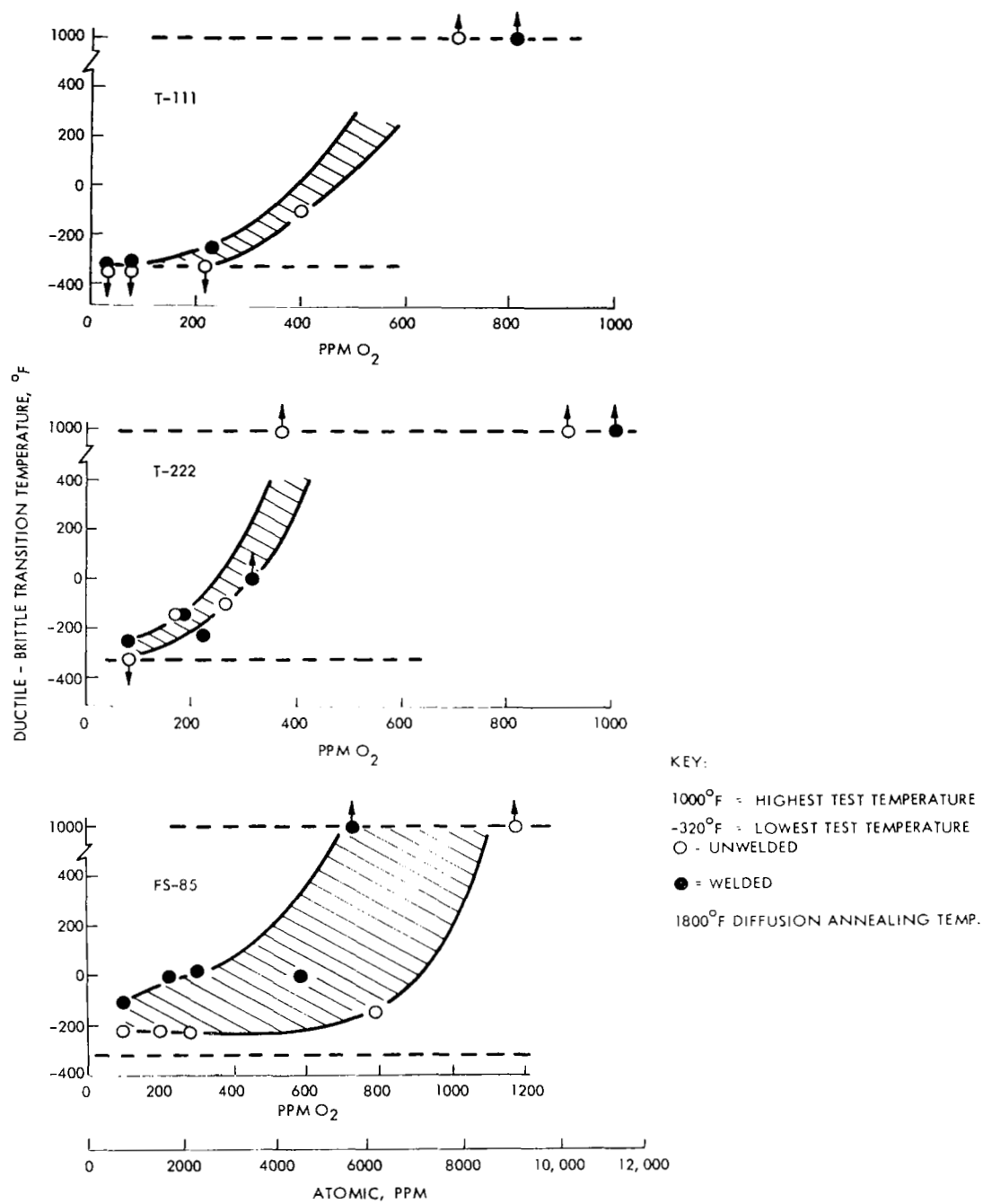


FIGURE 21 - Bend Ductility Versus Oxygen Content for 3 Alloys

## Tensile Properties

Tensile specimens were tested at all five oxygen contamination levels at four test temperatures including room temperature, 1500°F, 1800°F and 2200°F. The specimens were all transverse weld tensile specimens with the weld ground flush. The evaluation was designed to measure the effect of oxygen contamination on weld strength and ductility over a typical hardware operating temperature range. Because the specimen thermal history controls the character and resultant strengthening effects of the oxygen contamination, the specimens were diffusion annealed following oxygen contamination at temperatures corresponding to the ultimate tensile test temperature. An exception was the room temperature group of specimens which were diffusion annealed at 1800°F. As in the preparation of all the specimens in the program, the specimens were welded and tested following the diffusion annealing treatment. The tensile properties are presented in Tables 5, 6, and 7, and in Figures 22 thru 24. In general, oxygen additions produced an increase in tensile and yield strength and a loss in tensile elongation, especially at the lower test temperatures. The loss in ductility is more extreme than indicated by the elongation values. One T-111 specimen and three T-222 specimens failed either during specimen preparation or through the tensile grip hole during the initial load application. The loss in tensile ductility persists up to testing temperatures of 1800°F. At 2200°F all of the alloys except T-222 demonstrated at least 15% elongation at the highest oxygen contamination levels.

All of the transverse weld tensile specimens were wet ground following welding to remove 0.002" from each surface. The uniform cross-sectional area of ground specimens was required for tensile testing. It is possible that this operation may have altered the tensile behavior of the lower temperature specimens since, as was discussed in the background section of this report, a considerable surface-to-center oxygen concentration gradient existed following the 50 hour, 1500°F diffusion anneal. Hence, the effect of surface grinding would be to remove the high oxygen content layers from the 1500°F specimens. The weld and heat affected zones, however, would contain the normal complement of oxygen since the surface



TABLE 7. Tensile Test Properties of T-111 at Five Oxygen Levels

Tensile Test Temp. (°F)	50-Hr. Diffusion Temp. (°F)	Contamination Level PPM O <sub>2</sub>	Calculated <sup>(2)</sup> Total Oxygen Content	Specimen No.	Y. S. 0.2% Offset Psi x 10 <sup>3</sup>	Ultimate Stress Psi x 10 <sup>3</sup>	Elongation %	Fracture Location	Distance From weld Centerline (inches)
Room Temp.	1800	0	40	T1CU-3	75.3	86.6	19.5	Base (1)	1.00
		70	125	T1C4-1	62.7	85.2	14.0	HAZ (1)	0.12
		140	220	T1C3-1	85.3	96.0	9.0	HAZ (1)	0.16
		350	355	T1C1-3	88.5	99.0	3.5	HAZ (1)	0.12
		700	800	T1C2-2	87.6	94.1	2.0	HAZ (1)	0.12
1500	1500	0	40	T1CU-1	38.8	64.0	14.0	Base	0.47
		70	110	T1C4-2	40.9	66.8	14.0	Base	0.35
		140	210	T1C3-4	44.0	70.7	13.0	Base	0.47
		350	380	T1C1-2	50.6	70.6	8.0	Weld	0.05
		700	810	T1C2-1	56.5	72.8	5.0	Base	0.40
1800	1800	0	40	T1CU-4	33.9	57.3	15.0	Base	0.42
		70	110	T1C4-3	35.8	61.4	15.0	Base (1)	0.40
		140	225	T1C3-2	43.5	66.3	9.0	HAZ (1)	0.15
		350	370	T1C1-4	51.6	66.3	7.0	HAZ (1)	0.15
		700	810	T1C2-3	--	58.1	—Failed in Grip Hole—		
2200	2200	0	40	T1CU-2	29.0	42.4	24.0	Base	0.40
		70	125	T1C4-4	29.7	42.0	23.0	Base	0.55
		140	210	T1C3-3	31.8	44.3	22.0	Base	0.45
		350	380	T1C1-1	35.5	46.6	22.0	Base	0.42
		700	810	T1C2-4	41.5	48.9	16.0	Weld	0.01

(1) Heat Affected Zone

(2) Based on weight gain following diffusion annealing and as received oxygen content of 40 ppm.

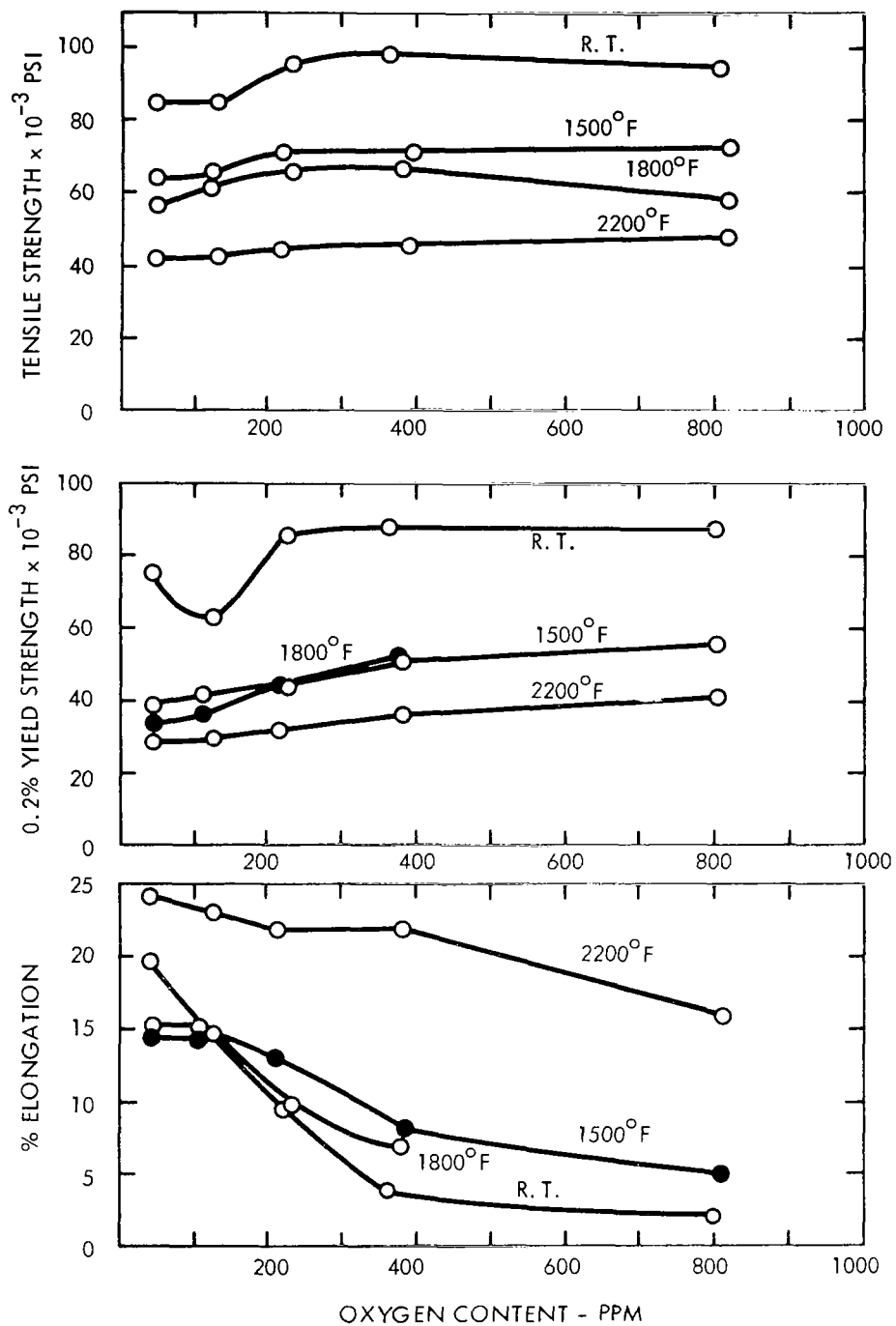


FIGURE 22 - Transverse Weld Tensile Properties of T-111

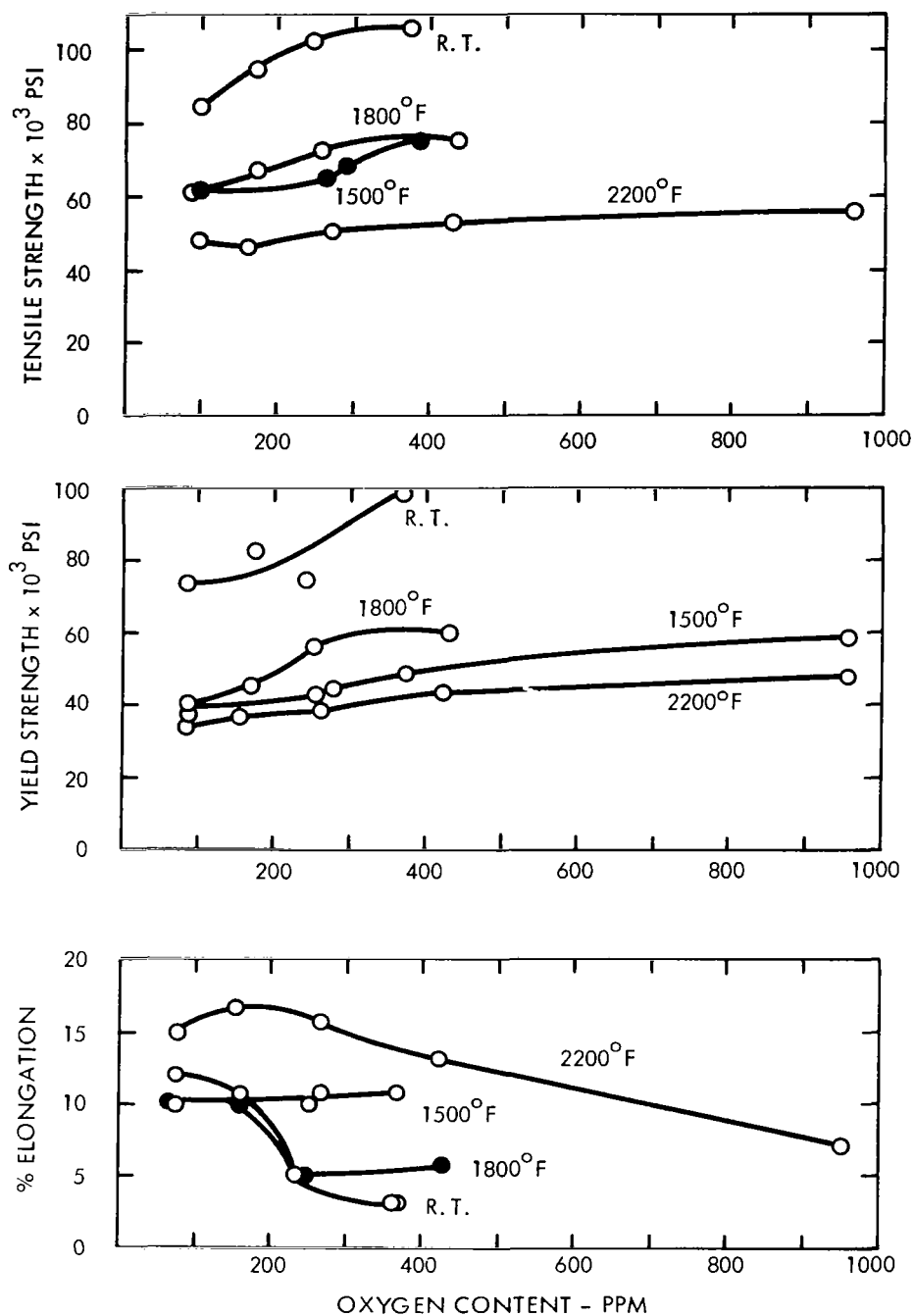


FIGURE 23 - Transverse Weld Tensile Properties of T-222

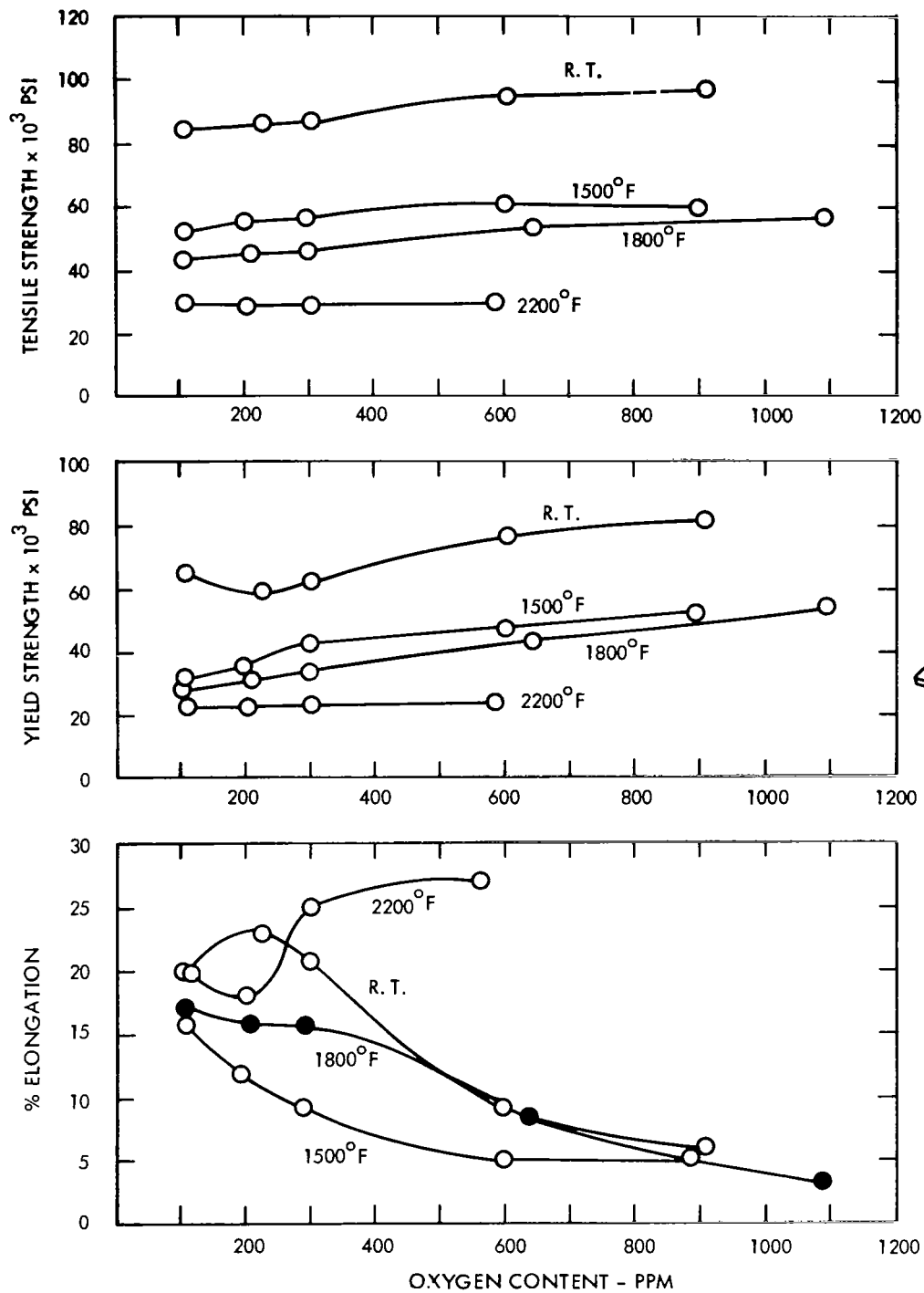


FIGURE 24 - Transverse Weld Tensile Properties of FS-85

oxides would be dissolved and diffused during the welding operation which preceeded the surface grinding operation. Thus, it would be assumed that the weld and possibly the heat affected zones of the 1500°F and 1800°F specimens contain more oxygen and under certain conditions are stronger than the base metal areas. An observation of the chemical analysis of surface ground tensile specimens shows from 10% to 20% oxygen loss for 1800°F and 2200°F specimens. No chemical analyses were obtained for the 1500°F specimens.

The tensile specimen fracture location is noted on Tables 7, 8 and 9. A mixed response in fracture location with oxygen content was observed although the previously described surface grinding may have disguised alloy to alloy and temperature dependent trends. Considering that the oxygen loss due to grinding is minimized at 2200°F, it is important to observe the 2200°F fracture location as shown on Tables 7, 8 and 9 and note that nearly all the tantalum alloy fractures are in the base metal.

A comparison of the 1800°F yield strength of T-111 and T-222 indicates little change from 1500°F. The high oxygen content specimens, especially for T-222, actually show an increase in yield strength from 1500°F. A comparison of previous T-111 and T-222 tensile strength data, shown on Figure 25 indicates a yield strength peak from 1600°F to 1800°F.<sup>(16)</sup> Although similar behavior could explain the strength peak observed in this program, a contributing factor may be that the oxygen contamination has diffused further into the 1800°F specimens than the 1500°F specimens prior to surface grinding thus resulting in a higher oxygen content in the tensile tested condition. The weld and heat affected zones, however would be expected to contain the total oxygen content listed on the tensile test curves. A ductility minimum is associated with the high tensile strength at 1800°F.

Examples of fracture profiles at 2200°F are shown in Figures 26, 27 and 28. The high oxygen content T-111 fracture shows signs of grain boundary sliding which is a normal failure mode for tantalum base alloys at temperatures above 2400°F. At 2200°F, all the fracture



TABLE 9. Tensile Test Properties of FS-85 at Five Oxygen Levels

Tensile Test Temp. (°F)	50-Hr. Diffusion Temp. (°F)	Contamination Level PPM O <sub>2</sub>	Calculated (2) Total Oxygen Level	Specimen No.	Y. S. 0.2% Offset Stress Psi x 10 <sup>3</sup>	Ultimate Stress Psi x 10 <sup>3</sup>	Elongation %	Fracture Location	Distance From Weld Centerline (inches)
Room Temp.	1800	0	105	C3CU-1	64.3	84.5	20.0	Weld	0.04
		100	225	C3C5-1	58.7	86.7	23.0	Base	0.20
		200	300	C3C2-3	60.8	87.7	21.0	Base	0.25
		500	600	C3C1-4	76.6	94.8	9.0	HAZ(1)	0.15
		1000	910	C3C4-1	80.3	96.1	6.0	Weld	0.05
1500	1500	0	105	C3CU-3	31.4	52.1	16.0	Base	0.35
		100	195	C3C5-3	35.4	56.0	12.0	Weld	0.00
		200	290	C3C2-1	41.1	57.7	9.0	HAZ(1)	0.12
		500	600	C3C1-1	47.2	60.0	5.0	Weld	0.00
		1000	890	C3C4-4	50.0	59.7	5.0	Weld	0.05
1800	1800	0	105	C3CU-2	28.9	42.9	17.0	Base	0.37
		100	210	C3C5-2	30.8	45.1	16.0	Base	0.40
		200	295	C3C2-2	33.3	45.9	16.0	Base	0.40
		500	640	C3C1-3	42.4	52.8	8.0	HAZ(1)	0.12
		1000	1090	C3C4-2	52.8	56.1	3.0	HAZ(1)	0.10
2200	2200	0	105	C3CU-4	22.4	29.2	20.0	Weld	0.00
		100	200	C3C5-4	21.9	28.6	18.0	Weld	0.00
		200	300	C3C2-4	22.0	28.8	25.0	Weld	0.00
		500	580	C3C1-2	23.7	29.3	27.0	Base	0.45
		1000	880	C3C4	No test				

(1) Heat affected zone

(2) Based on weight gain after diffusion anneal and as-received oxygen content of 105 ppm.

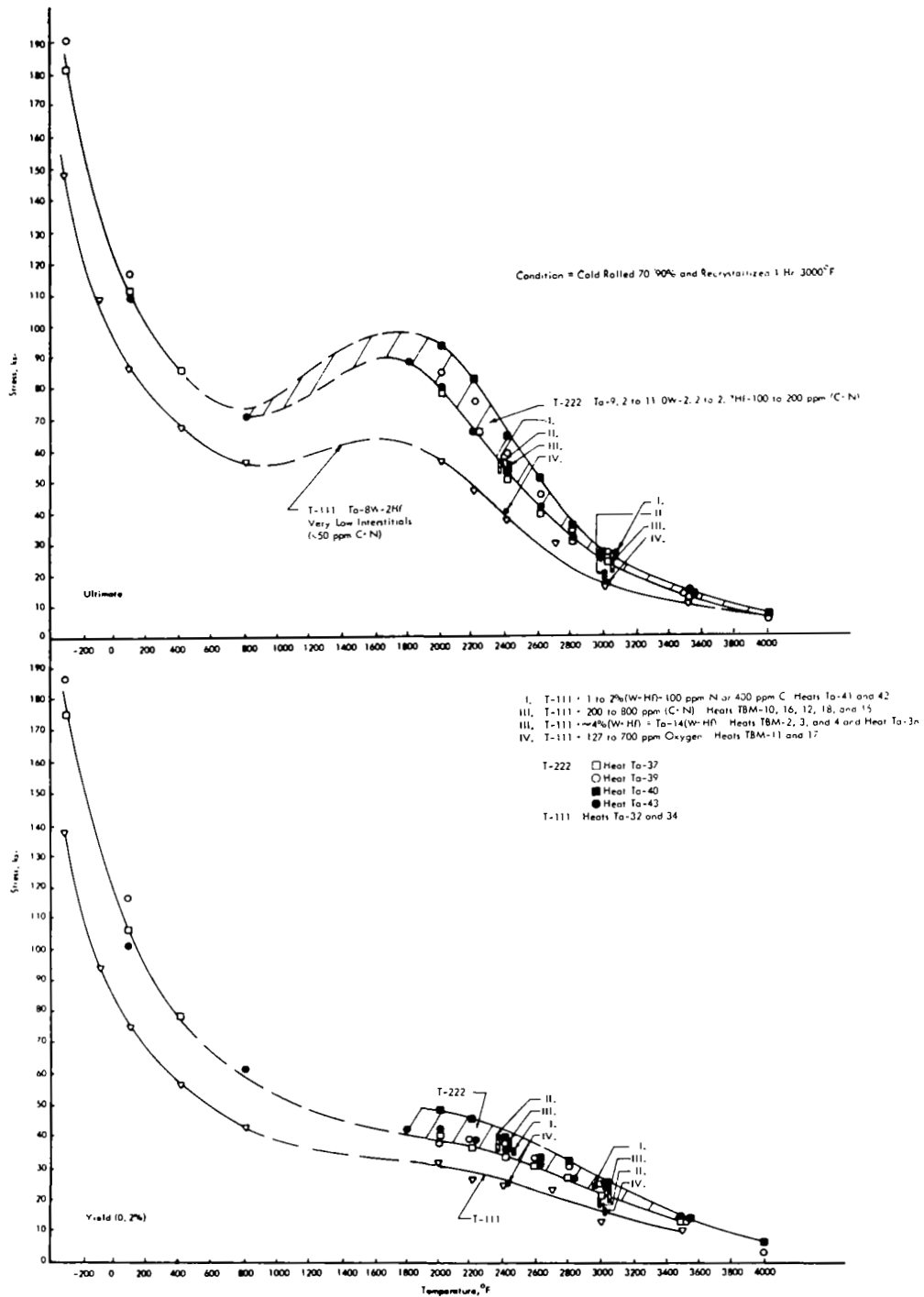
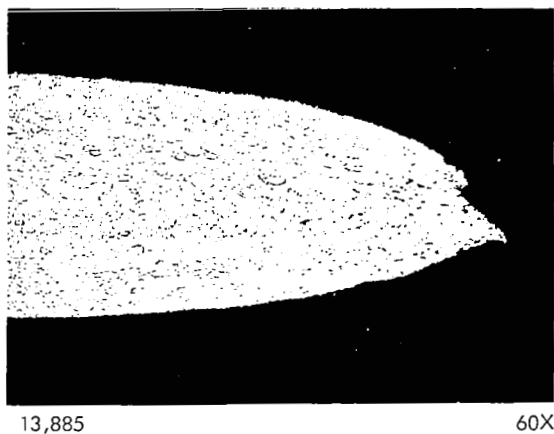


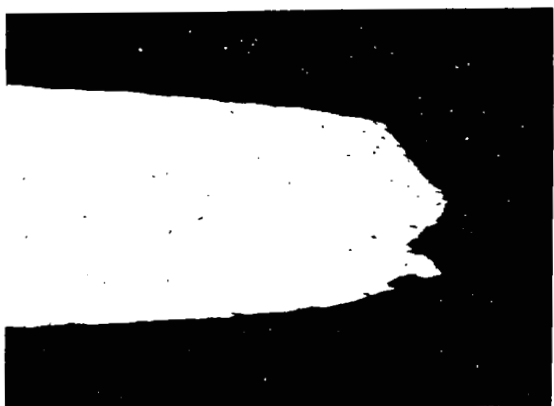
FIGURE 25 - Tensile Properties of Ta-W-Hf-C, N, O Alloys in the Recrystallized Condition as a Function of Temperature





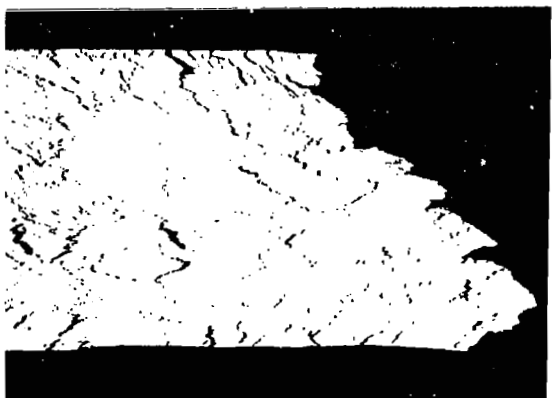
13,885

60X



12,170

60X



13,578

60X



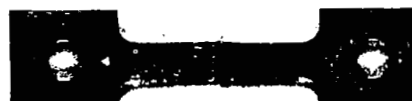
TICU-2

Base Metal Fracture  
Uncontaminated  
40 ppm Oxygen



TIC1-1

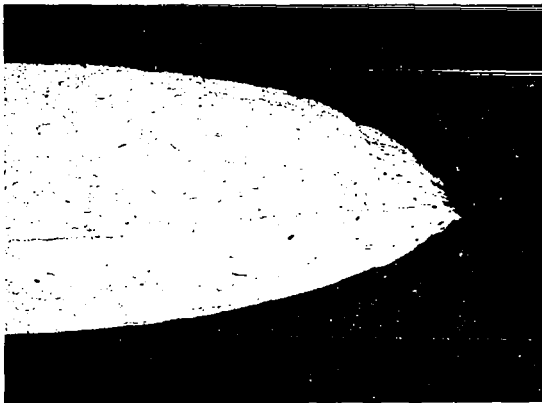
Base Metal Fracture  
380 ppm Oxygen



TIC2-4

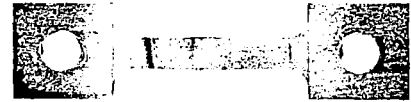
Weld Metal Fracture  
810 ppm Oxygen

FIGURE 26 - T-111, Photographs of 2200°F Tensile Specimens



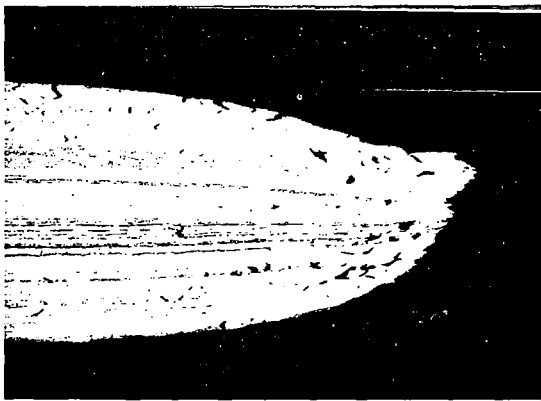
12,171

60X



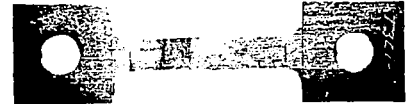
T3CU-3

Base Metal Fracture  
Uncontaminated  
75 ppm Oxygen



12,172

60X



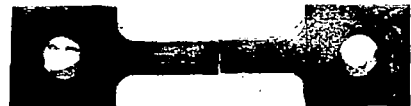
T3CI-1

Base Metal Fracture  
420 ppm Oxygen



13,580

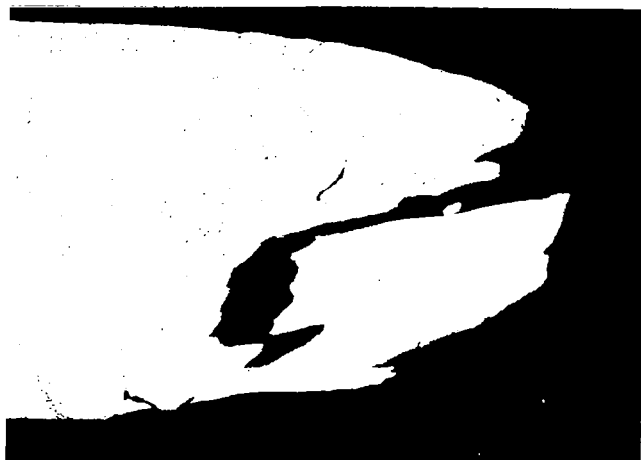
60X



T3C2-4

Weld Metal Fracture  
950 ppm Oxygen

FIGURE 27 - T-222, Photographs of 2200°F Tensile Specimens



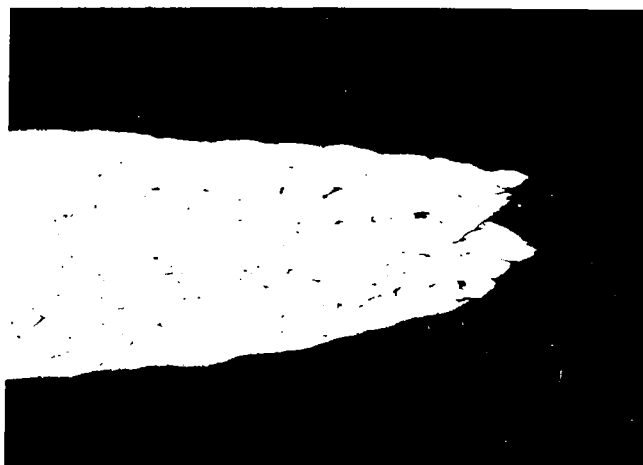
12,167

60X



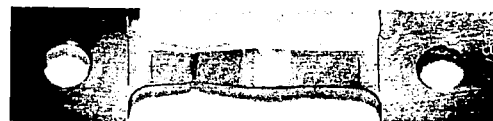
C3CU-4

Weld Failure  
Uncontaminated  
105 ppm Oxygen



12,168

60X



C3CI-2

Base Metal Fracture  
580 ppm Oxygen

No Test  
880 ppm Oxygen

FIGURE 28 - FS-85, Photographs of 2200°F Tensile Specimens

profiles of T-222 have a ductile appearance. An interesting fracture pattern is observed for FS-85, the columbium base alloy in Figure 28. The uncontaminated specimen failed intergranularly in the large grain size weld with a total elongation of 20%. Two of the high oxygen content specimens failed with a greater total elongation, 25 to 27%, and with greater reduction in area in the fracture profile. A possible explanation is that the oxygen contamination restricted grain growth in both the weld and base metal.

### Tensile Test Summary

If the alloys were compared on tensile behavior response to oxygen contamination, FS-85 would be rated marginally better than T-111 on the basis of minimum ductility loss at room temperature and 1500°F. T-222 was markedly brittle at the highest oxygen contamination levels with two of the specimens breaking during machining. On the basis of strength at temperature, however, the ranking order is reversed with T-222 being the strongest and FS-85 the weakest.

All of the tensile specimens were transverse weld specimens, and compared to the published tensile data on these alloys, some of which are shown in Figure 25, the weld material properties are not significantly different from the base metal properties.

### Weld Restraint Test

A weld restraint test in the form of a circular patch was used to measure the effect of oxygen content on restrained welds. Restrained weld tests are used as indicators for hot tearing tendencies during welding or residual weld stress cold cracking tolerances following welding. Figure 18 shows the circular patch test design both as-welded and as-tested with liquid dye penetrant. The restrained weld patch tests were inspected for cracks by dye penetrant inspection and radiography. The results are presented in Table 10. No failures were observed in the patch test specimens indicating that oxygen contamination does not contribute to weld hot tearing or weld, heat affected zone and base metal stress cracking.

TABLE 10. WELD RESTRAINT PATCH TEST INSPECTION RESULTS

			Inspection Results	
Alloy	Specimen	Oxygen Level ppm	Dye Penetrant	Radiograph
T-111	T1CU-7/8	40	✓	✓
	T1C4-7/8	120	✓	✓
	T1C3-7/8	220	✓	✓
	T1C1-7/8	360	✓	✓
	T1C2-7/8	840	✓	✓
T-222	T3CU-7/8	85	✓	✓
	T3C4-7/8	170	✓	✓
	T3C3-7/8	250	✓	✓
	T3C1-7/8	395	✓	(1)✓
	T3C2-7/8	1040	-NO TEST -	
FS-85	C3CU-7/8	100	✓	✓
	C3C5-7/8	200	✓	✓
	C3C2-7/8	275	✓	✓
	C3C1-7/8	645	✓	✓
	C3C4-7/8	950	✓	✓

✓ = CRACK FREE

(1) Initial butt weld was over penetrated and specimen fractured during attempted repair.

## Metallography

Microstructure. The microstructure of the weld interface in the three alloys is shown in Figures 29, 30 and 31. Examples of uncontaminated and the highest oxygen contamination level are shown. All of the specimens were contaminated with oxygen at 1000°F and diffusion annealed for 50 hours at 1800°F prior to welding. One effect of oxygen contamination was to minimize the heat affected zone grain growth during welding. This result is not unexpected based on analysis of Task I data. It was demonstrated in Task I that heat affected zone development was influenced significantly by the quantity and stability of reactive element precipitates. A band of general precipitation in the heat affected zone was produced in the oxygen contaminated tantalum base alloys, T-111 and T-222. Oxygen contamination also had a marked and consistent effect on the weld interface shape as shown graphically in Figure 32. The uncontaminated and low oxygen content welds displayed the typical cross section shown in the top photograph, with the top of the bead being considerably wider than the bottom, while the higher oxygen content welds were nearly of equal width from the surface to the underbead. Two mechanisms are suspected; one being oxide dissociation and consequent oxygen contamination of the helium arc which could produce a more concentrated arc and second, a general decrease in alloy thermal conductivity with increasing oxygen content. The effect was severe enough to produce overpenetration in the high oxygen content T-222 circular patch test.

## Hardness

Hardness measurements were used to help follow changes in material properties, such as in the weld and heat affected zone and to check for point to point variability through the material thickness and weld cross sections. Vickers DPH hardness traverses of uncontaminated and high oxygen level welds are shown in Figures 33, 34 and 35. The traverses were made along the material thickness centerline at 0.030" intervals. A marked strengthening effect of oxygen contamination on the base metal is observed for T-111 and T-222. This effect extends from the base metal into the HAZ. The weld metal hardness shows little change. The columbium



80X

Weld Interface

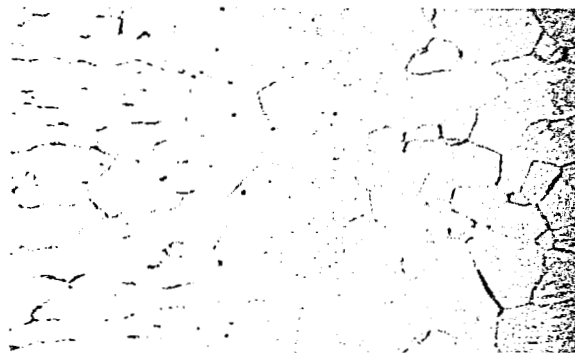


Weld Interface

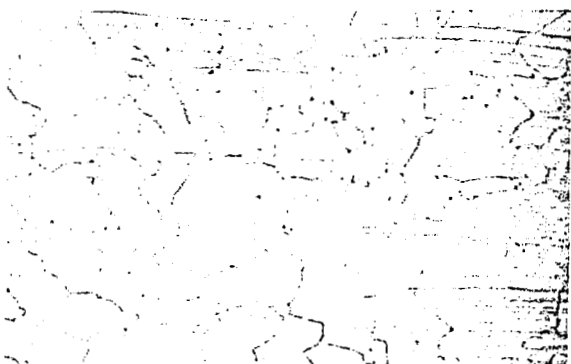


400X

Weld Interface



Weld Interface

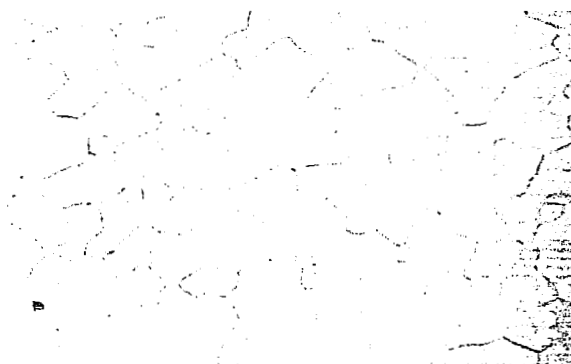


400X

Base Metal

10,942

UNCONTAMINATED

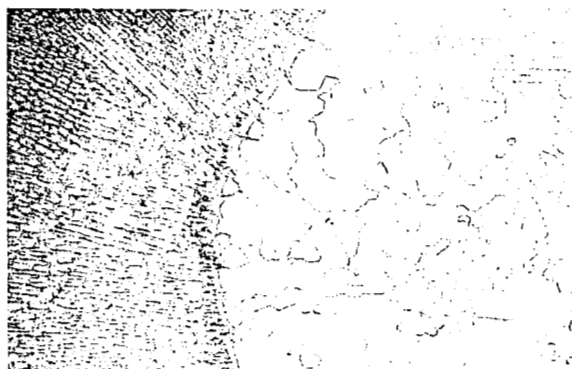


Base Metal

12,129

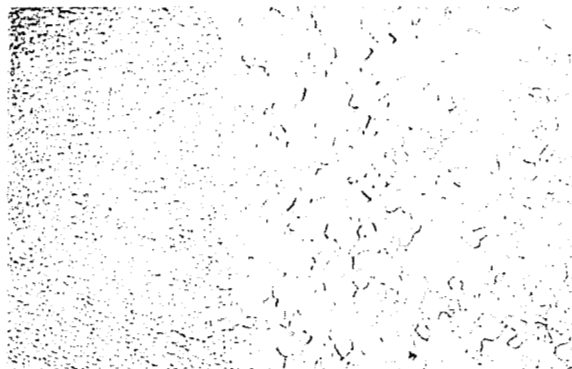
750 PPM OXYGEN

FIGURE 29 - T-111, As-Welded Following 1800°F-50 Hr. Diffusion Anneal



80X

Weld Interface



Weld Interface

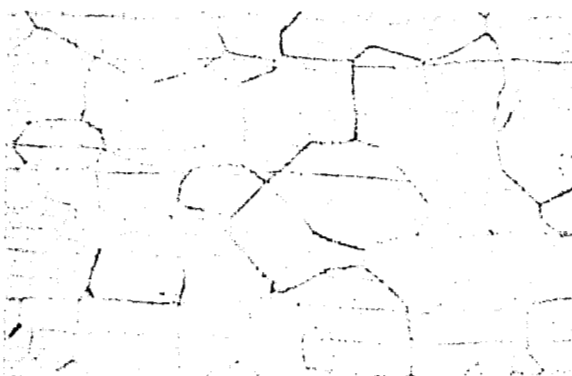


400X

Weld Interface



Weld Interface

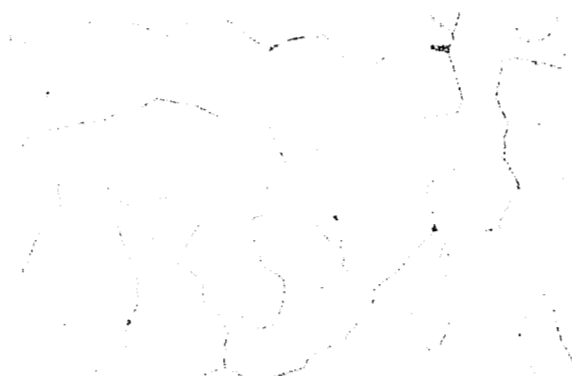


400X

Base Metal

10,943

UNCONTAMINATED



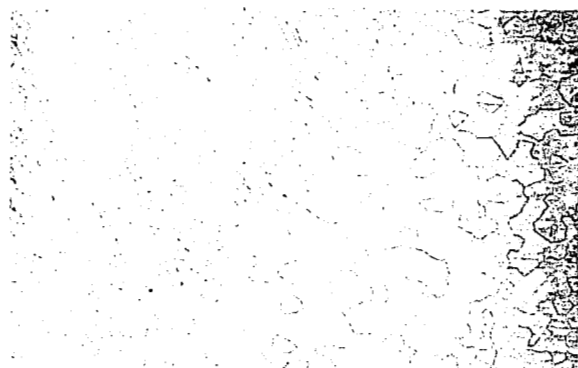
Base Metal

12,130

750 PPM OXYGEN

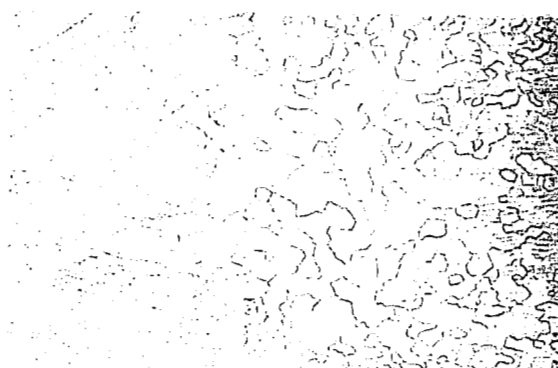
FIGURE 30 - T-222, As-Welded, Following 1800°F-50 Hr. Diffusion Anneal





80X

Weld Interface



Weld Interface



400X

Weld Interface



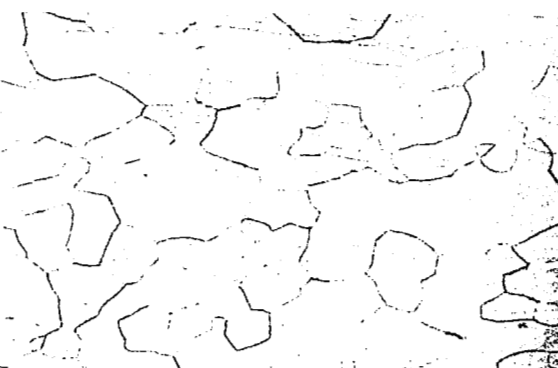
Weld Interface



Base Metal

10,940

UNCONTAMINATED

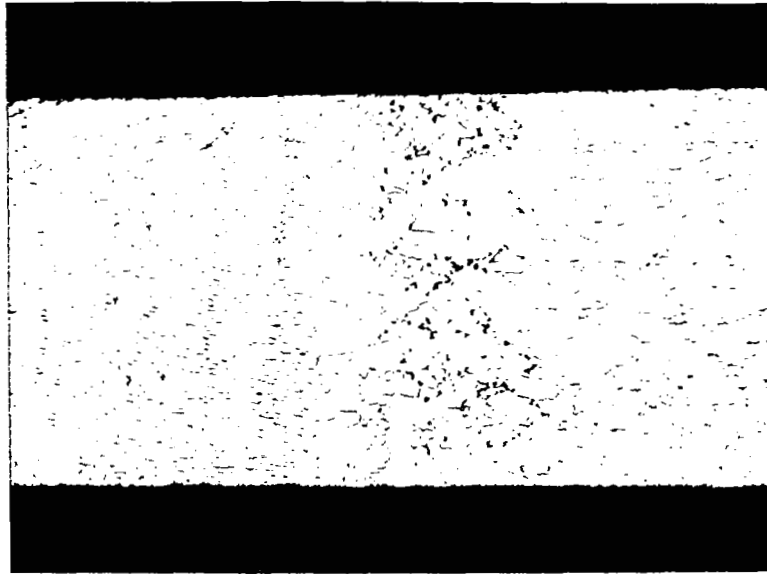


Base Metal

12,128

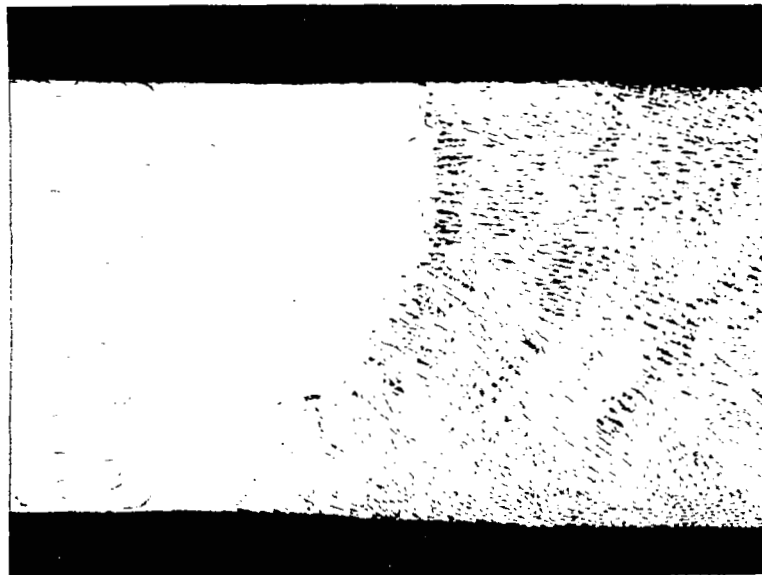
1000 PPM OXYGEN

FIGURE 31 - FS-85, As-Welded Following 1800°F-50 Hr. Diffusion Anneal



UNCONTAMINATED

15,874A



700 PPM  $O_2$

15,872

T-111, AGED 1000 HOURS AT 1500°F

FIGURE 32 - Effect of Oxygen Content on Weld Interface Shape

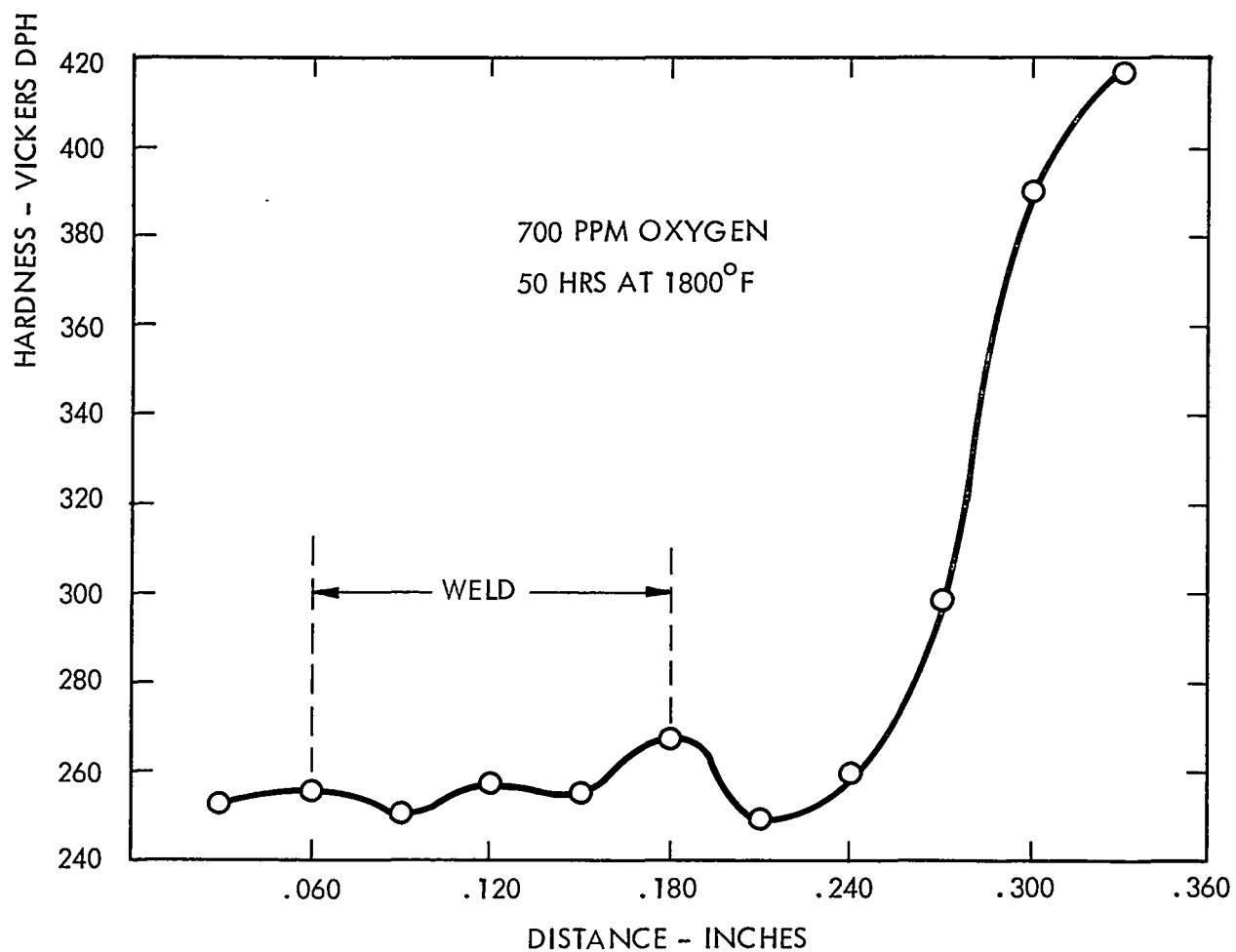
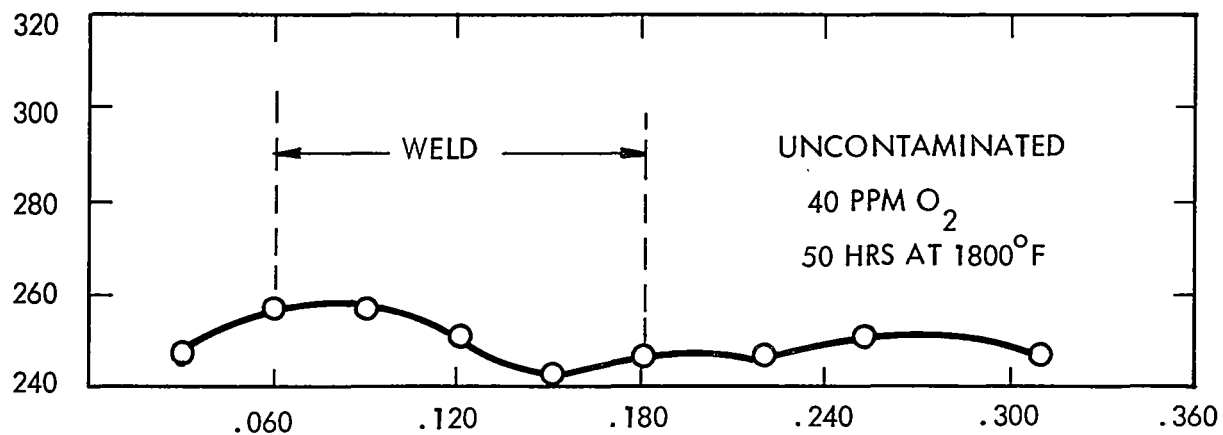


FIGURE 33 - Weld Hardness Traverse of T-111

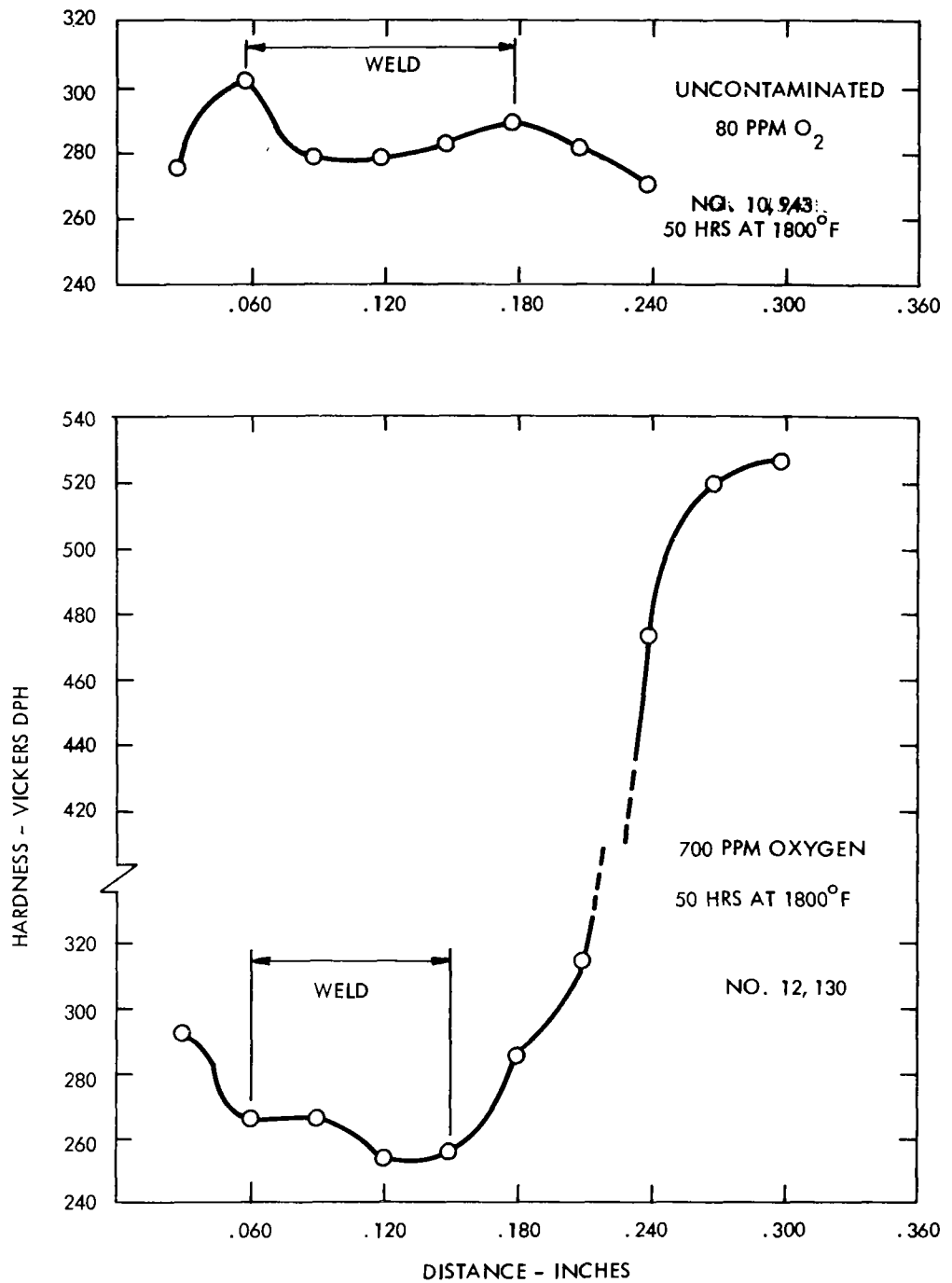


FIGURE 34 - Weld Hardness Traverse of T-222

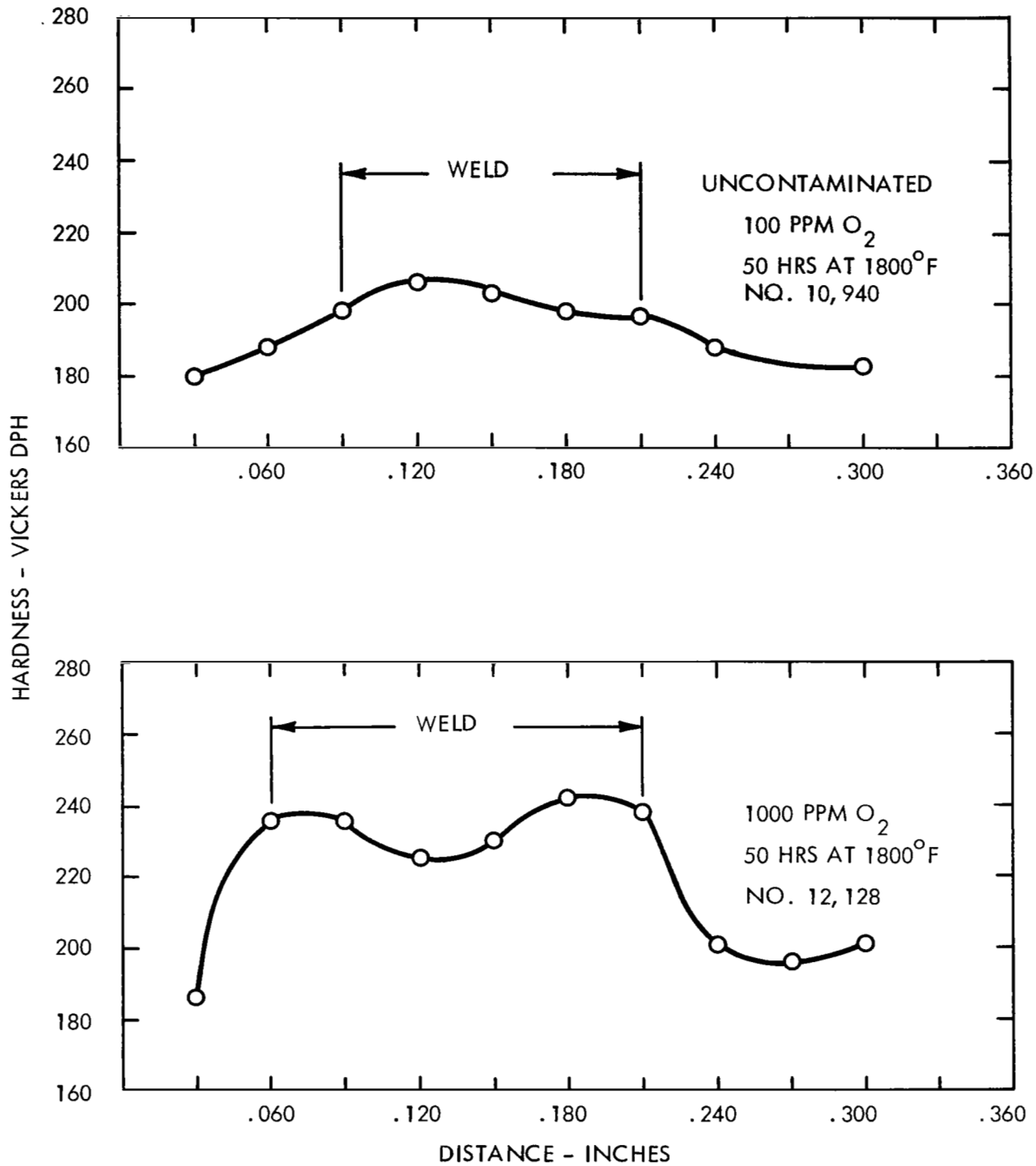


FIGURE 35 - Weld Hardness Traverse of FS-85

base alloy shows the opposite effect in the weld with an increase in weld hardness with oxygen content but no hardness increase in the HAZ. A general rationale based on classic oxygen strengthening mechanisms for gettered refractory metal alloys probably accounts for the observed behavior. In general low temperature internal oxidation produces the optimum size of hafnium or zirconium oxide precipitate for maximum strength. Higher temperature exposures produce an increase in precipitate size, lack of coherency with the matrix, and frequently a corresponding loss of strength. Contaminated weld metal representing melted and cast material should show a slight decrease in strength and hardness because the reactive metal exists as a massive oxide rather than in solid solution. At higher oxygen levels, however, all the available reactive metal addition is combined with oxygen, and further oxygen additions in cast structures will produce strengthening by interstitial solution hardening. This latter condition of supersaturation with oxygen should not be observed at the selected oxygen levels. Hence, strengthening was observed in the FS-85 weld metal which could be construed as anomalous. However, aging may be occurring during the diffusion annealing since this alloy tends to respond to aging much like Cb-1Zr. The 50 hour 1800°F diffusion anneal is comparable to the aging anneals identified for welds and cast metal in Cb-1Zr.<sup>(5, 6)</sup> Although T-111 weld hardness remained about constant, T-222 weld hardness decreased somewhat as could be predicted. Likewise the base metal hardness increases appear to have also been predictable.

The low hardness in Figure 35 for FS-85 base metal results from an oxygen gradient through the sheet thickness. The surface hardness in doped FS-85 is high compared to the centerline hardness as shown in Figure 36 for various diffusion annealing treatments. The weld hardness profile previously discussed represented a 1800°F-50 hour anneal prior to welding which produces a hardness gradient from surface to center of 190 to 290 Knoop hardness (100 gm load). Clearly hardness values do not provide a measure of the oxygen concentration since hardness is sensitive to the competing precipitation and solid solution mechanisms. However, if properly interpreted in terms of the most probable precipitation and strengthening mechanism as described above, hardness traverses proved useful in identifying potential mechanisms of response to contamination.

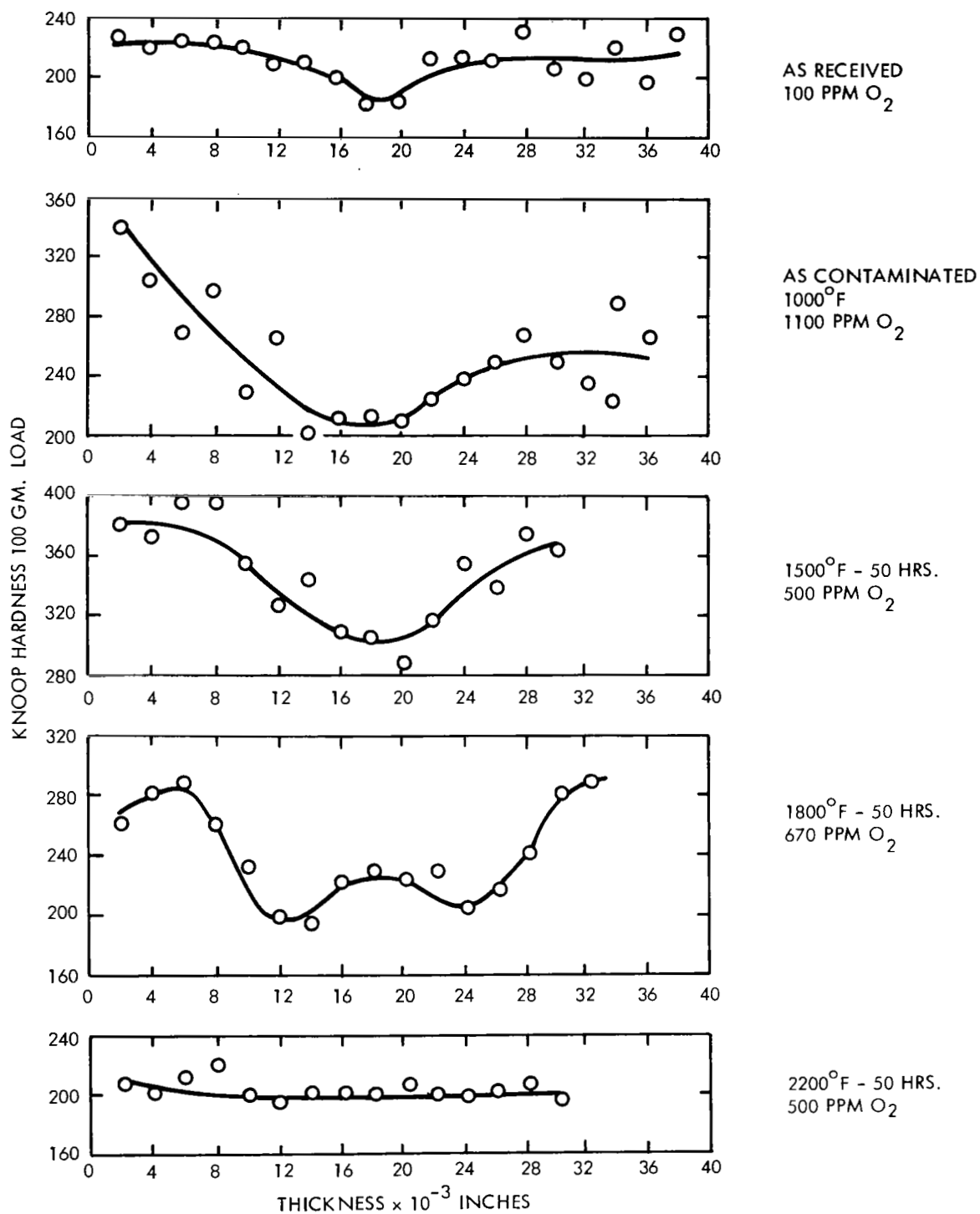


FIGURE 36 - Transverse Hardness Traverses for FS-85

### Effect of Oxygen Content on Hardness

Figure 37 summarizes the change in hardness for weld and base metal with oxygen content. The base metal hardness readings were all made on the material thickness centerline except for FS-85, in which both the centerline and surface hardness is presented. The effect of the oxygen gradient in FS-85 sheet is evident.

### Phase I - Summary

The effect of oxygen contamination on the strength and ductility of base and weld metal has been observed for three refractory metal alloys. A gradual increase in strength and loss in ductility with increased oxygen contamination was observed in this study as expected. The weld metal properties were in general less affected by the oxygen addition than the base metal because of a more favorable oxide morphology. Hence, repair welding per se of contaminated material did not introduce any special problems as compared with the normal deleterious effect of contamination on the base metal. In addition, the restrained weld circular patch tests did not indicate that contamination introduces hot tearing problems or strain induced brittle cleavage.

All three alloys displayed a fair tolerance to contamination. In comparing the three alloys, T-111 showed the least loss in bend ductility, especially in the welded condition, FS-85 maintained the greatest elongation in the tensile tests, and T-222 was the least tolerant to oxygen contamination. Based on these results, T-111 was chosen for more extensive evaluation in the second phase of the program.



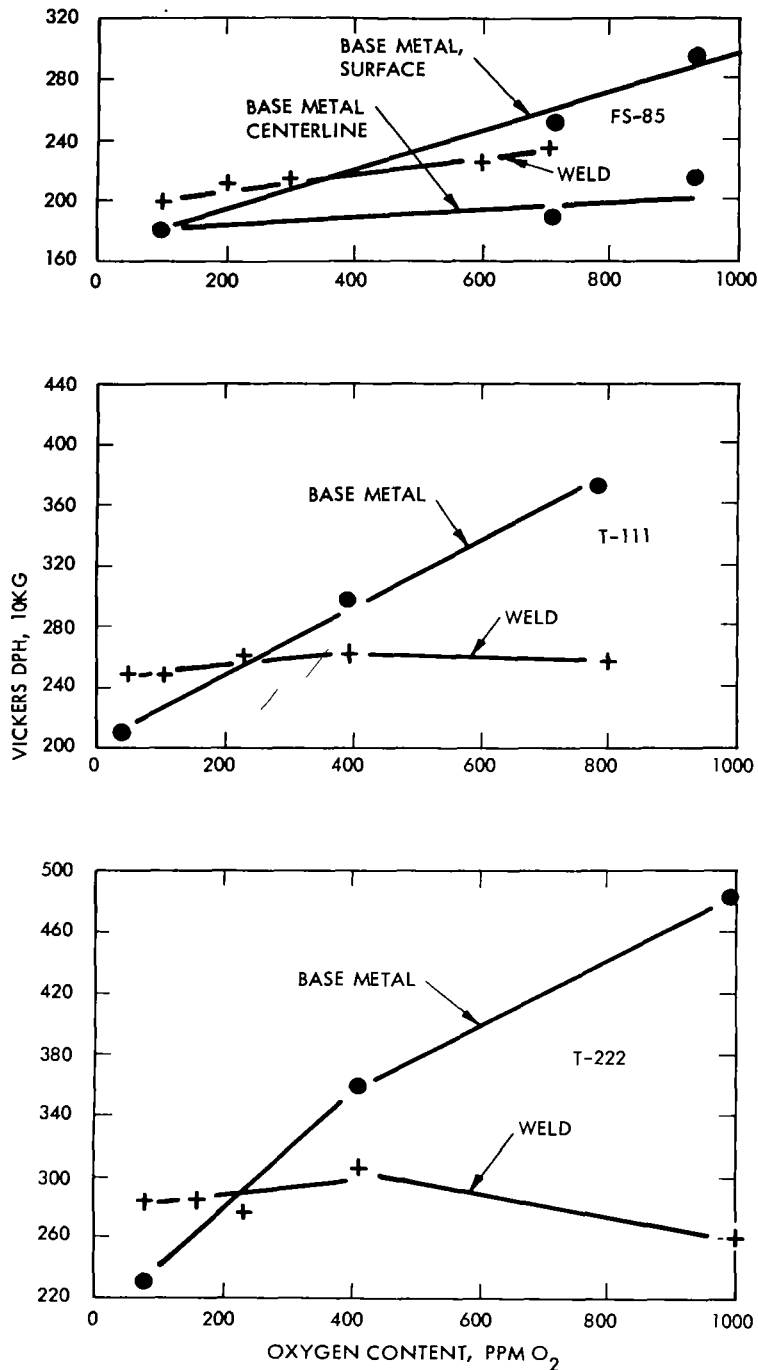


FIGURE 37 - Hardness Versus Oxygen Content for 3 Alloys

## Phase II

The second phase of the program was a more detailed evaluation of T-111 with the emphasis on the long time thermal stability of oxygen contaminated and welded material. Figure 38 shows the overall program outline. A change in the oxygen contamination levels as compared with Phase I was made. An intermediate contamination level of 500 ppm was substituted for the 70 ppm level. This was done to follow the change in bend ductility between 350 ppm O<sub>2</sub> and 700 ppm O<sub>2</sub>.

The alloy response to oxygen contamination was measured by bend ductility tests and tensile tests of material exposed for 1000 hours at three elevated temperatures. Bend tests were run for both welded and unwelded material. The complete specimen and test description is shown in Figure 17.

The oxygen contamination procedure was identical to the one used in Phase I with the parameters listed in Table 1, with the identification shown in Table 11.

## Bend Ductility

Similar to the first part of the program, bend ductility was the primary measure of the material response to oxygen contamination. The initial specimen preparation was identical; low temperature oxidation followed by vacuum diffusion annealing for 50 hours at one of three key temperatures, 1500, 1800 or 2200°F, instead of only 1800°F as in Phase I. The specimens were then welded if required and aged for 1000 hours at the same temperature used for diffusion annealing. All specimens were tested in the aged condition.

Figure 39 is a summary of the 30 bend ductile-brittle transition temperature curves developed for the aged specimens. The figure compares the transition temperature to oxygen contamination level and the obvious trend is an improvement in ductility with increasing aging temperature. Both welded and unwelded material follow the trend which at the 2200°F

(T-111, SELECTED FROM PHASE I)  
CONTAMINATE WITH OXYGEN

ANNEAL 50 HOURS



BASE METAL

GAS TUNGSTEN  
ARC WELD IN  
HELIUM  
ATMOSPHERE

AGE 1000 HOURS

$10^{-8}$  TO  $10^{-9}$  TORR  
HIGH VACUUM FURNACE  
1500°F  
1800°F  
2200°F

EVALUATE MECHANICAL PROPERTIES

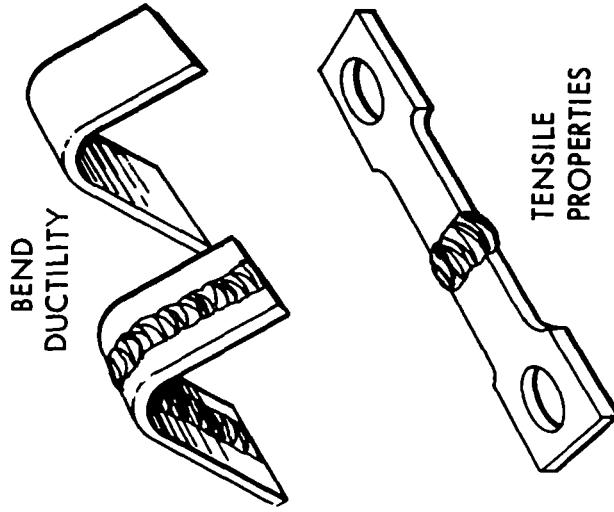


FIGURE 38 - Phase II Program Outline

TABLE 11. OXIDATION PROGRAM PHASE II DIFFUSION ANNEALING SCHEDULE

	1500°F - 50 HRS.		1800°F - 50 HRS.		2200°F - 50 HRS.		Prefix
	Unwelded	Welded	Unwelded	Welded	Unwelded	Welded	
700 ppm	BD-3	BD-6 RT-7 15-8	BD-1 RT-9 18-10	BD-2 RT-11 18-12	BD-4	BD-5 RT-13 22-14	2T1C4
500 ppm	BD-4	BD-3 RT-7 15-8	BD-1 RT-9 18-10	BD-2 RT-11 18-12	BD-5	BD-6 RT-13 22-14	2T1C3
350 ppm	BD-1	BD-2 RT-7 15-8	BD-3 RT-9 18-10	BD-4 RT-11 18-12	BD-5	BD-6 RT-13 22-14	2T1C1
140 ppm	BD-1	BD-2 RT-7 15-8	BD-3 RT-9 18-10	BD-4 RT-11 18-12	BD-5	BD-6 RT-13 22-14	2T1C2
Uncontaminated	BD-1	BD-2 RT-7 15-8	BD-3 RT-9 18-10	BD-4 RT-11 18-12	BD-5	BD-6 RT-13 22-14	2T1C4

BD = 1" WIDE  
 RT }  
 15 } = 1 1/2" WIDE  
 18 }  
 22 }

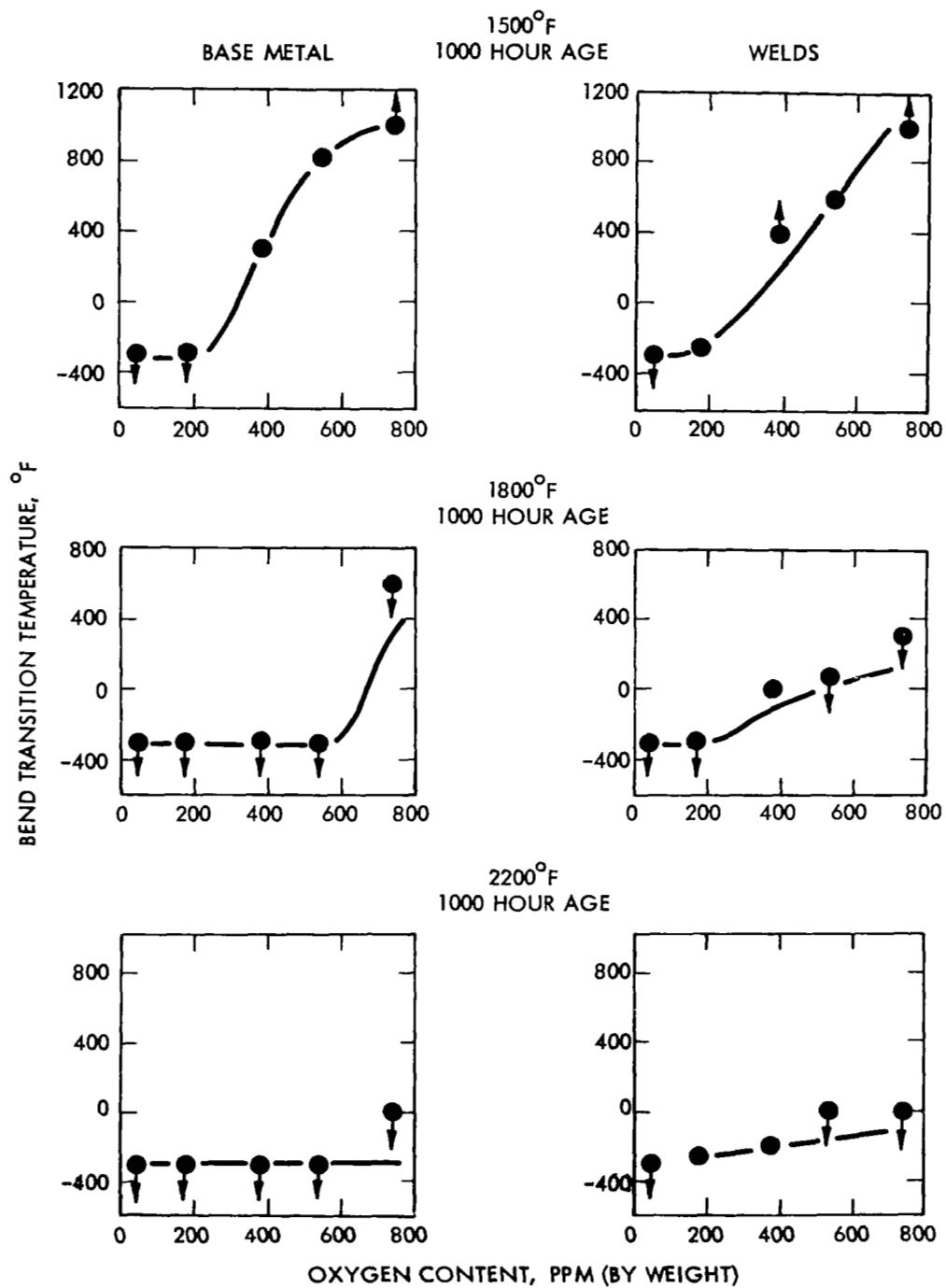


FIGURE 39 - Bend Transition Temperature Summary for Aged T-111

aging temperature results in ductile low temperature bends at the highest oxygen levels. Two mechanisms probably account for the change in behavior; (1) a higher temperature produces a coarser, less coherent oxide precipitate or zone and thus reduces the strengthening effect of oxygen and (2) the higher temperature also reduces the oxygen concentration gradient thereby lowering the oxygen concentration near the specimen surface, the most highly strained area of a bend test specimen.

In order to verify this general approach relating bend ductility to the oxygen gradient additional FS-85 specimens were contaminated with oxygen using a vacuum oxidizing procedure. In this case specimens were contaminated at 1700°F using a controlled leak to produce an oxygen partial pressure of  $5 \times 10^{-5}$  torr in an oil diffusion pumped, liquid nitrogen trapped system. A five hour exposure was required to produce an oxygen level of 500 ppm. The specimens were subsequently bend tested in the oxidized condition and as diffusion treated at 1800°F and 2200°F. Similar results are shown in Figure 40 for this process as were observed using the low temperature oxidation technique. Hence, the results are independent of the selected contamination technique. Further, layer chemical analyses were made to determine the oxygen concentration gradients of vacuum oxidized FS-85. These are shown in Figure 41. The data indicate that an appreciable concentration gradient is also produced by high temperature, low partial pressure, contamination. The FS-85 oxygen diffusion data is comparable to that measured for T-222, Figure 9.

The effect of aging for 1000 hours at 1800°F was to increase the ductility of the bend test specimens. Figure 42 compares the bend ductility of specimens aged for 1000 hours at 1800°F to T-111 bend test specimens from the initial phase of the program which were tested unaged. Again, one is inclined to suggest that coarsening of the oxide precipitates and flattening of concentration gradients most likely accounts for the improved ductility following aging.

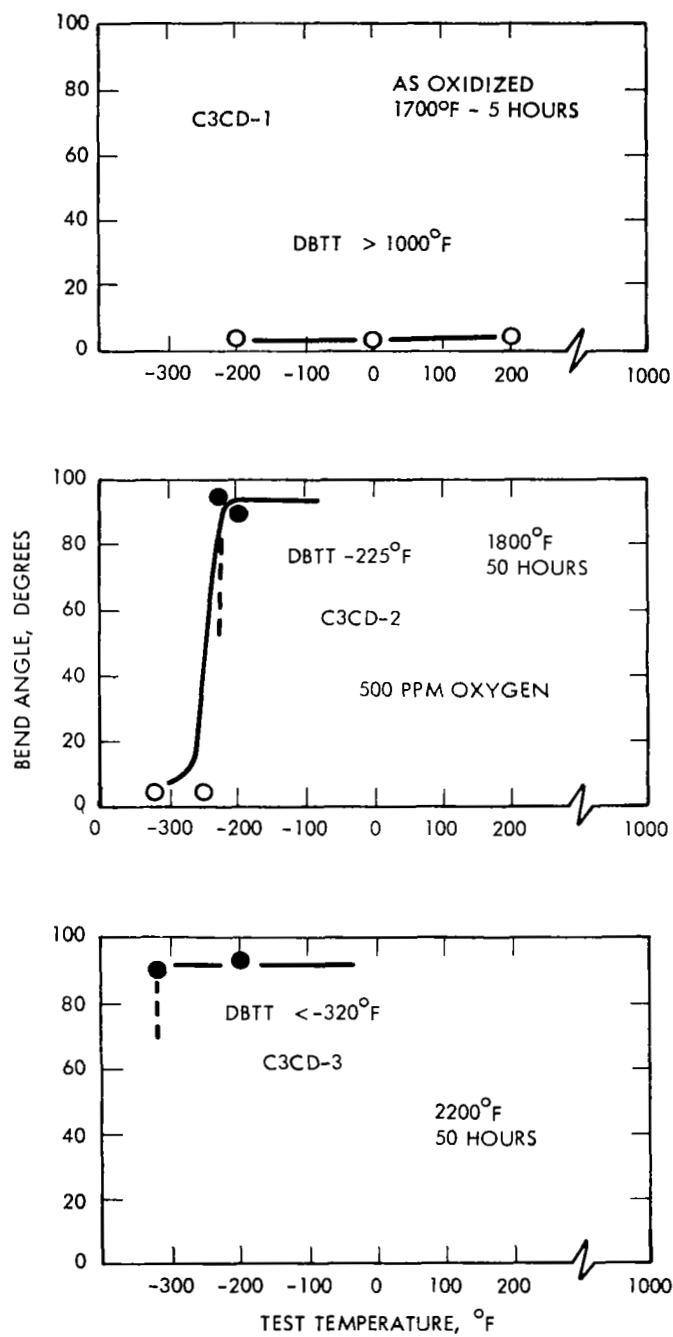


FIGURE 40 - Bend Ductility of Vacuum Oxidized FS-85

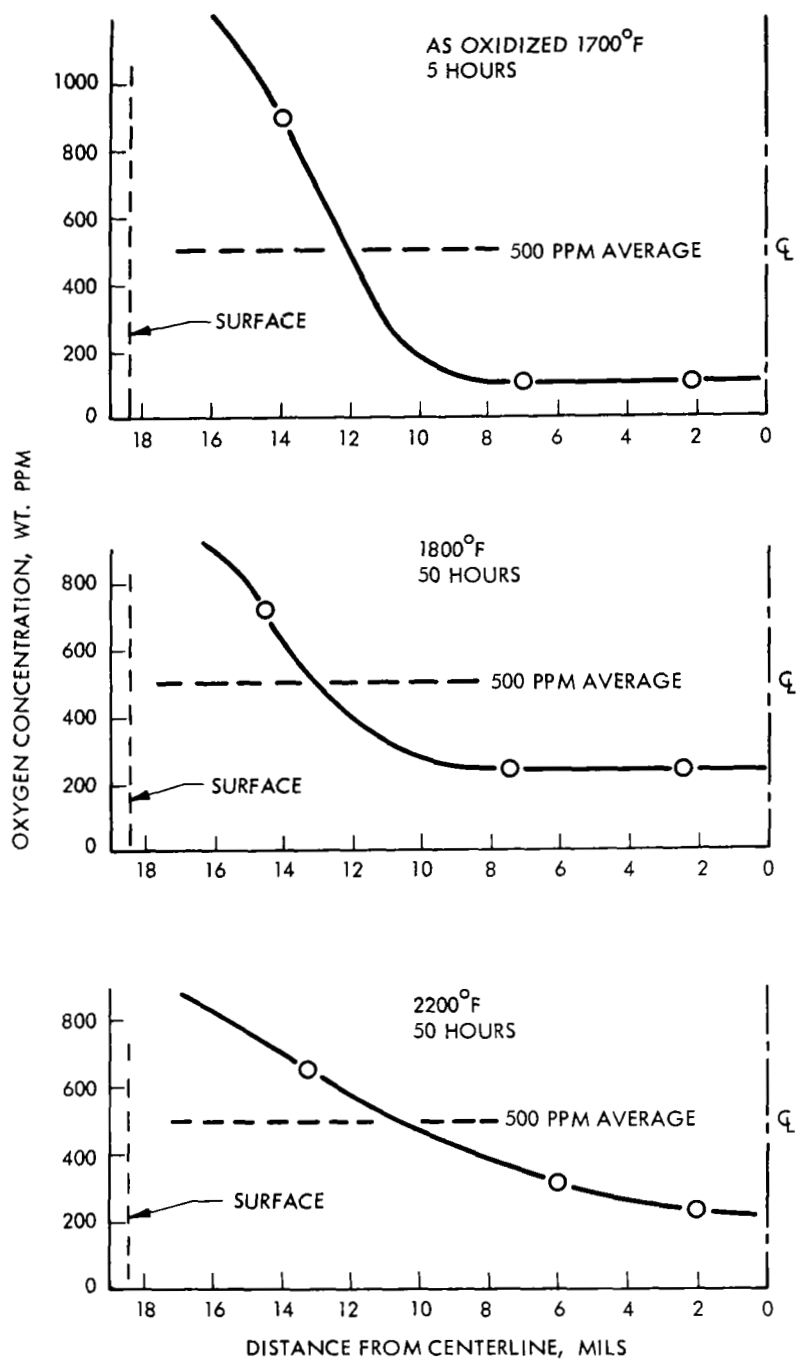


FIGURE 41 - Measured Oxygen Concentration Gradients for Vacuum Oxidized FS-85



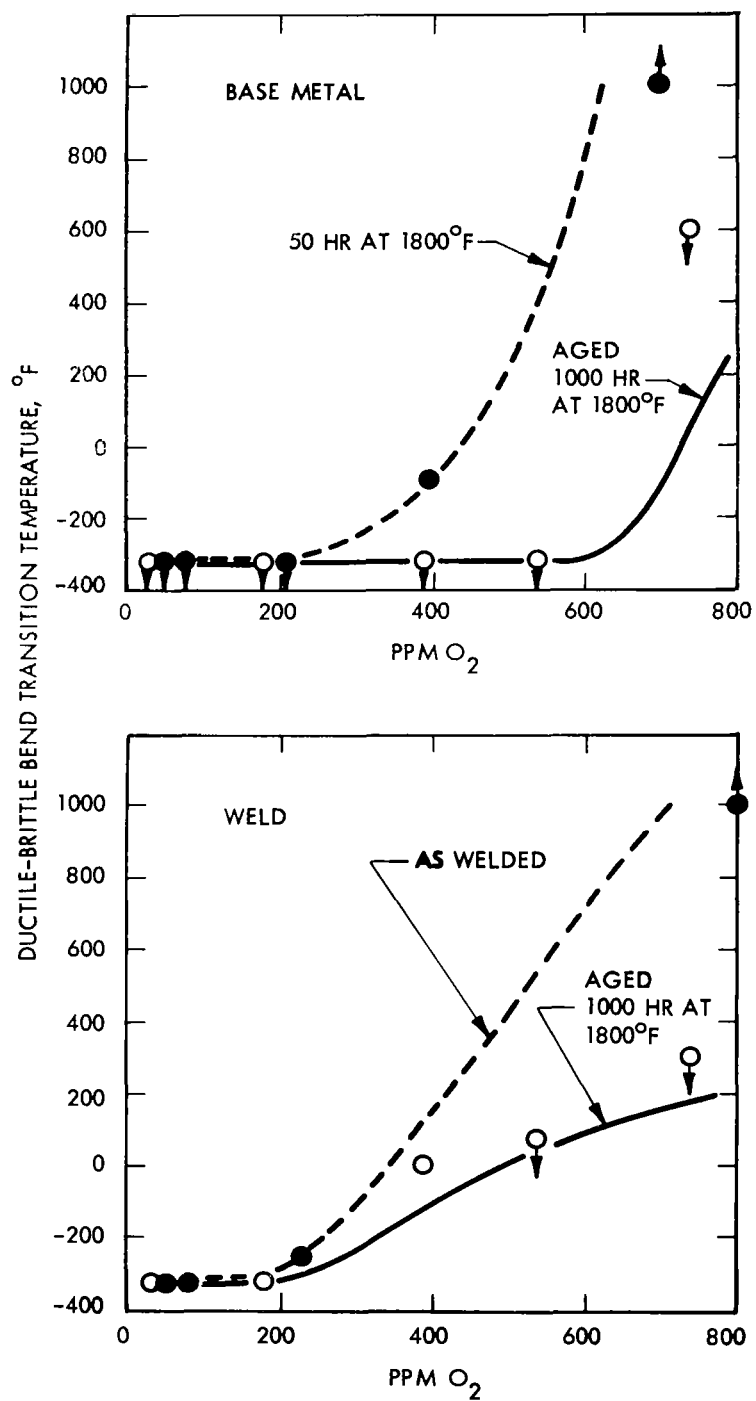


FIGURE 42 - Bend Ductility Comparison of Aged and Unaged T-111

TABLE 12 - Tensile Test Properties Aged T-111, Weld Specimens, 1500, 1800 and 2200°F

Test Temp. °F	Diffusion Anneal and 1000Hr. Temp. °F	Contamination Level PPM O <sub>2</sub>	Specimen Identification	Y.S. 0.2% Offset PSIX 10 <sup>3</sup>	Ultimate Stress PSIX 10 <sup>3</sup>	Elongation %	Fracture Location	Fracture Distance From Weld Centerline Inches	Reduction In Area %
1500	1500	0	2T1CU-8	40.4	59.6	10	HAZ	0.10	73
		140	2T1C2-8	42.3	64.3	10	HAZ	0.15	
		350	2T1C1-8	59.0	73.2	5	Base	0.60	
		500	2T1C3-8	59.8	66.0	2	Base	0.58	
		700	2T1C4-8		59.2		Grip	1.00	
1800	1800	0	2T1CU-12	35.7	55.4	11	HAZ	0.09	88
		140	2T1C2-12	42.5	58.9	8	HAZ	0.10	
		350	2T1C1-12	45.5	60.6	7	HAZ	0.10	
		500	2T1C3-12	50.4	62.6	4	HAZ	0.10	
		700	2T1C4-12	51.3	60.0	5	HAZ	0.10	
2200	2200	0	2T1CU-14	27.2	43.2	12	Weld	0.07	23
		140	2T1C2-14	26.2	42.3	14	HAZ	0.11	
		350	2T1C1-14	28.2	44.0	14	HAZ	0.10	
		500	2T1C3-14	31.2	45.3	13	HAZ	0.09	
		700	2T1C4-14	28.6	41.7	13	Weld	0.08	

TABLE 13 - Tensile Test Properties of Aged T-111, Weld Specimen, Room Temperature

Test Temp. °F	Diffusion Anneal and 1000Hr. Temp °F	Contamination Level PPM O <sub>2</sub>	Specimen Identification	Y.S. 0.2% Offset 3 PSIX 10 <sup>3</sup>	Ultimate Stress PSIX 10 <sup>3</sup>	Elongation %	Fracture Location	Fracture Distance From Weld Centerline Inches	Reduction In Area %	
↑ ROOM TEMP ↓	1500	0	2T1CU-7	78.0	88.4	18.0	Weld	0.10	62	
		140	2T1C2-7	83.3	94.4	14.0	HAZ	0.16		
		350	2T1C1-7	89.2	104.2	4.0	HAZ	0.13		
		500	2T1C3-7	89.1	104.8	3.0	HAZ	0.10		
	1800	700	2T1C4-7	85.3	103.1	3.0	HAZ	0.10	19	
		0	2T1CU-11	73.0	87.2	16.0	Weld	0.09		100
		140	2T1C2-11	70.0	89.1	12.0	HAZ	0.10		
		350	2T1C1-11	76.5	88.6	13.0	HAZ	0.10		
	2200	500	2T1C3-11	80.3	94.7	6.0	Weld	0.08	62	
		700	— NO TEST							
		0	2T1CU-13	68.5	80.0	17.0	HAZ	0.11		88
		140	2T1C2-13	70.9	83.2	13.0	HAZ	0.11		
	350	2T1C1-13	69.1	82.9	16.0	HAZ	0.11	65		
	500	2T1C3-13	69.5	84.9	14.0	Weld	0.10			
	700	2T1C4-13	71.8	86.9	15.0	Weld	0.08			

TABLE 14 - Tensile Test Properties of Aged T-111, Base Metal, R.T. and 1800°F

Test Temp. °F	Diffusion Anneal and 1000Hr. Temp °F	Contamination Level PPM O <sub>2</sub>	Specimen Identification	Y.S. 0.2% Offset PSIX 10 <sup>3</sup>	Ultimate Stress PSIX 10 <sup>3</sup>	Elongation %	Reduction In Area %
R.T.	1800	0	2T1CU-9	72.2	80.2	31	88
		140	2T1C2-9	79.4	93.0	23	
		350	2T1C1-9	83.4	101.0	21	
		500	2T1C3-9	88.6	111.7	21	
		700	2T1C4-9	113.6	141.8	19	
1800	1800	0	2T1CU-10	35.8	57.4	21	88
		140	2T1C2-10	41.9	60.5	16	
		350	2T1C1-10	45.5	68.0	16	
		500	2T1C3-10	50.8	75.8	12	
		700	— NO TEST				
							46

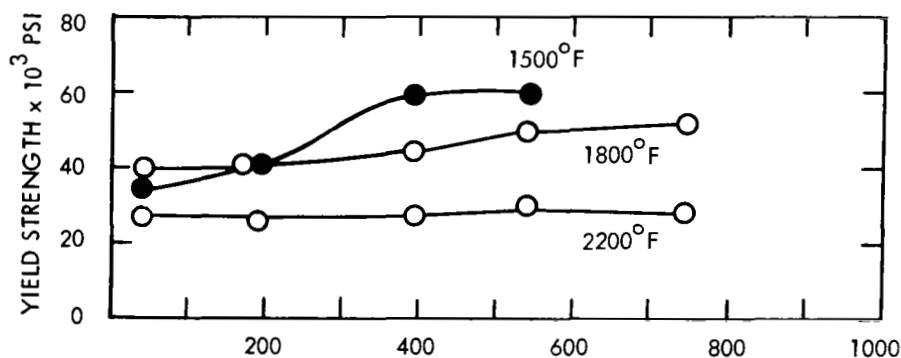
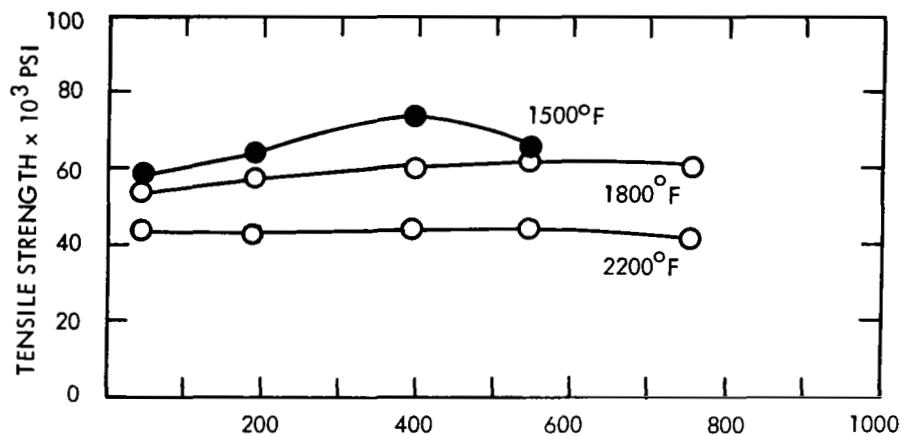
## Tensile Properties

Changes in tensile properties were used to observe the combined effect of oxygen contamination and 1000 hour aging at elevated temperatures simulating service conditions. Weld specimens were tested at room temperature, 1500°F, 1800°F and 2200°F, and base metal specimens were tested at room temperature and 1800°F. All weld specimens were tested in the transverse direction as in the first phase of the program.

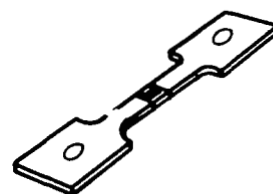
The tensile test results are listed in Tables 12, 13 and 14. Figure 43 presents the elevated temperature properties of welded and aged specimens as a function of oxygen content. Tensile elongation was most severely impaired with oxygen contamination in the 1500°F test specimens. The highest oxygen contamination level specimens fractured in the grip area during loading. For the room temperature tensile properties, Figure 44, three sets of curves are shown corresponding to the three aging temperatures used, but all of the specimens were tested at room temperature. Similar to the elevated temperature tests, the most pronounced loss in ductility with oxygen content occurred at 1500°F. Specimens aged at 2200°F, show almost no change in strength with increasing oxygen content while maintaining acceptable elongation values.

Fracture profiles of the elevated temperature and room temperature weld specimens are shown in Figures 50 and 51. The fracture reduction in area is similar to the total elongation except for the 2200°F fracture of an uncontaminated specimen shown in Figure 50 which fractured intergranularly in the weld. At the 2200°F aging and test temperature, the high oxygen level T-111 has greater elongation than the uncontaminated material, similarly to the FS-85 in the first phase of the program. A possible explanation is grain growth inhibition by the oxide precipitates providing a finer grained more ductile structure.

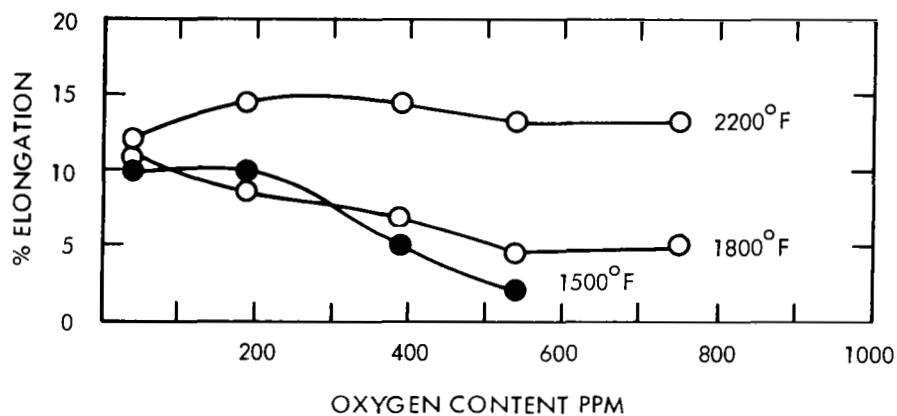
Unwelded tensile specimens were tested at 1800°F and at room temperature following aging at 1800°F. A comparison of the weld and base metal properties is shown in Figures 45 and 46. The most marked difference between welded and unwelded material in the lower



ALL SPECIMENS  
TRANSVERSE WELDS

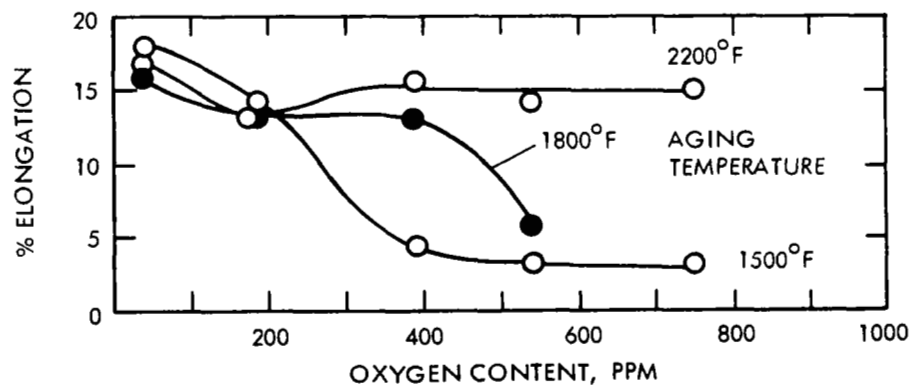
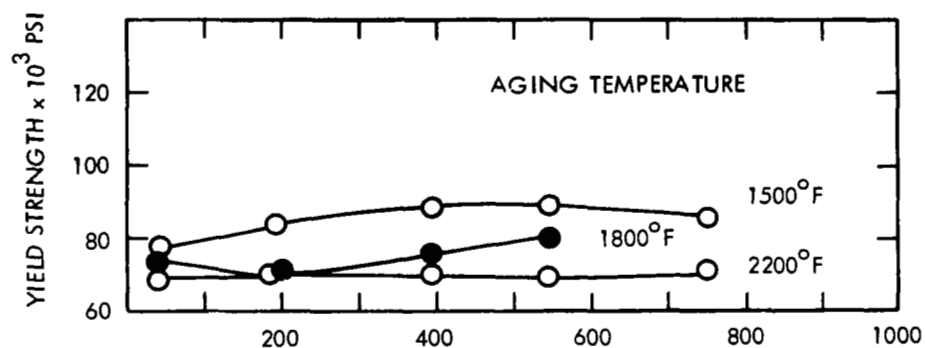
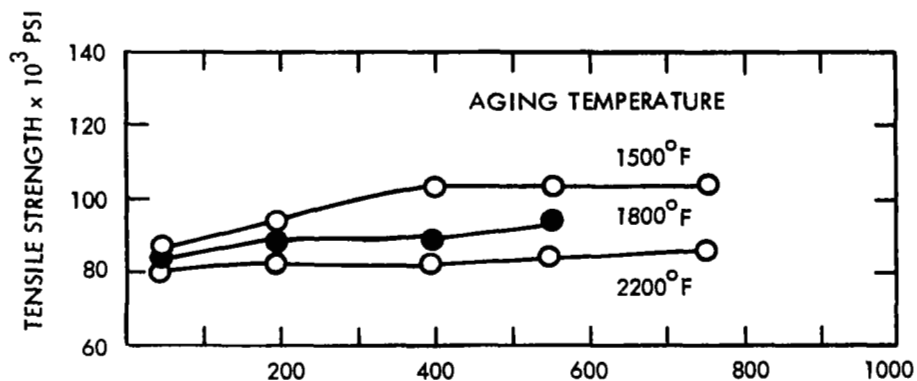


TEST TEMPERATURE  
LISTED

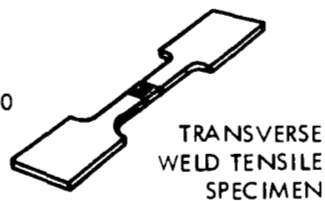


SPECIMENS AGED  
1000 HOURS AFTER  
WELDING AT THE  
INDICATED TEMPERATURE

FIGURE 43 - Elevated Temperature Transverse Weld Tensile Properties of T-111, Aged 1000 Hours



ROOM TEMPERATURE TESTS



1000 HOUR AGING TEMPERATURE AS LISTED

FIGURE 44 - Room Temperature Transverse Weld Tensile Properties of T-111, Aged 1000 Hours

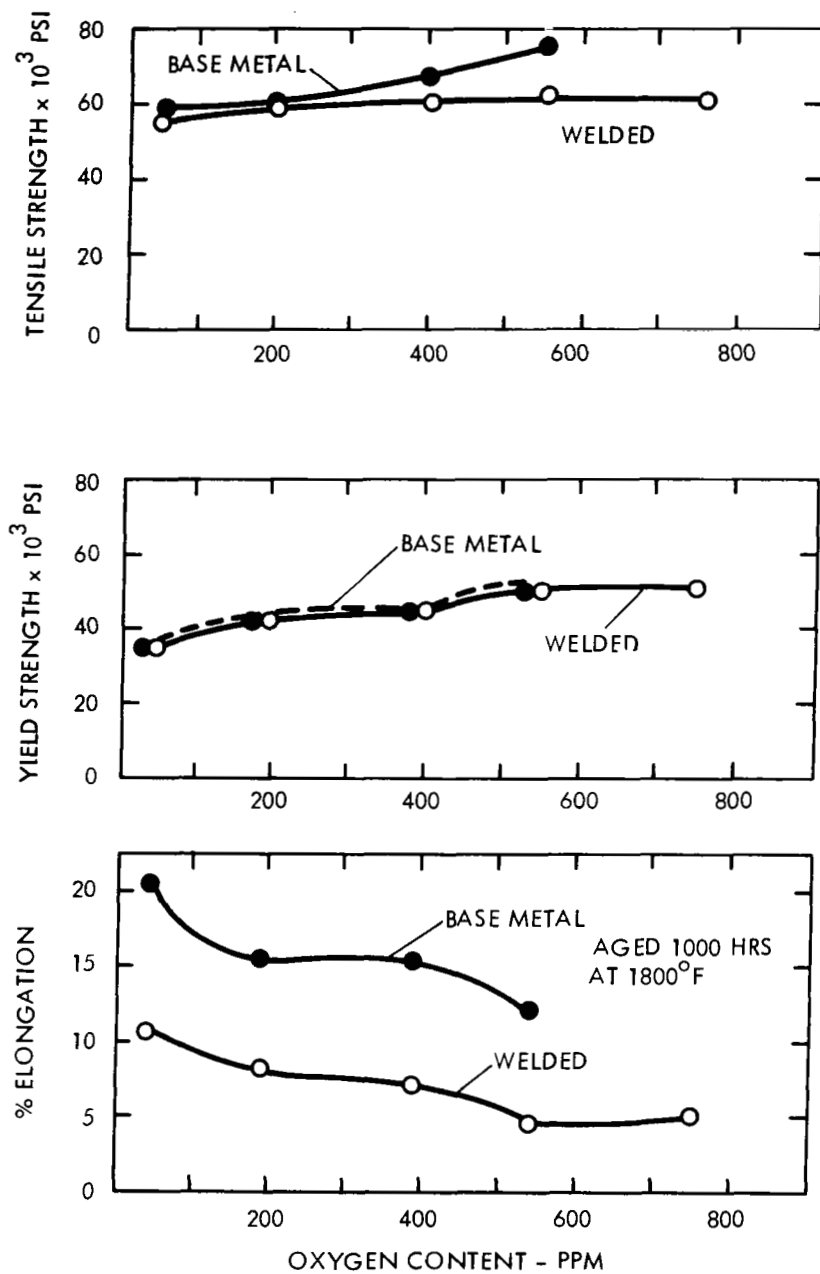
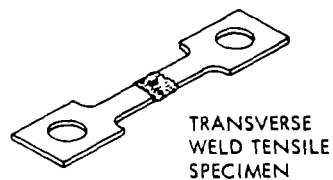
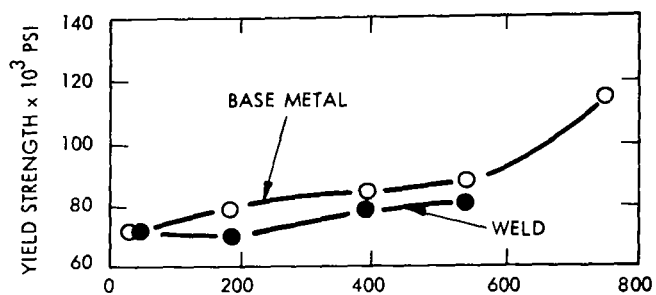
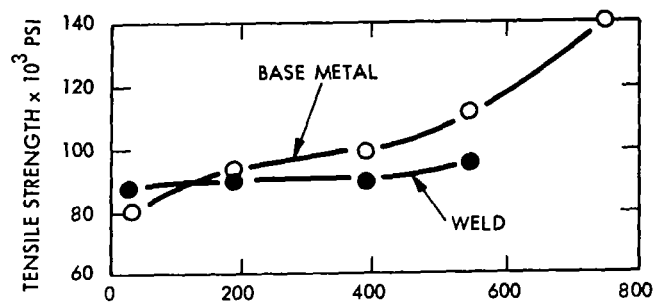
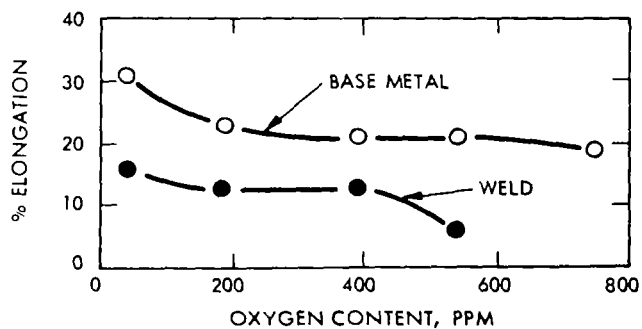


FIGURE 45 - 1800°F Comparison of Weld and Base Metal Tensile Properties





TRANSVERSE  
WELD TENSILE  
SPECIMEN



ALL SPECIMENS AGED 1000 HRS  
AT 1800°F  
ROOM TEMPERATURE TENSILE TESTS

FIGURE 46 - Room Temperature Comparison of T-111 Weld and  
Base Metal Tensile Properties

tensile elongation values obtained for welded material. The total elongation for weld specimens is consistently less than one half that of the base metal specimens at all oxygen concentration levels. Hence, weld metal appears no more sensitive to contamination than base metal. Since the weld specimens have reductions in area equivalent to the base metal specimens, the difference in total elongation is the more concentrated deformation at the weakest area in the weld and heat affected zone. Similarly, weld strength is nearly equal to base metal strength at all levels of contamination.

A comparison of aged and unaged material is shown for transverse weld specimens in Figures 47 through 49. The most pronounced difference between the aged and as-welded specimens is in the tensile elongation, shown in Figure 49. In comparing the various test conditions, it appears that aging is detrimental to the tensile elongation at 1500°F, but aging at higher temperatures 1800°F, 2200°F, results in almost equivalent or at room temperature even better properties than the as-welded material. Room temperature tensile strength, Figure 48, is very responsive to differences in thermal history.

#### Tensile Test Summary

Similar to the first phase of the program, specimens were contaminated with oxygen, diffusion annealed at temperatures corresponding to subsequent aging and test temperatures, welded, and machined to tensile specimen configuration. At this point the specimens were aged for 1000 hours under high vacuum conditions at 1500°F, 1800°F and 2200°F and tensile tested. The general effects of oxygen contamination were similar to the as-welded specimens; increasing oxygen content increased the strength and reduced the ductility of the specimens. A comparison of aged weld and base metal was available at 1800°F and room temperature which indicated the base metal specimens were slightly stronger and more ductile than weld specimens at all oxygen contamination levels. The main purpose of this phase of the program, a comparison of the aged and unaged properties, indicated that aging slightly decreased the strength and ductility of T-111 at elevated temperatures. The room temperature ductility of T-111 aged at 2200°F and 1800°F, however, was superior to the as-welded properties. This

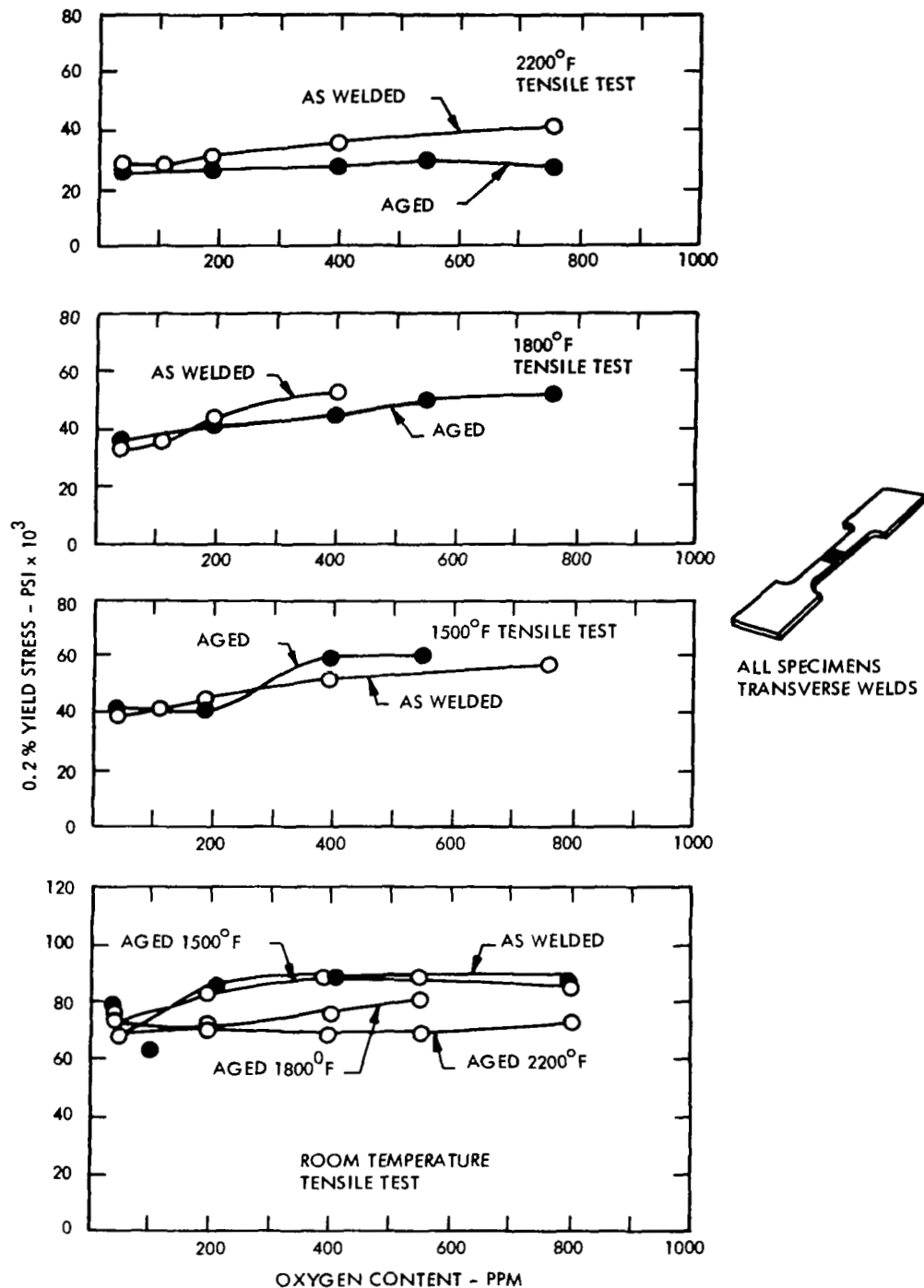


FIGURE 47 - Comparison of Aged and As-Welded Yield Strength

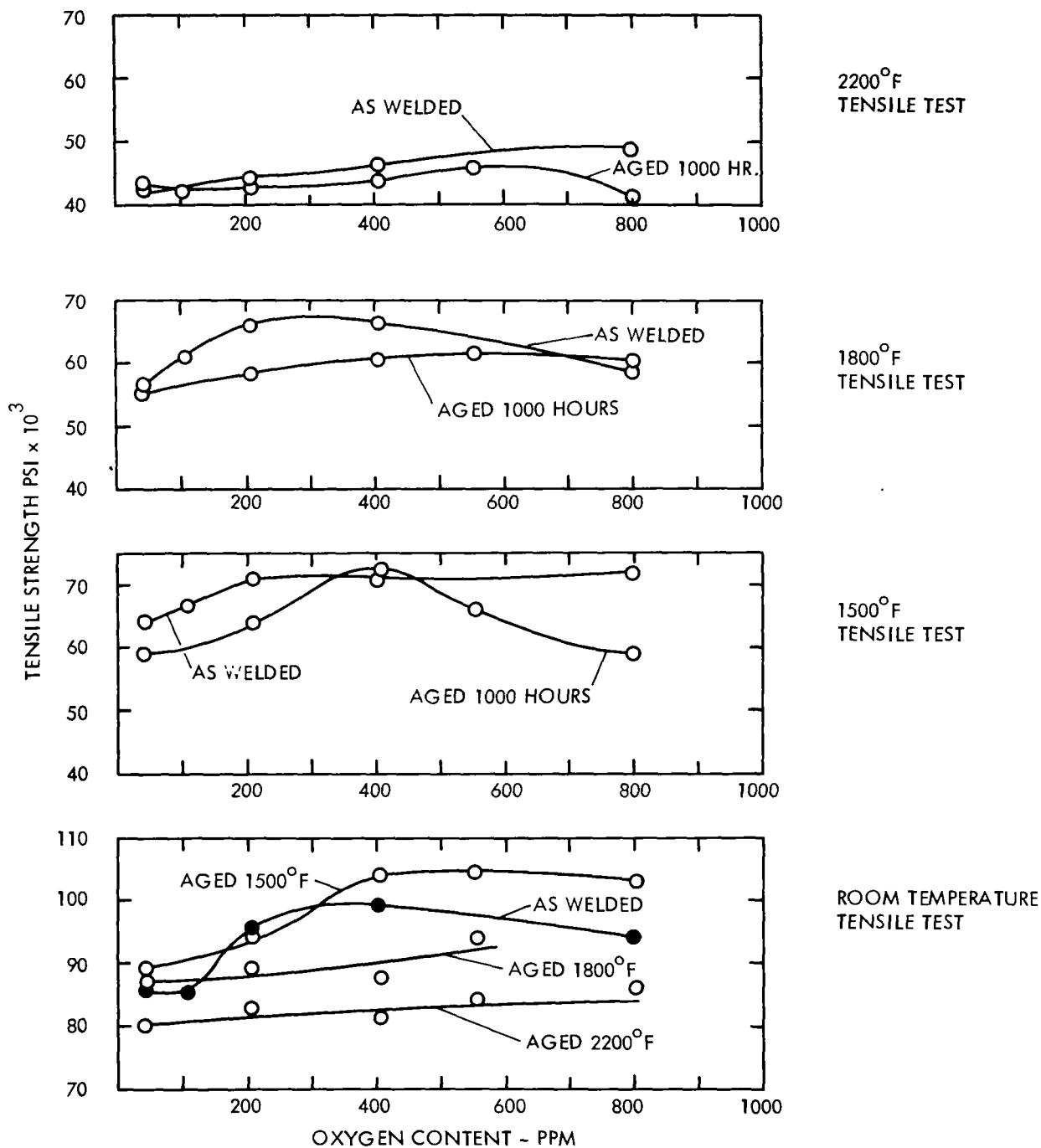


FIGURE 48 - Comparison of Aged and As-Welded Tensile Strength

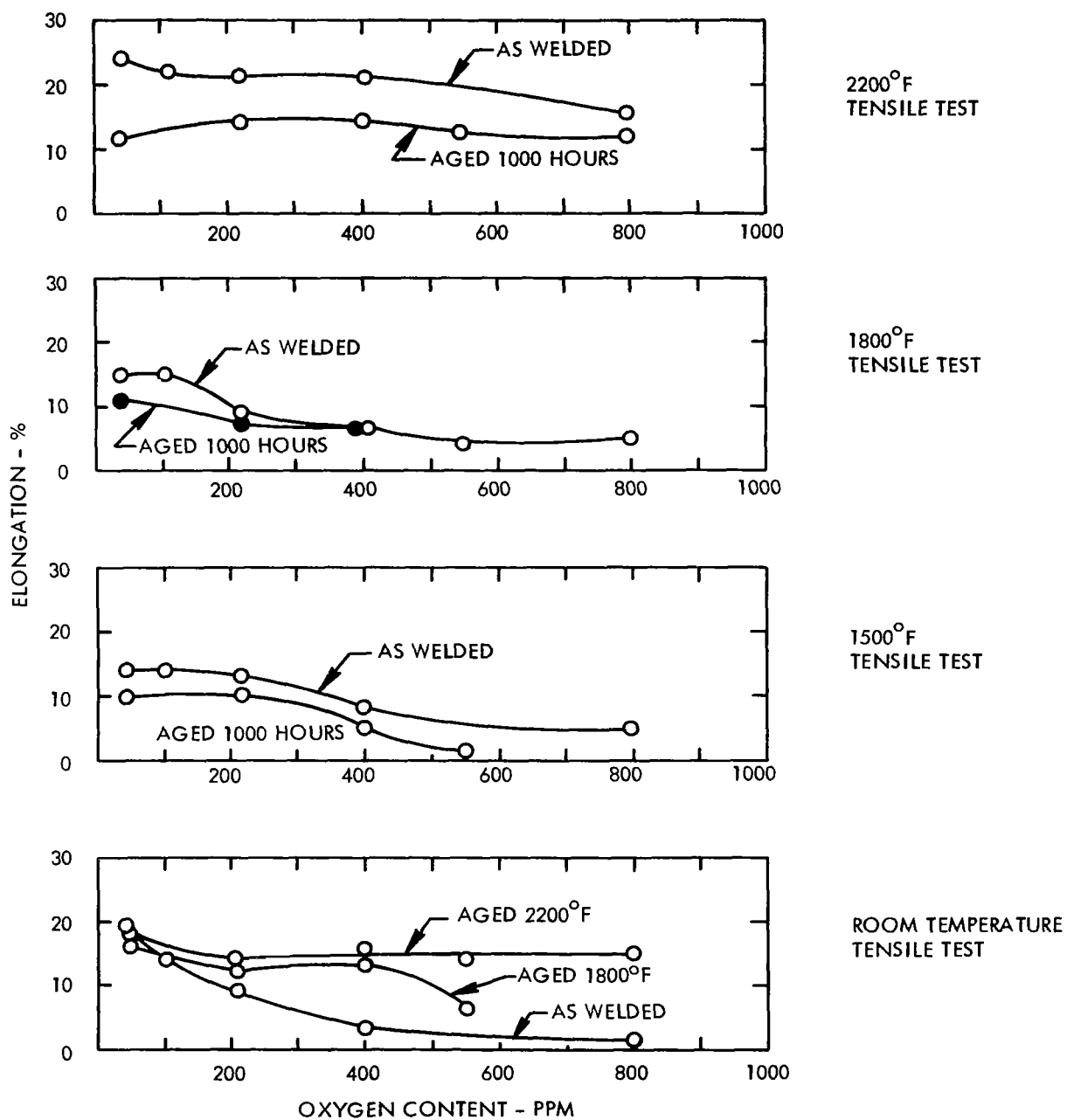


FIGURE 49 - Comparison of Aged and As-Welded Tensile Elongation

is somewhat analogous to the overaging of Cb-1Zr observed by Franco-Ferreira and Slaughter,<sup>(6)</sup> in that heat treatments over 2000°F were successful in preventing a loss in weld ductility during temperature aging. In general, tensile properties displayed a considerable tolerance to contamination.

### Weld Microstructure

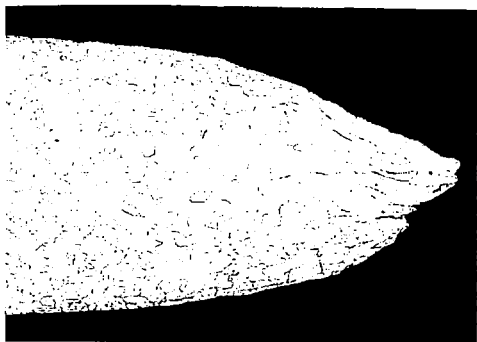
Details of the weld interface in aged T-111 are shown in Figures 53, 54, and 55. As noted for the as-welded microstructure, the addition of oxygen results in a general increase in grain boundary and matrix precipitate. A strong restriction to grain growth is observed at the weld interfaces and also in the base metal at the higher aging temperatures. At the 2200°F aging temperature, the weld precipitate is changed in appearance from an interdendritic precipitate to an intergranular precipitate.

### Weld Hardness Traverses

Weld interface hardness traverses of low and high oxygen content T-111 are shown in Figures 56 and 57. The as-welded material was diffusion annealed for 50 hours prior to welding resulting in a fairly high hardness in the base metal. The change in interface hardness in the high oxygen content T-111 follows the analogy shown in Figure 58. It is assumed that an area of the heat affected zone was exposed during welding to temperatures above 3000°F producing an effective solution anneal and a relatively low hardness in the as-welded condition.

Aging at 1500°F produces aging and high hardness in the heat affected zone. The 2200°F heat treating temperature produces an overaged structure and low hardness in all areas of the weld and heat affected zone.

The weld hardness traverse data is summarized in Figure 59 and shows the effect of increasing oxygen content on both weld and base metal. The maximum hardness in both the weld and base metal was achieved at 1500°F following a 1000 hour age. It would be expected



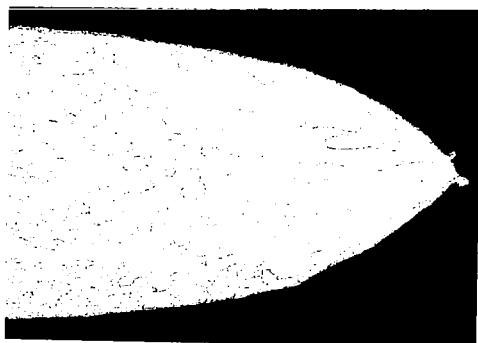
2TICU-8 Uncontaminated 26X  
40 ppm O<sub>2</sub> 16,169



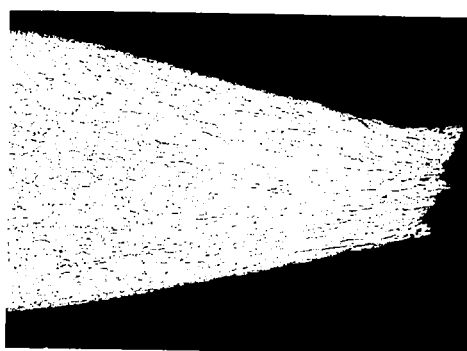
2TIC4-8 700 ppm O<sub>2</sub> 26X  
16,170

Aged 1000 Hrs.  
at 1500°F

1500°F  
TENSILE TEST



2TICU-12 Uncontaminated 26X  
40 ppm O<sub>2</sub> 16,165



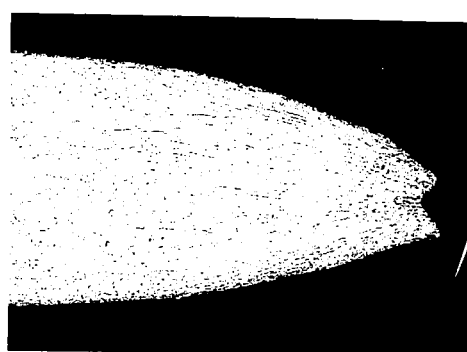
2TIC4-12 700 ppm O<sub>2</sub> 26X  
16,166

Aged 1000 Hrs.  
at 1800°F

1800°F  
TENSILE TEST



2TICU-14 Uncontaminated 26X  
40 ppm O<sub>2</sub> 16,163



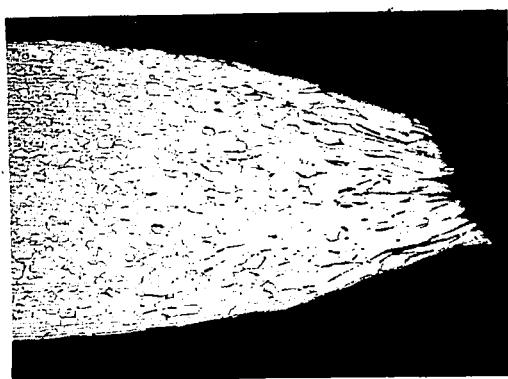
2TIC4-14 700 ppm O<sub>2</sub> 26X  
16,164

Aged 1000 Hrs.  
at 2200°F

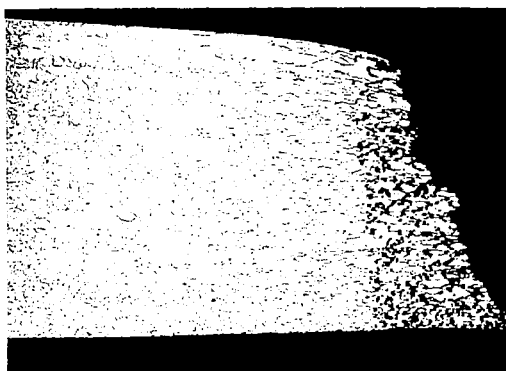
2200°F  
TENSILE TEST

FIGURE 50 - Elevated Temperature Fracture Profiles of T-111 Weld Tensile Specimens

Aged 1000 Hrs.  
at 1500°F

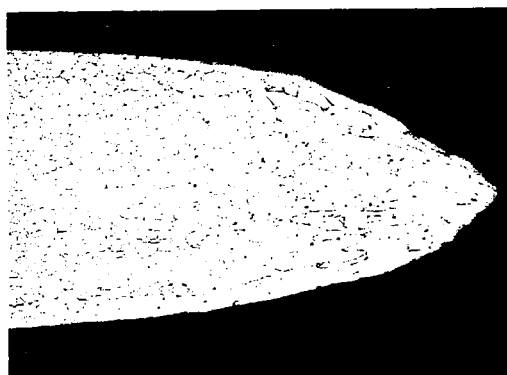


2TICU-7 Uncontaminated 26X  
400 ppm O<sub>2</sub> 16,177

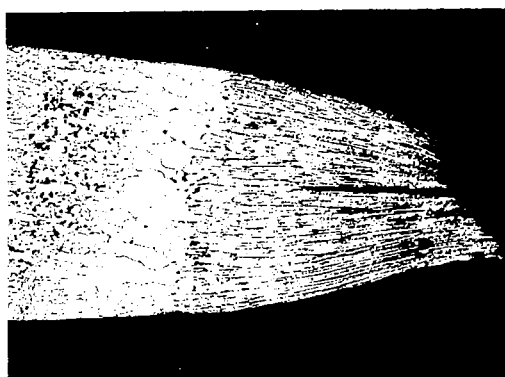


2TIC4-7 700 ppm O<sub>2</sub> 26X  
16,178

Aged 1000 Hrs.  
at 1800°F

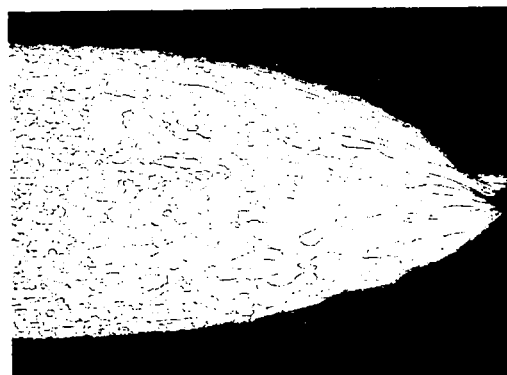


2TICU-11 Uncontaminated 26X  
400 ppm O<sub>2</sub> 16,173

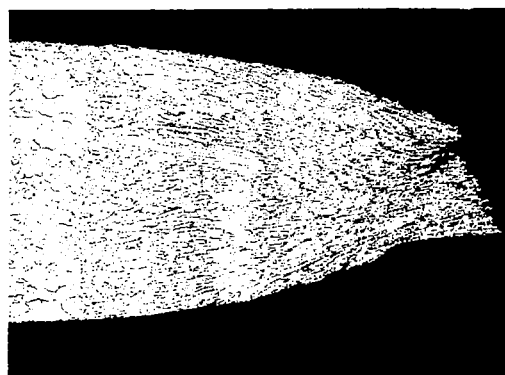


2TIC3-11 500 ppm O<sub>2</sub> 26X  
16,174

Aged 1000 Hrs.  
at 2200°F



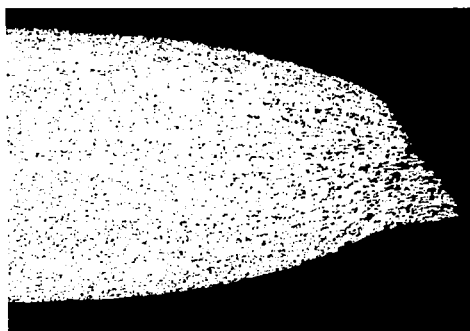
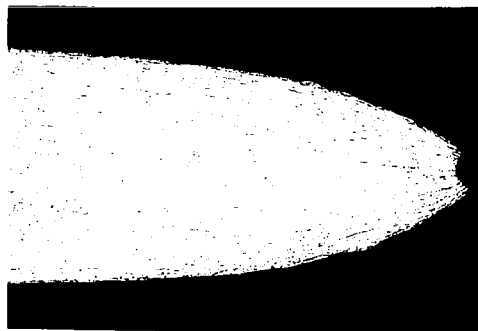
2TICU-13 Uncontaminated 26X  
400 ppm O<sub>2</sub> 16,171



2TIC4-13 700 ppm O<sub>2</sub> 26X  
16,172

FIGURE 51 - Room Temperature Fracture Profiles of T-111 Weld Specimens



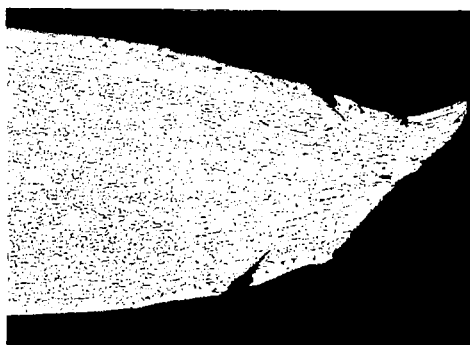
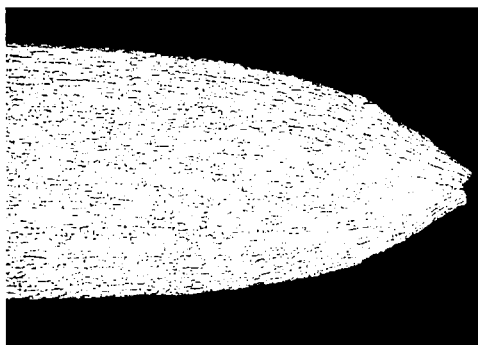


Aged 1000 Hrs.  
at 1800°F

ROOM TEMP.  
TENSILE TEST

2TICU-9    Uncontaminated    26X  
              40 ppm O<sub>2</sub>        16,175

2TIC4-9    700 ppm O<sub>2</sub>        26X  
   16,176



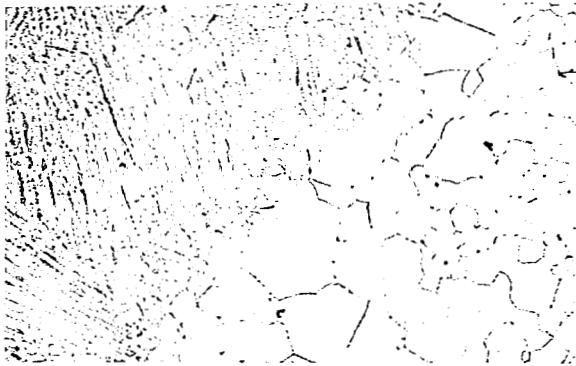
Aged 1000 Hrs.  
at 1800°F

1800°F  
TENSILE TEST

2TICU-10    Uncontaminated    26X  
              40 ppm O<sub>2</sub>        16,167

2TIC3-10    500 ppm O<sub>2</sub>        26X  
   16,168

FIGURE 52 - Fracture Profiles of T-111 Base Metal Specimens



80X

Weld Interface

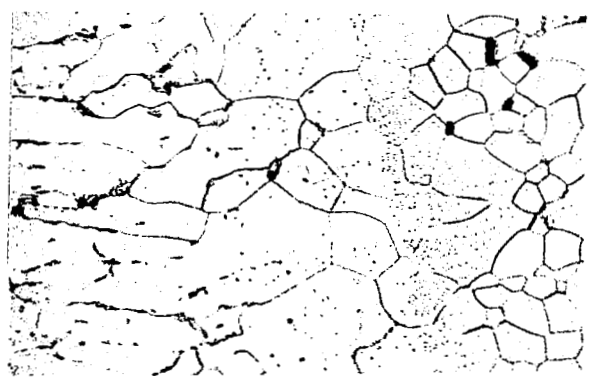


Weld Interface



400X

Weld Interface



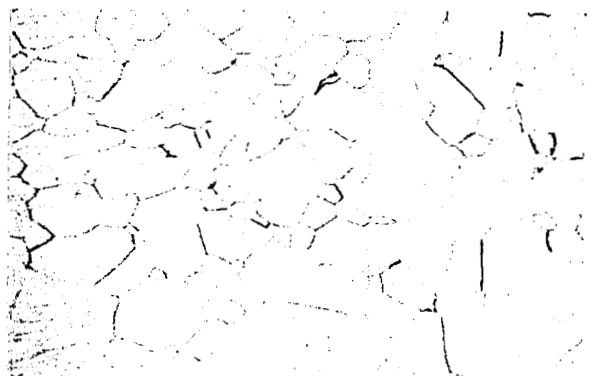
Weld Interface



400X

Base Metal

14,984



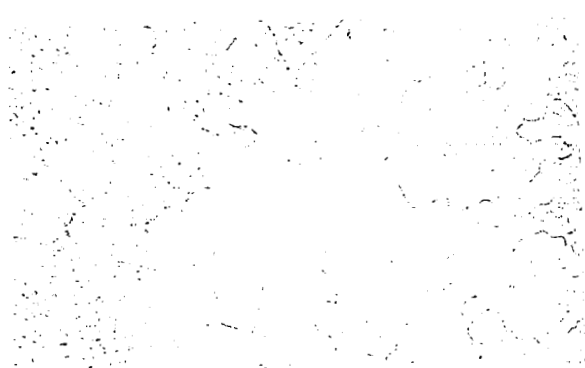
Base Metal

14,988

UNCONTAMINATED

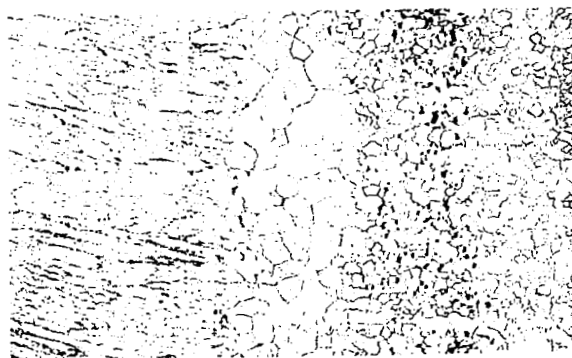
750 PPM OXYGEN

FIGURE 53 - T-111, Aged 1000 Hours at 1500°F

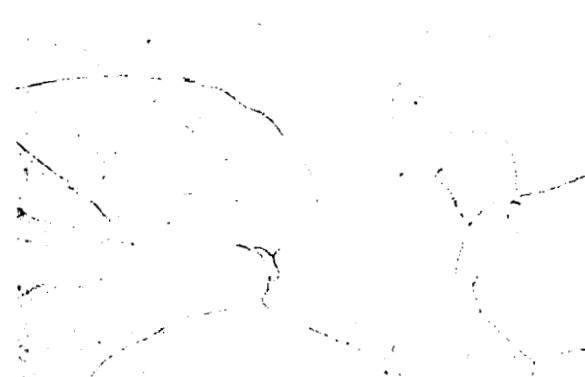


80X

Weld Interface



Weld Interface

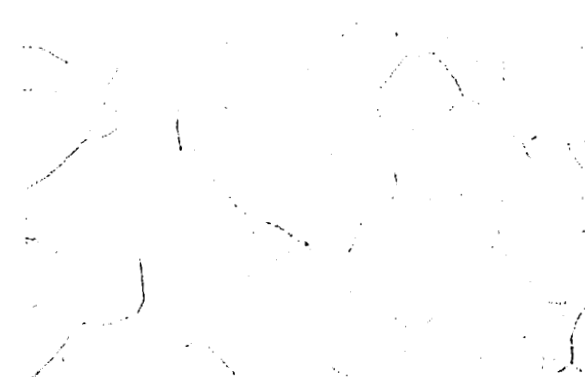


400X

Weld Interface



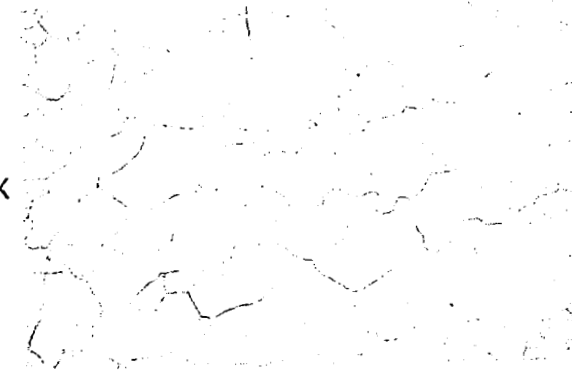
Weld Interface



400X

Base Metal

14,989



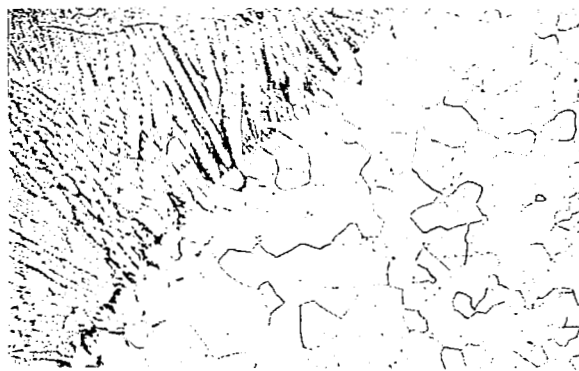
Base Metal

14,993

UNCONTAMINATED

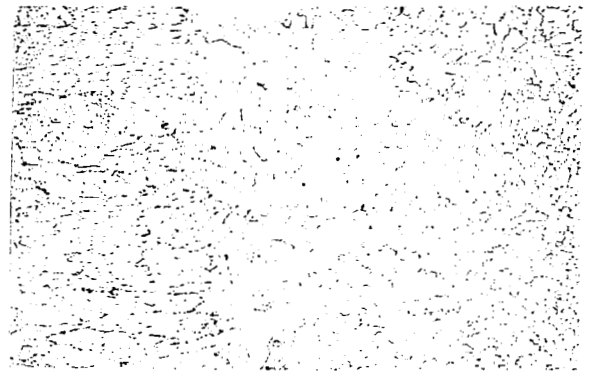
750 PPM OXYGEN

FIGURE 54 - T-111, Aged 1000 Hours at 1800°F



80X

Weld Interface

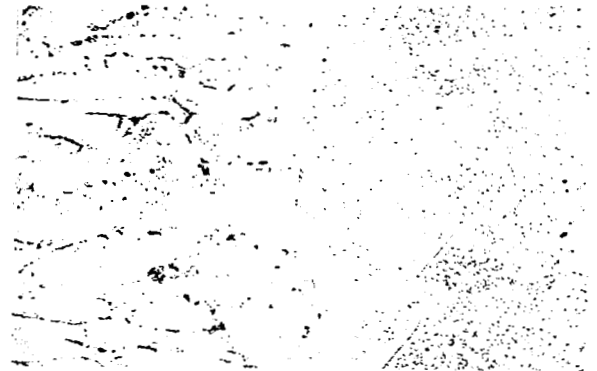


Weld Interface



400X

Weld Interface



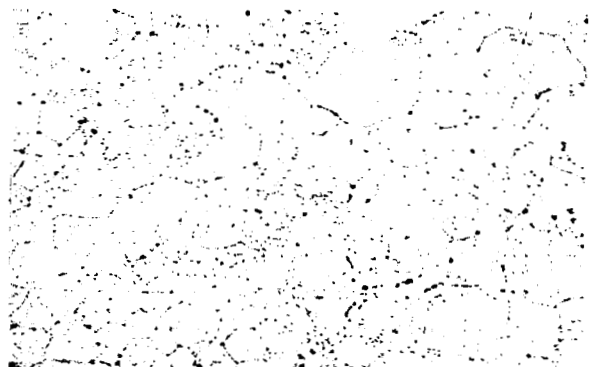
Weld Interface



400X

Base Metal

14,994



Base Metal

14,998

UNCONTAMINATED

750 PPM OXYGEN

FIGURE 55 - T-111, Aged 1000 Hours at 2200°F

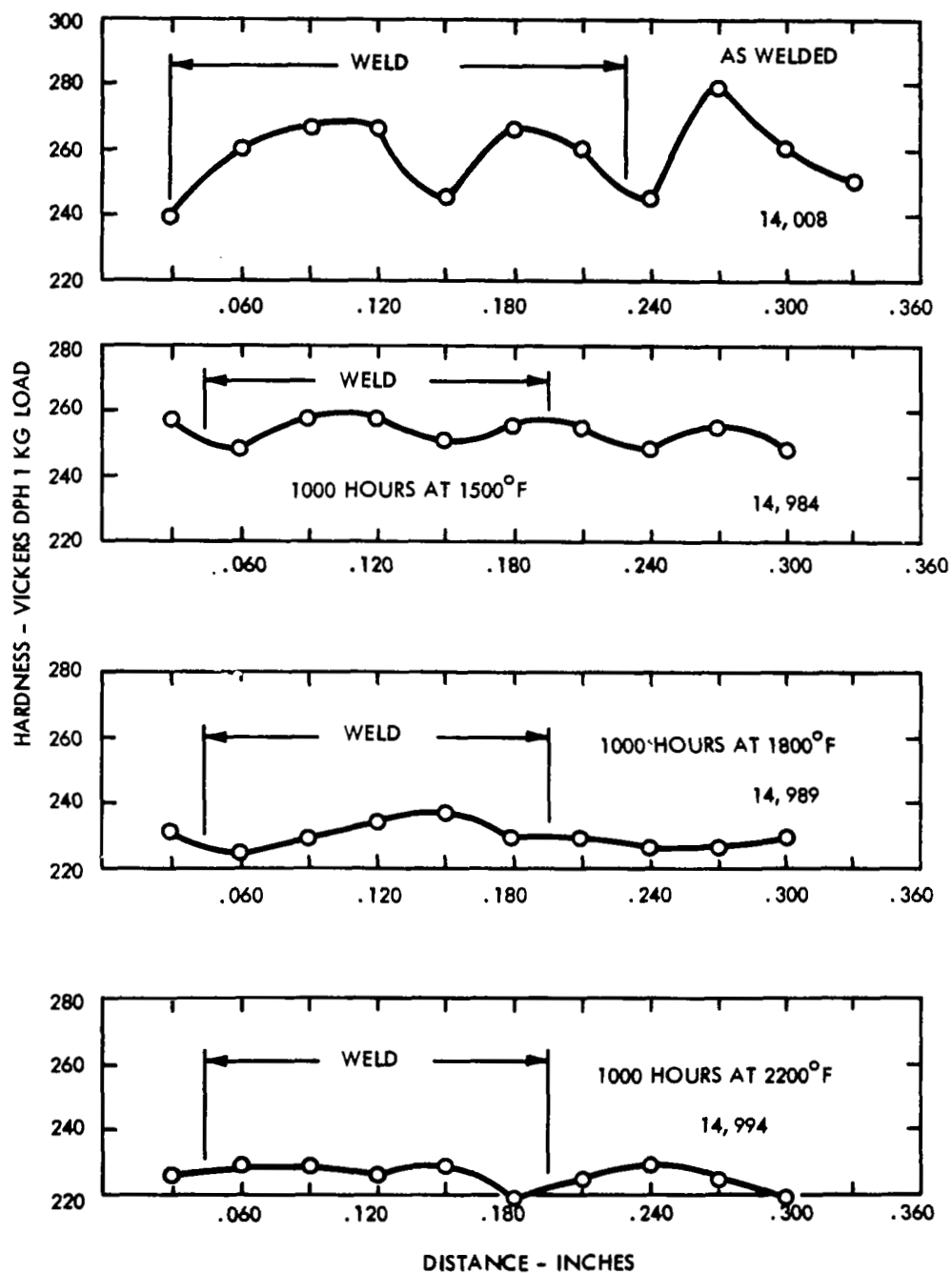


FIGURE 56 - Weld Hardness Traverse of T-111 Uncontaminated (40 ppm O<sub>2</sub>)

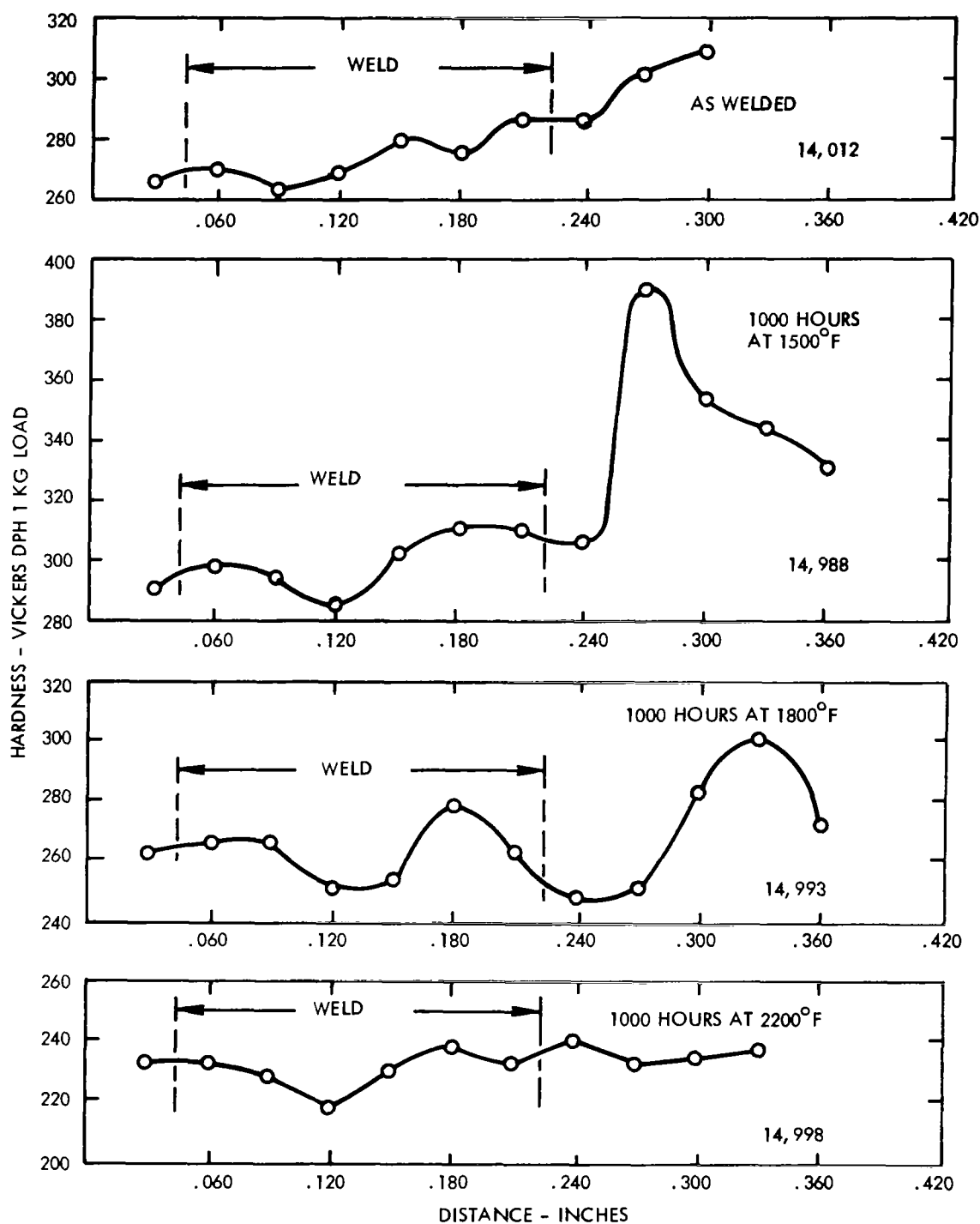


FIGURE 57 - Weld Hardness Traverse of T-111  
(700 ppm O<sub>2</sub>)

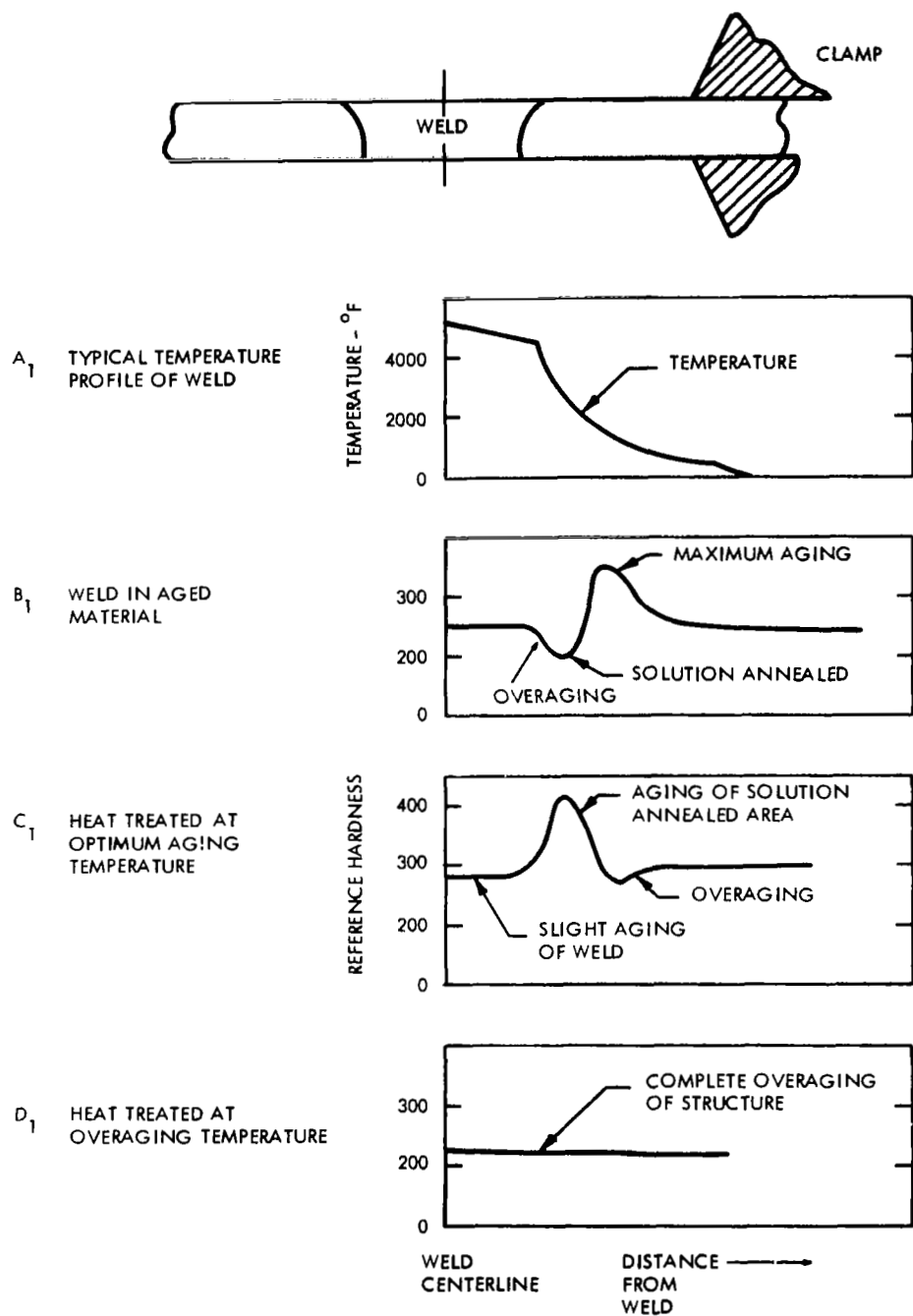


FIGURE 58 - Weld Hardness Profiles Expected in Age Hardenable Material

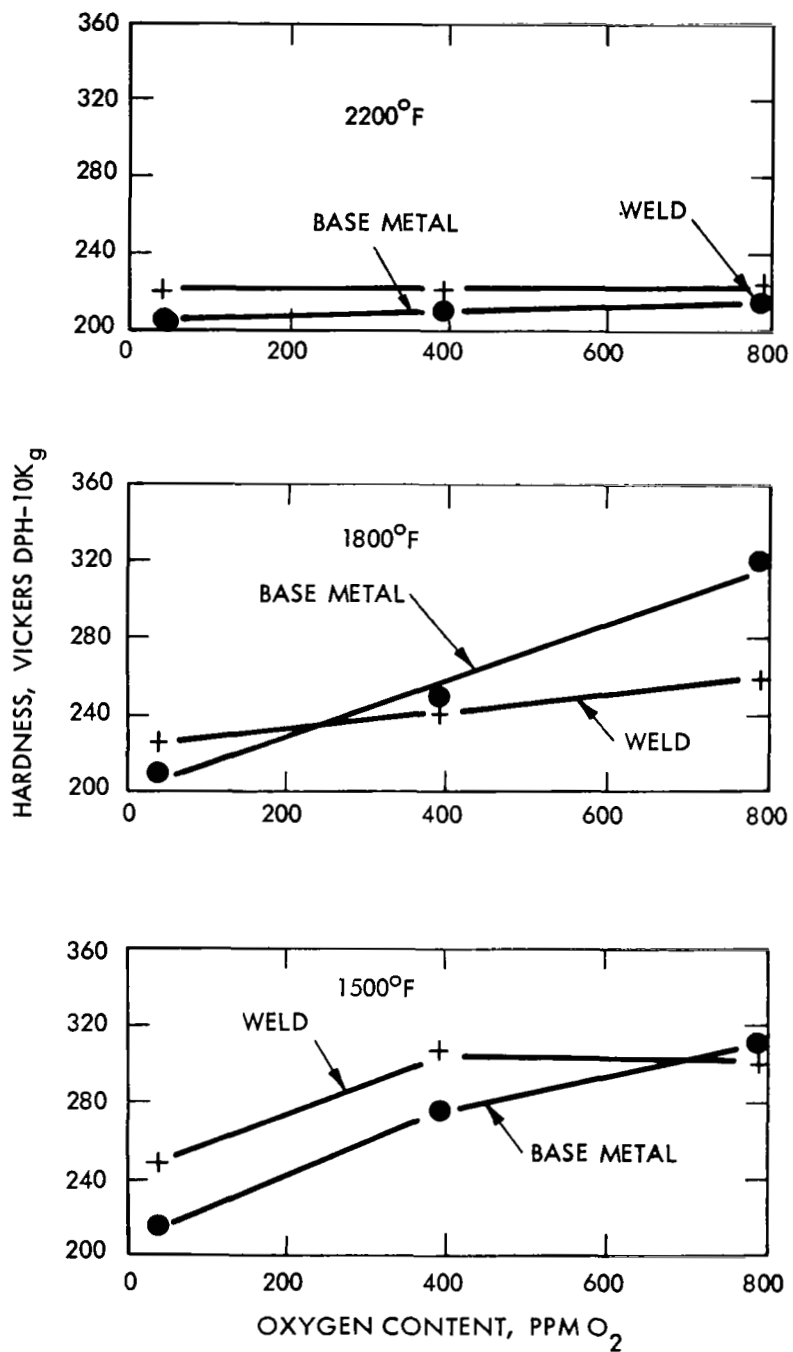


FIGURE 59 - Hardness Versus Oxygen Content for Aged T-111



that shorter aging times would require higher temperatures for maximum aging. Figure 60 compares the aged and unaged hardness of weld and base metal at 1800°F, the only temperature at which a comparison was available. The unaged T-111 is stronger and also indicates that T-111 is slightly overaged at 1000 hours at 1800°F.

### Strengthening Mechanism Identification

High magnification optical and electron microscopy techniques have supported the precipitation hardening analyses of the behavior of T-111. Figure 61 shows the microstructure of high oxygen content T-111 at 1800°F and 2200°F, representing an aged and overaged condition respectively. At 1800°F, a broadened zone is observable around the grain boundaries, and at 2200°F a general precipitate occurs at the grain boundaries and in the matrix. It is speculated that the broadened grain boundaries observed in the 1800°F specimens represent an area of coherent  $\text{HfO}_2$  precipitate. Since grain boundary diffusion of oxygen is rapid it may be assumed that the surface oxygen contamination first diffuses along the grain boundaries and forms an adjacent zone of coherent oxide precipitates. At 2200°F, a non-coherent precipitate is formed throughout the matrix and in the grain boundaries.

Bromine solution extraction and concentration techniques for oxide precipitates were used to corroborate the surface replica observations and electron micrographs of the precipitates are shown in Figure 62. In general, very little material was extracted from the 1800°F specimen. This is not unusual with coherent precipitates which because of their structural similarity to the matrix are also dissolved by the extraction solution. A few platelets were obtained as shown in Figure 62 and are suspected to be the remains of grain boundary films. The 2200°F specimens yielded a large extraction residue, also shown in Figure 62, which is suspected to be large non-coherent precipitates of  $\text{HfO}_2$ . Subsequent x-ray diffraction analysis indicated the 1800°F residue to be monoclinic  $\text{HfO}_2$  and the 2200°F residue to be a mixture of monoclinic and cubic  $\text{HfO}_2$ .

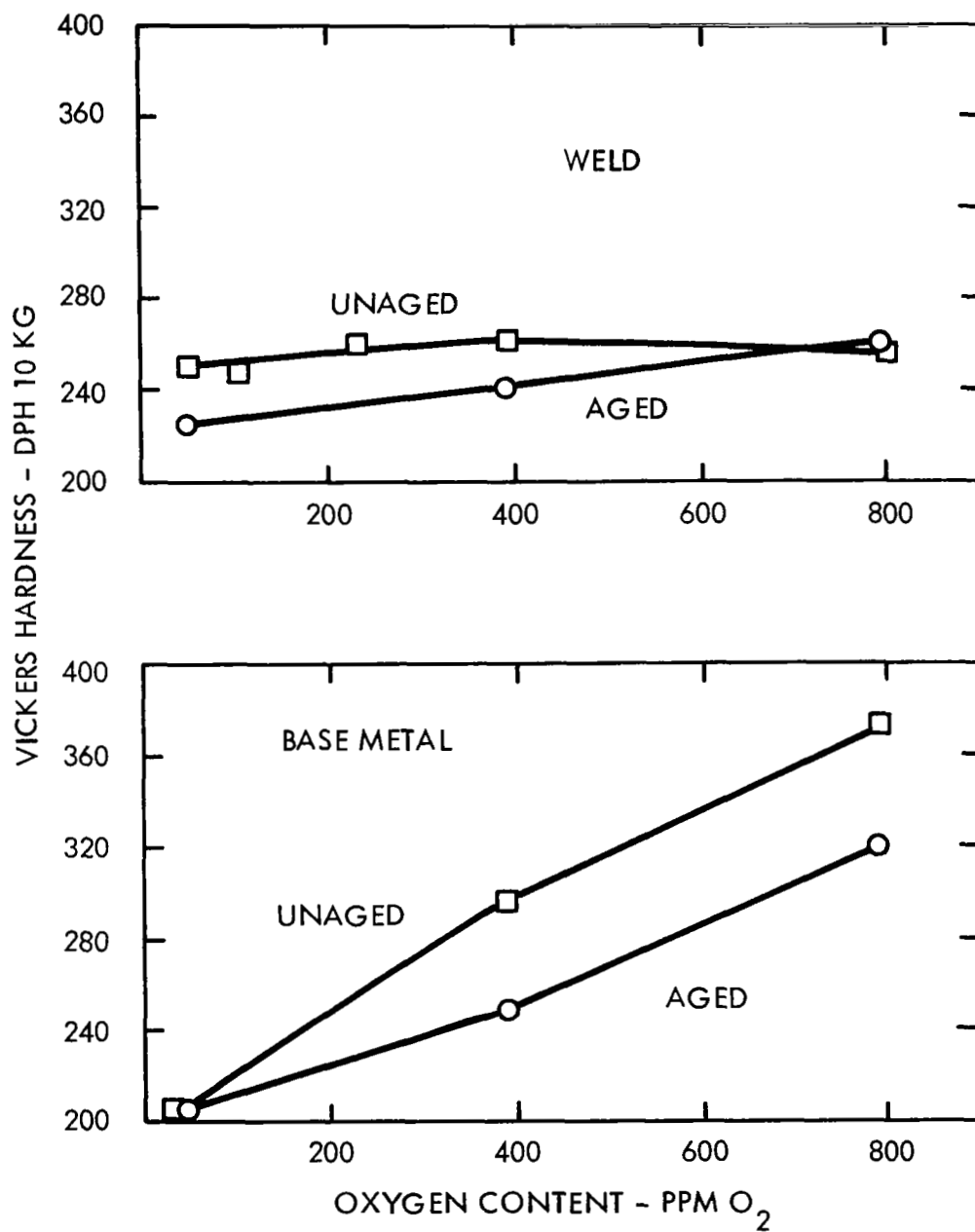
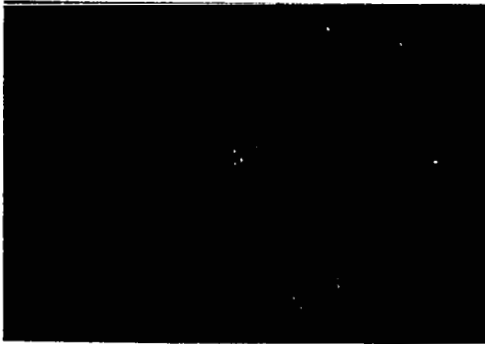



FIGURE 60 - Effect of Aging at 1800°F on Weld and Base Metal Hardness



1μ 

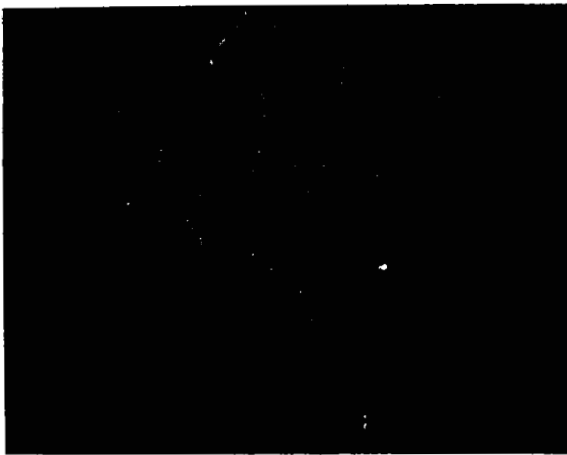
1800°F - 1000 Hrs.




10μ 

2200°F - 1000 Hrs.


700 ppm O<sub>2</sub>  
Base Metal  
Electron Microscope Replica



10μ 

1800°F - 1000 hrs.

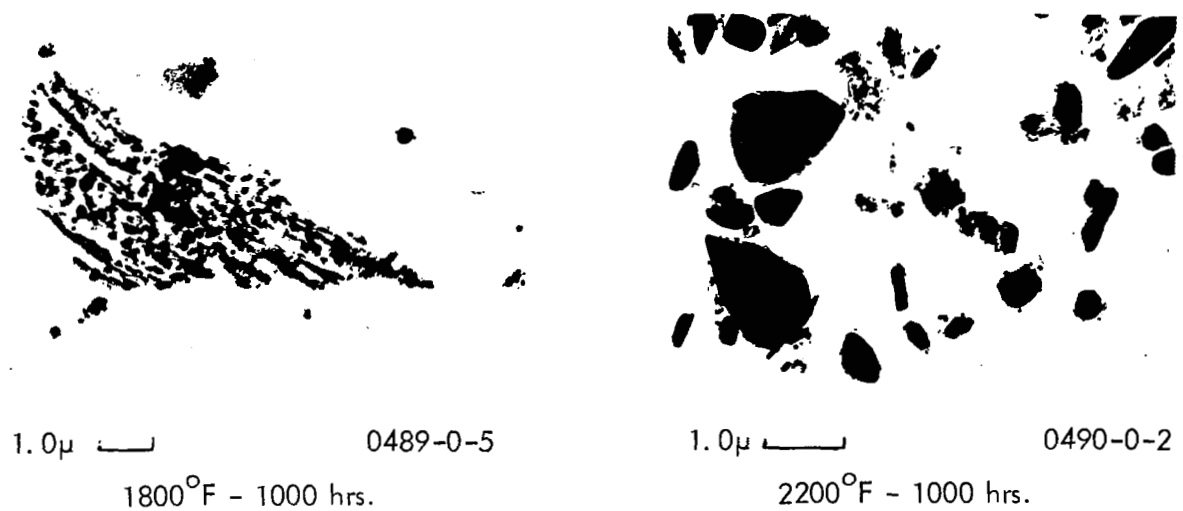


10μ 

2200°F - 1000 hrs.

700 ppm O<sub>2</sub>  
Base Metal  
Oblique Light

FIGURE 61 - Microstructure of Oxygen Contaminated T-111



Bulk extractions from T-111 contaminated with 700 ppm  $O_2$ . Base metal.

FIGURE 62 - Electron Micrograph of  $HfO_2$  Precipitates

## Phase II - Summary

In the second phase of the program, the effect of 1000 hour aging an oxygen contaminated T-111 was determined and a more complete understanding of the oxygen strengthening and embrittlement reaction was obtained.

Aging at 1800°F and 2200°F improved the ductility of oxygen contaminated T-111. Although a direct comparison of aged and as-welded T-111 was not available at 1500°F, the limited data and the aging rationale of hardening behavior indicate that long time exposure at temperatures near 1500°F may result in severe embrittlement of oxygen contaminated material.

Although a summary of the aging effects on tensile behavior is complicated by the lack of base metal specimens, the general trend is a slight loss of both strength and ductility at elevated temperatures. The room temperature tensile tests however indicate a marked improvement in ductility following aging at 1800°F and 2200°F.

Electron microscopy and x-ray diffraction techniques have indicated that changes in the form of a  $\text{HfO}_2$  precipitate are responsible for the marked effect of thermal exposure on the strength and ductility of oxygen contaminated T-111. At temperatures over 2000°F, a coarse non-coherent precipitate is formed which does not impair the ductility of T-111.

#### IV. CONCLUSIONS

The effect of oxygen contamination on the weldability and subsequent high temperature service life was determined for three fabricable tantalum and columbium base alloys (T-111, T-222 and FS-85).

1. T-111 and FS-85 displayed a considerable tolerance to contamination and were appreciably more tolerant to oxygen contamination than T-222. In view of the better performance of welded T-111, this alloy was more extensively evaluated including 1000 hour high vacuum aging at 1500°F, 1800°F and 2200°F.
2. Oxygen contamination increased the hardness and strength and reduced the ductility of all three alloys. Oxygen contamination levels of 200 ppm or greater produced significant losses in bend ductility of both welded and unwelded material.
3. The bend ductility behavior of welded FS-85 was appreciably worse than base metal, whereas little difference between weld and base metal was noted for T-111 and T-222.
4. Hot tearing or weld cracking was not aggravated by oxygen contamination.
5. Although weld and base metal tensile behavior indicated a loss in total tensile elongation, excellent ductility was generally achieved based on reduction in area.
6. The thermal exposure of oxygen contaminated T-111 was found to have greater influence on the resultant physical properties than the total oxygen content. Apparently, oxygen contamination produces an increase in strength and a loss of ductility by the formation of coherent oxide precipitates. At temperatures above 2000°F, a coarser, non-coherent oxide precipitate was formed which has little strengthening effect. Maximum strengthening was produced in the 1500°F to 1800°F temperature range.
7. The combined effect of time and temperature on oxygen contaminated T-111 was similar to a classic aging response even though the apparent metallurgical system, weld zone and oxygen gradient, requires a considerably more sophisticated treatment. The maximum strengthening from oxygen contamination was produced in the 1500°F to 1800°F range and overaging seemed to occur

at 2200°F. Bend ductility following aging for 1000 hours at 1800°F was considerably better than the unaged bend ductility. The aged weld tensile properties were equal to the unaged properties at all temperatures but 1500°F, where the tensile elongation was significantly reduced. 1500°F would appear to be near maximum aging temperature for the 1000 hour aging time.

8. The aging tests indicate that extended service times at temperatures above 1800°F would not impair the performance of oxygen contaminated T-111. Long time service at temperatures below 1800°F, however, may be expected to produce a severe loss in ductility.
9. A practical guideline can be proposed for welding oxygen contaminated columbium or tantalum base alloys. If the contamination has occurred at very low temperatures where a surface film is produced, the film may be mechanically removed to avoid subsequent oxidation. If the oxidation temperature has produced a high strength and low ductility condition, the alloys could be heat treated at temperatures of 2200°F and above to improve ductility. A post weld anneal of 2200°F is recommended to avoid further aging embrittlement of oxygen contaminated alloys. This anneal is compatible with current practice required for inhibiting corrosion resistance in liquid alkali metals.

## V. REFERENCES

1. R. T. Begley and L. L. France, Effect of Oxygen and Nitrogen on Workability and Mechanical Properties of Columbium, Symposium on Newer Metals, ASTM Special Publication No. 272, 1959.
2. W. N. Platte, Welding Columbium and Columbium Alloys, Welding Journal, Vol. 42, No. 2, Feb. 1963, Research Supplement 695-835.
3. G. G. Lessmann, Welding Evaluation of Experimental Columbium Alloys, Welding Journal, March 1964, Research Supplement.
4. H. Inouye, The Contamination of Refractory Metals in Vacua Below  $10^{-6}$  Torr, AIME Symposium, Los Angeles, December 1963.
5. D. O. Hobson, Aging Phenomena in Columbium-Base Alloys, High Temperature Materials II - Publication of AIME Conference in April, 1961.
6. E. A. Franco-Ferreira, G. M. Slaughter, Welding of Columbium-1% Zirconium, Welding Journal, Vol. 42, No. 1, Jan. 1963, Research Supplement 185-245.
7. W. Jost, Diffusion in Solids, Liquids, Gases, Academic Press, Inc., New York, 1960.
8. N. L. Peterson, Diffusion in Refractory Metals, WADD 60-793, AMR-1107, Dec. 1960.
9. R. W. Harrison, and E. J. Delgrosso, Low Pressure Oxidation of Columbium-1 Zirconium, Pratt & Whitney Aircraft - CANEL - Contract AT(30-1)-2789, April 30, 1964.
10. P. Kofstad, et al, High Temperature Oxidation of Niobium, ASTIA S1 Publ. No. 282, April 1960, WADC, Wright Field, Contract AF 61(052)-90.
11. W. D. Klopp, C. T. Sims and R. I. Jaffee, Effects of Alloying on the Kinetics of Oxidation of Niobium, Second International Conference on the Peacetime Uses of Atomic Energy, Geneva, Switzerland, September, 1958.
12. P. Kofstad, "Low Pressure Oxidation of Tantalum at 1300-1800°F," Journal of Less Common Metals, Vol. 7, 1964, Pgs. 241-266.
13. R. A. Pasternak, "High Temperature Oxidation and Nitridation of Niobium in Ultra High Vacuum," Final Report - AEC Contract AT(04-3)-115 Stanford Research Institute, November 15, 1964.



14. D. R. Stoner, and G. G. Lessmann, Operation of  $10^{-10}$  Torr Vacuum Heat Treating Furnaces in Routine Processing, American Vacuum Society - Proceedings of 8th Annual Vacuum Metallurgy Conference, June 1965.
15. D. R. Stoner and G. G. Lessmann, Measurement and Control of Weld Chamber Atmospheres, Welding Journal, August 1965.
16. R. L. Ammon and D. L. Harrod, Strengthening Effects in Ta-W-Hf Alloys, W.ANL-SP-013, AIME Symposium, October 3, 1965.